3.01
Composition of the Continental Crust

R. L. Rudnick

University of Maryland, College Park, MD, USA

and

S. Gao

China University of Geosciences, Wuhan, People's Republic of China and Northwest University, Xi'an, People's Republic of China

3.01.1 INTRODUCTION

The Earth is an unusual planet in our solar system in having a bimodal topography that reflects the two distinct types of crust found on our planet. The low-lying oceanic crust is thin (~7 km on average), composed of relatively dense rock types such as basalt and is young (≤200 Ma old) (see Chapter 3.13). In contrast, the high-standing continental crust is thick (~40 km on average), is composed of highly diverse lithologies (virtually every rock type known on Earth) that

yield an average intermediate or "andesitic" bulk composition (Taylor and McLennan (1985) and references therein), and contains the oldest rocks and minerals yet observed on Earth (currently the 4.0 Ga Acasta gneisses (Bowring and Williams, 1999) and 4.4 Ga detrital zircons from the Yilgarn Block, Western Australia (Wilde *et al*., 2001)), respectively. Thus, the continents preserve a rich geological history of our planet's evolution and understanding their origin is critical for understanding the origin and differentiation of the Earth.

The origin of the continents has received wide attention within the geological community, with hundreds of papers and several books devoted to the topic (the reader is referred to the following general references for further reading: Taylor and McLennan (1985), Windley (1995), and Condie (1997). Knowledge of the age and composition of the continental crust is essential for understanding its origin. Patchett and Samson (Chapter 3.10) review the present-day age distribution of the continental crust and Kemp and Hawkesworth (Chapter 3.11) review secular evolution of crust composition. Moreover, to understand fully the origin and evolution of continents requires an understanding of not only the crust, but also the mantle lithosphere that formed more-or-less contemporaneously with the crust and translates with it as the continents move across the Earth's surface. The latter topic is reviewed in Chapter 2.05.

This chapter reviews the present-day composition of the continental crust, the methods employed to derive these estimates, and the implications of the continental crust composition for the formation of the continents, Earth differentiation, and its geochemical inventories.

3.01.1.1 What is the Continental Crust?

In a review of the composition of the continental crust, it is useful to begin by defining the region under consideration and to provide some generalities regarding its structure. The continental crust, as considered here, extends vertically from the Earth's surface to the Mohorovicic discontinuity, a jump in compressional wave speeds from $\sim 7\ \mathrm{km\ s^{-1}}$ to $\sim 8\ \mathrm{km\ s^{-1}}$ that is interpreted to mark the crust–mantle boundary. In some regions the Moho is transitional rather than discontinuous and there may be some debate as to where the crust–mantle boundary lies (cf. Griffin and O'Reilly, 1987; McDonough *et al*., 1991). The lateral extent of the continents is marked by the break in slope on the continental shelf. Using this definition, ~31% of continental area is submerged beneath the oceans (Figure 1; Cogley, 1984), and is thus less accessible to geological sampling. For this reason, most estimates of continental crust composition derive from exposed regions of the continents. In some cases the limited geophysical data for submerged continental shelves reveal no systematic difference in bulk properties between the shelves and exposed continents; the shelves simply appear to be thinned regions of the crust. In other cases, such as volcanic rifted margins, the submerged continent is characterized by high-velocity layers interpreted to represent massive basaltic intrusions associated with continental breakup (Holbrook and Kelemen, 1993). Depending on the extent of the latter type of continental margin (which is yet to be quantified), crust compositional estimates derived from exposed regions may not be wholly representative of the total continental mass.

The structure of the continental crust is defined seismically to consist of upper-, middle-, and

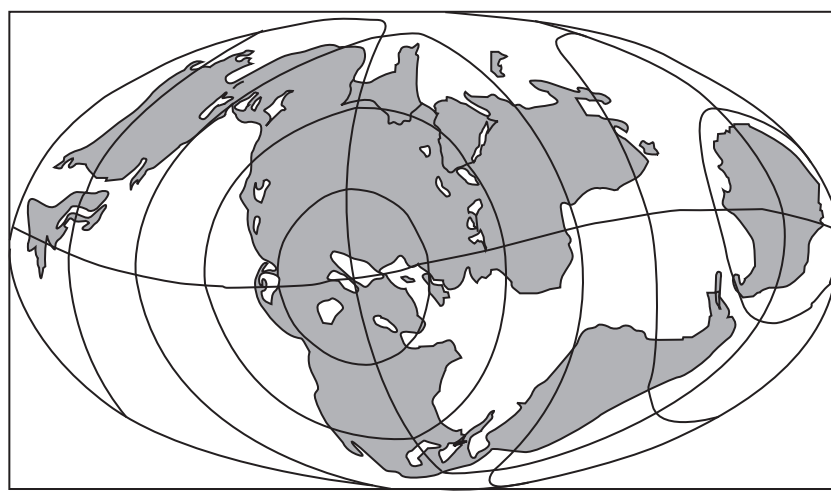

Figure 1 Map of continental regions of the Earth, including submerged continents (Cogley (1984); reproduced by permission of American Geophysical Union from *Rev. Geophys. Space Phys.*, **1984**, *22*, 101–122).

lower crustal layers (Christensen and Mooney, 1995; Holbrook *et al*., 1992; Rudnick and Fountain, 1995). The upper crust is readily accessible to sampling and robust estimates of its composition are available for most elements (Section 3.01.2). These show the upper crust to have a granodioritic bulk composition, to be rich in incompatible elements, and generally depleted in compatible elements. The deeper reaches of the crust are more difficult to study. In general, three probes of the deep crust are employed to unravel its composition: (i) studies of high-grade metamorphic rocks (amphibolite or granulite facies) exposed in surface outcrops (Bohlen and Mezger, 1989) and, in some cases, in uplifted cross-sections of the crust reaching to depths of 20 km or more (Fountain *et al*., 1990a; Hart *et al*., 1990; Ketcham, 1996; Miller and Christensen, 1994); (ii) studies of granulite-facies xenoliths (foreign rock fragments) that are carried from great depths to the Earth's surface by fast-rising magmas (see Rudnick (1992) and references therein); and (iii) remote sensing of lower crustal lithologies through seismic investigations (Christensen and Mooney, 1995; Holbrook *et al*., 1992; Rudnick and Fountain, 1995; Smithson, 1978) and surface heat-flow studies (see Chapter 3.02). Collectively, the observations from these probes show that the crust becomes more mafic with depth (Section 3.01.3). In addition, the concentration of heat-producing elements drops off rapidly from the surface downwards. This is due, in part, to an increase in metamorphic grade but is also due to increasing proportions of mafic lithologies (see Chapter 3.02). Thus, the crust is vertically stratified in terms of its chemical composition.

In addition to this stratification, the above studies also show that the crust is heterogeneous from place to place, with few systematics available for making generalizations about crustal structure and composition for different tectonic settings. For example, the crust of Archean cratons in some regions is relatively thin and has low seismic velocities, suggesting an evolved composition (e.g., Yilgarn craton (Drummond, 1988); Kaapvaal craton (Durrheim and Green, 1992; Niu and James, 2002); and North China craton (Gao *et al*., 1998a,b)). However, in other cratons, the crust is thick (40–50 km) and the deep crust is characterized by high velocities, which imply mafic-bulk compositions (Wyoming craton (Gorman *et al*., 2002) and Baltic shield (Luosto and Korhonen, 1986; Luosto *et al*., 1990)). The reasons for these heterogeneities are not fully understood and we return to this topic in Section 3.01.3. Similar heterogeneities are observed for Proterozoic and Paleozoic regions (see Rudnick and Fountain (1995) and references therein). Determining an average composition of such a heterogeneous mass is difficult and, at first glance, may seem like a futile endeavor. Yet it is just such averages that allow insights into the relative contribution of the crust to the whole Earth-chemical budget and the origin of the continents. Thus, deriving average compositions is critical to studies of the continents and the whole Earth.

3.01.1.2 The Importance of Determining Crust Composition

Although the continental crust constitutes only ~0.6% by mass of the silicate Earth, it contains a very large proportion of incompatible elements (20–70%, depending on element and model considered; Rudnick and Fountain (1995)), which include the heat-producing elements and members of a number of radiogenic-isotope systems (Rb–Sr, U–Pb, Sm–Nd, Lu–Hf). Thus the continental crust factors prominently in any mass-balance calculation for the Earth as a whole and in estimates of the thermal structure of the Earth (Sclater *et al*., 1980).

In addition, knowledge of the bulk composition of the crust and determining whether this composition has changed through time is important for: (i) understanding the processes by which the crust is generated and modified and (ii) determining whether there is any secular evolution in crust generation and modification processes (see Chapter 3.11). The latter has important implications for the evolution of our planet as a whole.

In this chapter we review the composition of the upper, middle, and lower continental crust (Sections 3.01.2 and 3.01.3). We then examine the bulk crust composition and the implications of this composition for crust generation and modification processes (Sections 3.01.4 and 3.01.5). Finally, we compare the Earth's crust with those of the other terrestrial planets in our solar system (Section 3.01.6) and speculate about what unique processes on Earth have given rise to this unusual crustal distribution.

3.01.2 THE UPPER CONTINENTAL CRUST

The upper continental crust, being the most accessible part of our planet, has long been the target of geochemical investigations (Clarke, 1889). There are two basic methods employed to determine the composition of the upper crust: (i) establishing weighted averages of the compositions of rocks exposed at the surface and (ii) determining averages of the composition of insoluble elements in fine-grained clastic sedimentary rocks or glacial deposits and using these to infer upper-crust composition.

The first method was utilized by F. W. Clarke and colleagues over a century ago (Clarke, 1889; Clarke and Washington, 1924) and entails

Table 1 Major element composition[a] (in weight percent oxide) of the upper continental crust. Columns 1–9 represent averages of surface exposures and glacial clays. Columns 10–11 are derivative compositions from these data. Column 12 shows our recommended values.

Element	*1 Clarke (1889)*	*2 Clarke and Washington (1924)*	*3 Goldschmidt (1933)*	*4 Shaw et al. (1967)*	*5 Fahrig and Eade (1968)*	*6 Ronov and Yaroshevskiy (1976)*	*7 Condie (1993)*	*8 Gao et al. (1998a)*	*9 Borodin (1998)*	*10 Taylor and McLennan (1985)*	*11 Wedepohl (1995)*	*12 This Study*[b]
SiO_2	60.2	60.30	62.22	66.8	66.2	64.8	67.0	67.97	67.12	65.89	66.8	66.62
TiO_2	0.57	1.07	0.83	0.54	0.54	0.55	0.56	0.67	0.60	0.50	0.54	0.64
Al_2O_3	15.27	15.65	16.63	15.05	16.10	15.84	15.14	14.17	15.53	15.17	15.05	15.40
FeO_T[c]	7.26	6.70	6.99	4.09	4.40	5.78	4.76	5.33	4.94	4.49	4.09	5.04
MnO	0.10	0.12	0.12	0.07	0.08	0.10		0.10	0.00	0.07	0.07	0.10
MgO	4.59	3.56	3.47	2.30	2.20	3.01	2.45	2.62	2.10	2.20	2.30	2.48
CaO	5.45	5.18	3.23	4.24	3.40	3.91	3.64	3.44	3.51	4.19	4.24	3.59
Na_2O	3.29	3.92	2.15	3.56	3.90	2.81	3.55	2.86	3.21	3.89	3.56	3.27
K_2O	2.99	3.19	4.13	3.19	2.91	3.01	2.76	2.68	3.01	3.39	3.19	2.80
P_2O_5	0.23	0.31	0.23	0.15	0.16	0.16	0.12	0.16	0.00	0.20	0.15	0.15
Mg#	53.0	48.7	46.9	50.1	47.4	48.1	47.9	46.7	43.2	46.6	50.1	46.7

Mg# = molar $100 \times Mg/(Mg + Fe_{tot})$.
[a] Major elements recast to 100% anhydrous. [b] See Table 3 for derviation of this estimate. [c] Total Fe as FeO.

large-scale sampling and weighted averaging of the wide variety of rocks that crop out at the Earth's surface. All major-element (and a number of soluble trace elements) determinations of upper-crust composition rely upon this method.

The latter method is based on the concept that the process of sedimentation averages wide areas of exposed crust. This method was originally employed by Goldschmidt (1933) and his Norwegian colleagues in their analyses of glacial sediments to derive average composition of the crystalline rocks of the Baltic shield and has subsequently been applied by a number of investigators, including the widely cited work by Taylor and McLennan (1985) to derive upper-crust composition for insoluble trace elements. In the following sections we review the upper-crust composition determined from each of these methods, then provide an updated estimate of the composition of the upper crust.

3.01.2.1 Surface Averages

In every model for the composition of the upper-continental crust, major-element data are derived from averages of the composition of surface exposures (Table 1). Several surface-exposure studies have also provided estimates of the average composition of a number of trace elements (Table 2). For soluble elements that are fractionated during the weathering process (e.g., sodium, calcium, strontium, barium, etc.), this is the only way in which a reliable estimate of their abundances can be obtained.

The earliest of such studies was the pioneering work of Clarke (1889), who, averaging hundreds of analyses of exposed rocks, determined an average composition for the crust that is markedly similar to present-day averages of the bulk crust (cf. Tables 1 and 9). Although Clarke's intention was to derive the average crust composition, his samples are limited to the upper crust; there was little knowledge of the structure of the Earth when these studies were undertaken; oceanic crust was not distinguished as different from continental and the crust was assumed to be only 16 km thick. Clarke's values are, therefore, most appropriately compared to upper crustal estimates. Later, Clarke, joined by H. S. Washington, used a larger data set to determine an average composition of the upper-crust that is only slightly different from his original 1889 average (Clarke and Washington, 1924; Table 1). Compared to more recent estimates of upper-crust composition, these earliest estimates are less evolved (lower silicon, higher iron, magnesium, and calcium), but contain similar amount of the alkali elements, potassium and sodium.

The next major undertakings in determining upper-crust composition from large-scale surface

Table 2 Estimates of the trace-element composition of the upper continental crust. Columns 1–4 represent averages of surface exposures. Columns 5–8 are estimates derived from sedimentary and loess data. Column 9 is a previous estimate, where bracketed data are values derived from surface exposure studies. Column 10 is our recommended value (see Table 3).

Element	*Units*	*1* *Shaw et al. (1967, 1976)*	*2* *Eade and Fahrig (1973)*	*3* *Condie (1993)*	*4* *Gao et al. (1998a)*	*5* *Sims et al. (1990)*	*6* *Plank and Langmuir (1998)*	*7* *Peucker-Ehrenbrink and Jahn (2001)*	*8* *Taylor and McLennan (1985, 1995)*	*9* *Wedepohl (1995)*[a]	*10* *This study*[b]
Li	μg g^{-1}	22			20				20	[22]	21
Be	”	1.3			1.95				3	3.1	2.1
B	”	9.2			28				15	17	17
N	”									83	83
F	”	500			561					611	557
S	”	600			309					953	621
Cl	”	100			142					640	370
Sc	”	7	12	13.4	15				13.6[c]	[7]	14.0
V	”	53	59	86	98				107[c]	[53]	97
Cr	”	35	76	112	80				85[c]	[35]	92
Co	”	12		18	17				17[c]	[12]	17.3
Ni	”	19	19	60	38				44[c]	[19]	47
Cu	”	14	26		32				25	[14]	28
Zn	”	52	60		70				71	[52]	67
Ga	”	14			18				17	[14]	17.5
Ge	”				1.34				1.6	1.4	1.4
As	”				4.4	5.1			1.5	2	4.8
Se	”				0.15				0.05	0.083	0.09
Br	”									1.6	1.6
Rb	”	110	85	83	82				112	110	84
Sr	”	316	380	289	266				350	[316]	320
Y	”	21	21	24	17.4				22	[21]	21
Zr	”	237	190	160	188				190	[237]	193
Nb	”	26		9.8	12		13.7		12[c]	[26]	12
Mo	”				0.78	1.2			1.5	1.4	1.1
Ru	ng g^{-1}							0.34			0.34
Pd	”				1.46			0.52	0.5		0.52
Ag	”				55				50	55	53
Cd	μg g^{-1}	0.075			0.079				0.098	0.102	0.09
In	”								0.05	0.061	0.056
Sn	”				1.73				5.5	2.5	2.1
Sb	”				0.3	0.45			0.2	0.31	0.4

(continued)

Table 2 (continued).

Element	*Units*	*1* *Shaw et al. (1967, 1976)*	*2* *Eade and Fahrig (1973)*	*3* *Condie (1993)*	*4* *Gao et al. (1998a)*	*5* *Sims et al. (1990)*	*6* *Plank and Langmuir (1998)*	*7* *Peucker-Eherenbrink and Jahn (2001)*	*8* *Taylor and McLennan (1985, 1995)*	*9* *Wedepohl (1995)*[a]	*10* *This study*[b]
I	”									1.4	1.4
Cs	”				3.55		7.3		4.6[c]	5.8	4.9
Ba	”	1070	730	633	678				550	668	624
La	”	32.3	71	28.4	34.8				30	[32.3]	31
Ce	”	65.6		57.5	66.4				64	[65.7]	63
Pr	”								7.1	6.3	7.1
Nd	”	25.9		25.6	30.4				26		27
Sm	”	4.61		4.59	5.09				4.5	4.7	4.7
Eu	”	0.937		1.05	1.21				0.88	0.95	1.0
Gd	”			4.21					3.8	2.8	4.0
Tb	”	0.481		0.66	0.82				0.64	[0.5]	0.7
Dy	”	2.9							3.5	[2.9]	3.9
Ho	”	0.62							0.8	[0.62]	0.83
Er	”								2.3		2.3
Tm	”								0.33		0.30
Yb	”	1.47		1.91	2.26				2.2	[1.5]	2.0
Lu	”	0.233		0.32	0.35				0.32	[0.27]	0.31
Hf	”	5.8		4.3	5.12				5.8	[5.8]	5.3
Ta	”	5.7		0.79	0.74		0.96		1.0[c]	1.5	0.9
W	”				0.91	3.3			2	1.4	1.9
Re	ng g^{-1}							0.198	0.4		0.198
Os	”							0.031	0.05		0.031
Ir	”	0.02						0.022	[0.02]		0.022
Pt	”							0.51			0.5
Au	”	1.81			1.24				[1.8]		1.5
Hg	μg g^{-1}	0.096			0.0123					0.056	0.05
Tl	”	0.524			1.55				0.75	0.75	0.9
Pb	”	17	18	17	18				17[c]	17	17
Bi	”	0.035			0.23				0.13	0.123	0.16
Th	”	10.3	10.8	8.6	8.95				10.7	[10.3]	10.5
U	”	2.45	1.5	2.2	1.55				2.8	[2.5]	2.7

[a] Wedepohl's upper crust is largely derived from the Canadian Shield composites of Shaw *et al.* (1967, 1976). Values taken directly from Shaw *et al.* are shown in brackets. [b] See Table 3 for derviation of this estimate.
[c] Updated in McLennan (2001b).

sampling campaigns did not appear until twenty years later in studies centered on the Canadian, Baltic, and Ukranian Shields. It is these studies that form the foundation on which many of the more recent estimates of upper-crust composition are constructed (e.g., Taylor and McLennan, 1985; Wedepohl, 1995).

Shaw *et al*. (1967, 1976, 1986) and Eade and Fahrig (1971, 1973) independently derived estimates for the average composition of the Canadian Precambrian shield. Both studies created composites from representative samples taken over large areas that were weighted to reflect their surface outcrop area. The estimates of Shaw *et al*. are based on a significantly smaller number of samples than that of Eade and Fahrig's (i.e., ~430 versus ~14,000) and cover different regions of the shield, but the results are remarkably similar (Figure 2). All major elements agree to within ~10% except for CaO, which is ~20% higher, and MnO, which is 15% lower in the estimates of Shaw *et al*. estimates.

Shaw *et al*. (1967, 1976, 1986) also measured a number of trace elements in their shield composites and these are compared to the smaller number of trace elements determined by Eade and Fahrig in Table 2 and Figure 3. As might be expected, considering the generally greater variability in trace-element concentrations and the greater analytical challenge, larger discrepancies exist between the two averages. For example, scandium, chromium, copper, lanthanum, and

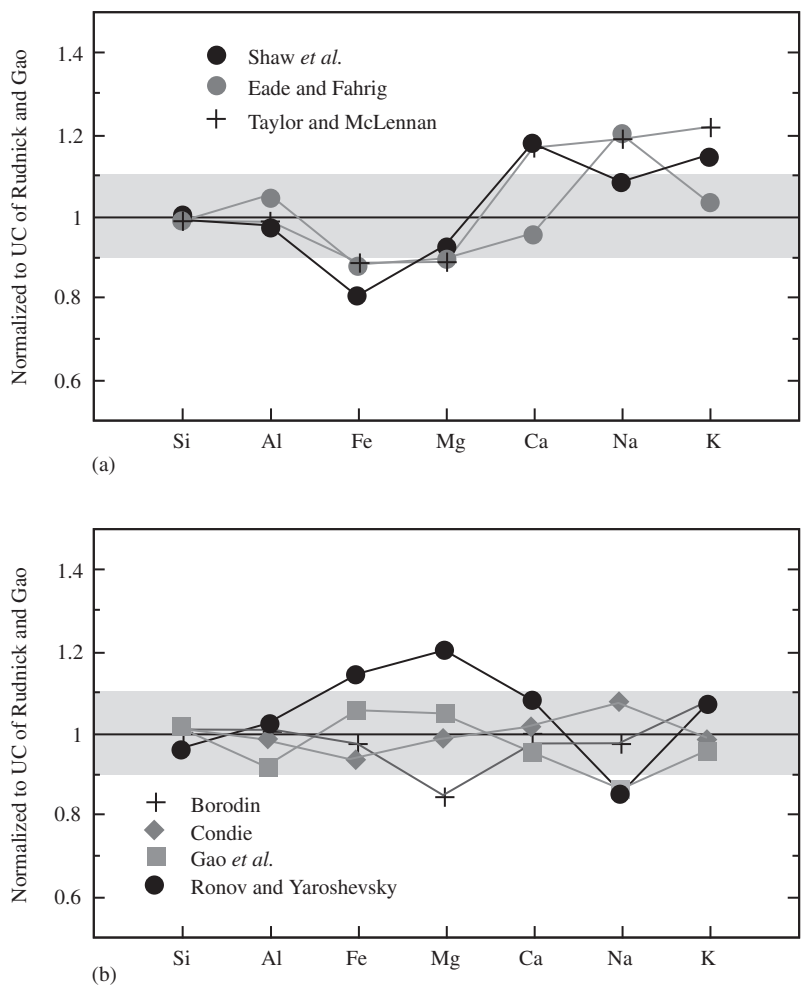

Figure 2 Comparison of different models for the major-element composition of the upper continental crust. All values normalized to the new composition provided in Table 3. Gray shaded field represents ±10% variation from this value. (a) Compositions derived from Canadian Shield samples (Shaw *et al*., 1967, 1976, 1986; Fahrig and Eade, 1968; Eade and Fahrig, 1971, 1973) and the Taylor and McLennan model (1985, 1995, as modified by McLennan, 2001b). (b) Compositions derived from surface sampling of the former Soviet Union (Ronov and Yaroshevsky, 1967, 1976; Borodin, 1998) and China (Gao *et al*., 1998a) and a global compilation of upper crustal rock types weighted in proportion to their areal distribution (Condie, 1993). The Canadian shield averages appear to be more evolved (having lower Mg, Fe, and higher Na and K) than other estimates.

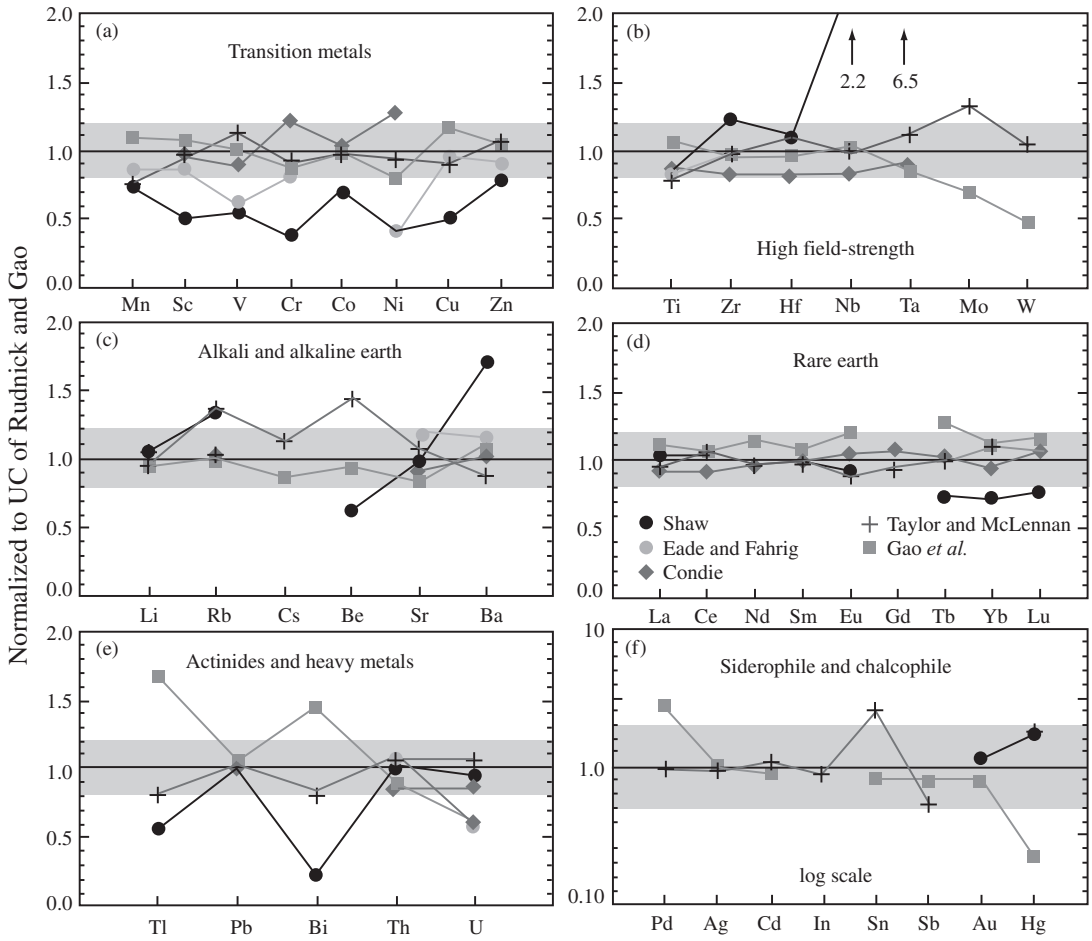

Figure 3 Comparison of different models for the trace-element composition of the upper-continental crust. All values normalized to the new composition provided in Table 3. Gray shaded field represents ±20% variation from this value for all panels except (f), in which gray field represents a factor of two variation. Trace elements are divided into the following groups: (a) transition metals, (b) high-field strength elements, (c) alkali, alkaline-earth elements, (d) REEs, (e) actinides and heavy metals, and (f) highly siderophile and chalcophile elements (note log scale). Data from Tables 1 and 2; lanthanum estimate from Eade and Fahrig (1973) is omitted from panel D.

uranium values vary by ~50% or more. In some cases this may reflect compromised data quality (e.g., lanthanum was determined by optical-emission spectroscopy in the Eade and Fahrig study) and in other cases it may reflect real differences in the composition between the two averages. However, for a number of trace elements (e.g., vanadium, nickel, zinc, rubidium, strontium, zirconium, and thorium), the averages agree within 30%.

In a similar study, Ronov and Yaroshevsky (1967, 1976) determined the average major-element composition of the upper crust based on extensive sampling of rocks from the Baltic and Ukranian shields and the basement of the Russian platform (Table 1). While the SiO_2, Al_2O_3, and K_2O values fall within 5% of those of the average Canadian Shield, as determined by Eade and Fahrig (1971, 1973), FeO_T, MgO, and CaO are ~10–30% higher, and Na_2O is ~30% lower than the Canadian average, suggesting a slightly more mafic composition.

The generally good correspondence between these independent estimates of the composition of shield upper crust lends confidence in the methodologies employed. However, questions can be raised about how representative the shields are of the global upper continental crust. For example, Condie (1993) suggests that shield averages may be biased because (i) shields are significantly eroded and thus may not be representative of the 5–20 km of uppermost crust that has been removed from them and (ii) they include only Precambrian upper crust and largely ignore any Phanerozoic contribution to upper crust. Condie (1993) derived an upper-crust composition based on over 3,000 analyses of upper crustal rock types weighted according to their distributions on geologic maps and stratigraphic sections, mainly covering regions of North America, Europe, and

Australia. He utilized two methods in calculating an average upper-crust composition: (i) using the map distributions, irrespective of level of erosion and (ii) for areas that have been significantly eroded, restoring the eroded upper crust, assuming it has a ratio of supracrustal rocks to plutonic rocks similar to that seen in uneroded upper crustal regions. The latter approach was particularly important for his study, as one of his primary objectives was to evaluate whether there has been any secular change in upper crust composition. However, in this review, we are interested in the present-day composition of the upper crust (eroded or not), so it seems most appropriate to consider his "map model" for comparisons with other models (for a discussion of the secular evolution of the continents, see Chapter 3.11).

Condie's "map model" is compared with other estimates of the upper crust in Tables 1 and 2 and Figures 2 and 3. For major elements, his upper crust composition is within 10% of the Canadian Shield values of Eade and Fahrig. It is also within 10% of some of the major elements estimated by Shaw, but has generally higher magnesium and iron, and lower calcium and potassium compared to Shaw's estimate (Figure 2). Many trace elements in Condie's upper-crust composition are similar (i.e., within 20%) to those of Shaw's Canadian Shield composites (Figure 3), including the light rare-earth elements (LREEs), strontium, yttrium, thorium, and uranium. However, several trace elements in Condie's average vary by $\geqslant$50% from those of Shaw *et al*. (1967, 1976, 1986) as can be seen in the figure. These include transition metals (scandium, vanadium, chromium, and nickel), which are considerably higher in Condie's upper crust, and niobium, barium and tantalum, which are significantly lower in Condie's upper crust compared to Shaw's. These differences may reflect regional variations in upper crust composition (i.e., the Canadian Shield is not representative of the worldwide upper crust) or inaccuracies in either of the estimates due to data quality or insufficiency. As will be discussed below, it is likely that Condie's values for transition metals, niobium, tantalum, and barium are the more robust estimates of the average upper crust composition.

A recent paper by Borodin (1998) provides an average composition of the upper crust that includes much Soviet shield and granite data not included in most other worldwide averages. For this reason, it makes an interesting comparison with other data sets. Like other upper crustal estimates, major elements in the Borodin average upper crust (Table 1 and Figure 2) fall within 10% of the Eade and Fahrig average for the Canadian Shield, except for TiO_2 and FeO, which are ~13% higher, and Na_2O, which is ~20% lower than the Canadian average. Borodin's limited trace element averages (for chromium, nickel, rubidium, strontium, zirconium, niobium, barium, lanthanum, thorium, and uranium—not given in table or figures) fall within 50% of Shaw's Canadian Shield values except for niobium, which, like other upper crustal estimates, is about a factor of 2 lower than the Canadian average.

The more recent and comprehensive study of upper-crust composition derived from surface exposures was carried out by Gao *et al*. (1998a). Nine hundred and five composite samples were produced from over 11,000 individual rock samples covering an area of 9.5×10^5 km^2 in eastern China, which includes samples from Precambrian cratons as well as Phanerozoic fold belts. The samples comprised both crystalline basement rocks and sedimentary cover, the thickness of which was determined from seismic and aeromagnetic data. Averages were derived by combining compositions of individual map units weighted according to their thicknesses (in the cases of sedimentary cover) and areal exposure, for shields. The upper crust is estimated to be ~15 km thick based on seismic studies (Gao *et al*., 1998a) and the crystalline rocks exposed at the surface area assumed to maintain their relative abundance through this depth interval. Average upper crust was calculated both as a grand average and on a carbonate-free basis; carbonates comprise a significant rock type (7–22%) in many of the areas sampled (e.g., Yangtze craton). The grand average (including carbonate) has a significantly different bulk composition than other estimates of the upper crust (Gao *et al*., 1998a; Table 2). Most of the latter are derived from crystalline shields and so a difference is expected. However, Condie's map model incorporates sedimentary cover as well as crystalline basement. The differences between Condie's map model and Gao *et al*. grand-total upper crust suggest that the carbonate cover in eastern China is thicker than most other areas. For this reason, we use Gao *et al*. (1998a) carbonate-free compositions in further discussions, but with the caveat that carbonates may be an overlooked upper crustal component in many upper crustal estimates.

The Gao *et al*. (1998a) major- and trace-element results are presented in Tables 1 and 2 and plotted in Figures 2 and 3, respectively. Unlike the model of Condie (1993), several of the major elements fall beyond 10% of Eade and Fahrig's Canadian Shield data (Figures 2 and 3). These include TiO_2, FeO, MnO, and MgO, which are higher, and Na_2O, which is lower in the eastern China upper crust compared to the Canadian Shield. Gao *et al*. (1998a) attribute these differences to erosional differences between the two areas. Whereas the Canadian Shield composites comprised mainly metamorphic

rocks of the amphibolite facies, the eastern China composites contain large proportions of unmetamorphosed supracrustal units that are considered to have, on average, higher proportions of mafic volcanics. In this respect, the Gao *et al*. model composition compares favorably to Condie's map model and the Russian estimates for all major elements. However, the Na_2O content of the eastern China upper crust is one of lowest of all (~20% lower than Condie's average and 10% lower than Borodin's values, but similar to Ronov and Yaroshevsky's average) (Figure 2).

The trace-element composition estimated by Gao *et al*. (1998a) for the Chinese upper crust is very similar to that of Condie (1993). Like the latter model, many lithophile trace elements in the Gao *et al*. model are within 50% of the Canadian Shield averages of Shaw *et al*. (e.g., LREEs, yttrium, rubidium, strontium, zirconium, hafnium, thorium, and uranium), and the Chinese average has significantly higher transition metals and lower niobium, barium, and tantalum than the Canadian Shield average. In addition, Gao *et al*. (1998a) provide values for some of the less well-constrained element concentrations. Of these, averages for lithium, beryllium, zinc, gallium, cadmium, and gold fall within 40% of the Shaw *et al*. averages, but boron, thallium, and bismuth are significantly higher, and mercury is significantly lower in Gao's average than in Shaw's. There is too little information for these elements in general to fully evaluate the significance of these differences.

Several generalizations can be made from the above studies of surface composites.

(i) Major element data are very consistent from study to study, with most major-element averages falling within 10% of Eade and Fahrig's Canadian Shield average. When differences do occur, they appear to reflect a lower percentage of mafic lithologies in the Canadian averages: all other estimates (including the Russian shield data) have higher FeO and TiO_2 than the Canadian averages and most also have higher CaO and MgO (Figures 2 and 3). The Eade and Fahrig average also has higher Na_2O than all other estimates (including Shaw's estimate for the Canadian Shield).

(ii) Trace elements show more variation than major elements from study to study, but some lithophile trace elements are relatively constant: rare earth elements (REEs), yttrium, lithium, rubidium, caesium, strontium, zirconium, hafnium, lead, thorium, and uranium do not vary beyond 50% between studies. Transition metals (scandium, cobalt, nickel, chromium, and vanadium) are consistently lower in the Canadian Shield estimates than in other studies, which may also be attributed to a lower percentage of mafic lithologies in the Canadian Shield (a conclusion supported by studies of sediment composition, as discussed in the next section). Barium is ~40% higher in the Shaw *et al*. average than in all other averages, including that of Eade and Fahrig, suggesting that this value is too high. Finally, niobium and tantalum are both about a factor of 2 higher in the Shaw *et al*. average than in any other average, suggesting that the former is not representative of the upper continental crust, a conclusion reached independently by Plank and Langmuir (1998) and Gallet *et al*. (1998) based on the composition of marine sediments and loess (see next section).

3.01.2.2 Sedimentary Rocks and Glacial Deposit Averages

While the large-scale sampling campaigns outlined above are the primary means by which the major-element composition of the upper continental crust has been determined, many estimates of the trace-element composition of the upper crust rely on the natural wide-scale sampling processes of sedimentation and glaciation. These methods are used primarily for elements that are insoluble during weathering and are, therefore, transported quantitatively from the site of weathering/glacial erosion to deposition. This methodology has been especially useful for determining the REE composition of the upper crust (see Taylor and McLennan (1985) and references therein). The averages derived from each of these natural large-scale samples are discussed in turn. When the upper crustal concentration of elements is discussed, the element name is printed in italic text so that the reader can quickly scan the text to the element of interest.

3.01.2.2.1 Sedimentary rocks

Processes that produce sedimentary rocks include weathering, erosion, transportation, deposition, and diagenesis. Elemental fractionation during weathering is discussed in detail by Taylor and McLennan (1985) (see also Chapters 5.01 and 7.01) and the interested reader is referred to these works for more extensive information. Briefly, elements with high solubilities in natural waters (Figure 4) have greater potential for being fractionated during sedimentary processing; thus, their concentration in fine-grained sedimentary rocks may not be representative of their source region. These elements include the alkali and alkaline-earth elements as well as boron, rhenium, molybdenum, gold, and uranium.

In contrast, a number of elements have very low solubilities in waters. Their concentrations in sedimentary rocks may, therefore, provide robust

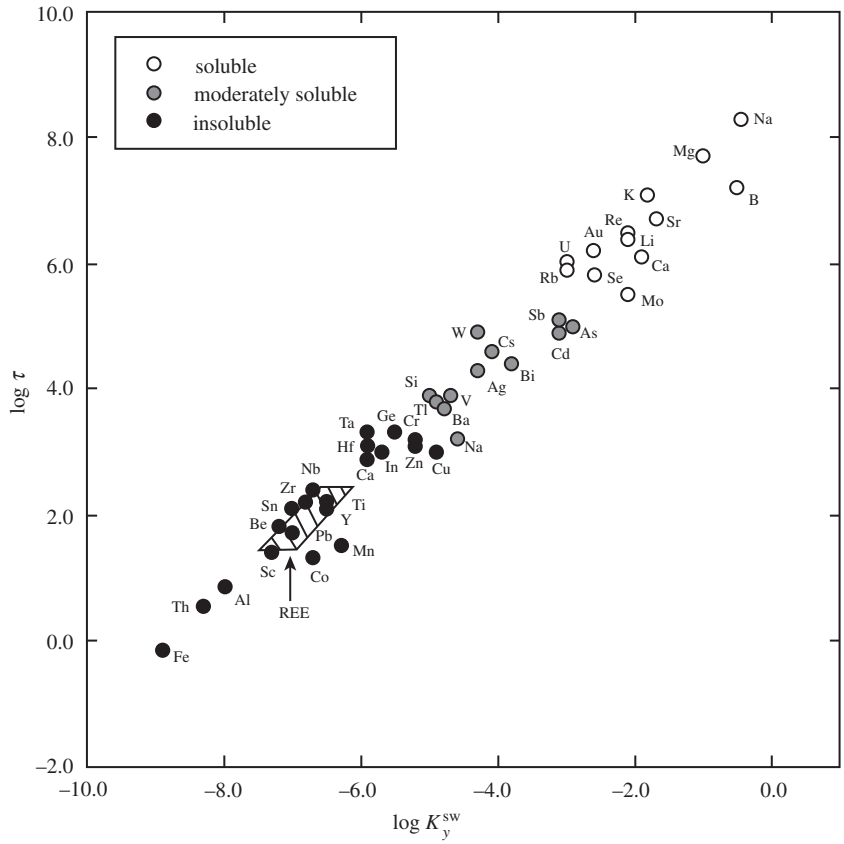

Figure 4 Plot of residence time (expressed as log τ) against seawater upper crust partition coefficient (expressed as K_y^{sw}) (source Taylor and McLennan, 1985).

estimates of the average composition of their source regions (i.e., average upper-continental crust). Taylor and McLennan (1985) identified that REEs, yttrium, scandium, thorium, and possibly cobalt as being suitably insoluble and thus providing useful information on upper crust composition.

The *REE* patterns for post-Archean shales show striking similarity worldwide (Figure 5): they are light REE enriched, with a negative europium anomaly and relatively flat heavy REEs. This remarkable consistency has led to the suggestion that the REE patterns of shales reflect that of the average upper-continental crust (Taylor and McLennan (1985) and references therein). Thus, Taylor and McLennan's (1985) upper crustal REE pattern is parallel to average shale, but lower in absolute abundances due to the presence of sediments with lower REE abundances such as sandstones, carbonates, and evaporites. Using a mass balance based on the proportions of different types of sedimentary rocks, they derive an upper crustal REE content that is 80% that of post-Archean average shale.

Comparison of various upper crustal REE patterns is provided in Figure 5. All estimates, whether from shales, marine sediments, or surface sampling, agree to within 20% for the LREEs and ~50% for the heavy rare-earth elements (HREEs). The estimate of Shaw *et al*. (1976) has the lowest HREEs and if these data are excluded, the HREEs agree to within 15% between the models of Condie (1993), Gao *et al*. (1998a), and Taylor and McLennan (1985). Thus, the REE content of the upper continental crust is established to within 10–25%, similar to the uncertainties associated with its major-element composition.

Once the REE concentration of the upper crust has been established, values for other insoluble elements can be determined from their ratios with an REE. Using the constant ratios of La/Th and La/Sc observed in shales, McLennan *et al*. (1980) and Taylor and McLennan (1985) estimated the upper crustal *thorium* and *scandium* contents at 11 ppm and 10.7 ppm, respectively. The scandium value increased slightly (to 13.7 ppm) and the thorium value remained unchanged when a more comprehensive sediment data set was employed by McLennan (2001b). The sediment-derived scandium and thorium averages agree to within 20% of the surface-sample averages (Table 2 and Figure 3).

Other insoluble elements include the high-field strength elements (HFSEs—titanium, zirconium,

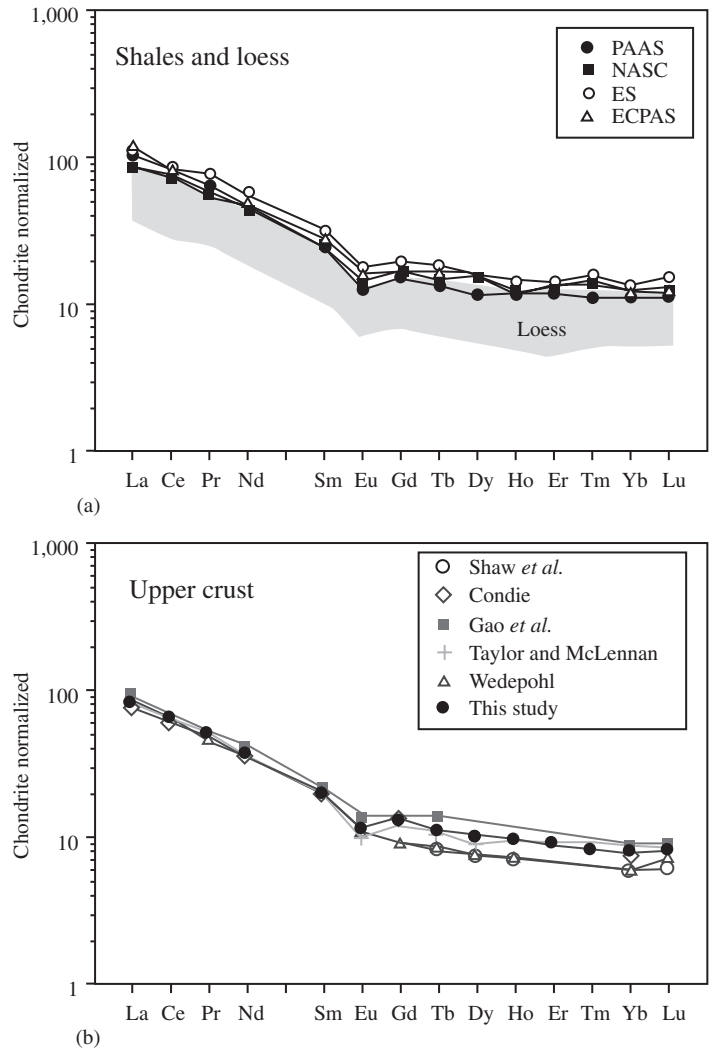

Figure 5 Comparison of REE patterns between (a) average post-Archean shales and loess and (b) various estimates of the upper continental crust composition. PAAS = post-Archean Australian Shale (Taylor and McLennan, 1985); NASC = North American shale composite (Haskin *et al*., 1966); ES = European shale composite (Haskin and Haskin, 1966); ECPAS = Eastern China post-Archean shale (Gao *et al*., 1998a). The loess range includes samples from China, Spitsbergen, Argentina, and France (Gallet *et al*., 1998; Jahn *et al*., 2001). Chondrite values are from Taylor and McLennan (1985).

hafnium, niobium, tantalum, molybdenum, tungsten), beryllium, aluminum, gallium, germanium, indium, tin, lead, and a number of transition metals (chromium, cobalt, nickel, copper, and zinc). Taylor and McLennan (1985) noted that some of these insoluble elements (e.g., HFSEs) may be fractionated during sedimentary processing if they reside primarily in heavy minerals. More recent evaluations have suggested that this effect is probably not significant for niobium and tantalum, and fractionations of zirconium and hafnium due to heavy mineral sorting are only really apparent in loess (Barth *et al*., 2000; McLennan, 2001b; Plank and Langmuir, 1998). Plank and Langmuir (1998) noted that the *niobium*, *tantalum*, and *titanium* concentrations derived for the upper crust using marine sediments are considerably different from those of the Taylor and McLennan's upper continental crust composition. As oceanic processes are unlikely to fractionate these elements, Plank and Langmuir (1998) suggested that marine sediments provide a reliable estimate of the average composition of the upper continental crust. Using correlations between Al_2O_3 and niobium, they derived a niobium concentration for the upper crust of 13.7 ppm, and tantalum of 0.96 ppm (assuming Nb/Ta = 14); these values are about a factor of 2 lower than Taylor and McLennan's (1985) upper crustal estimates. Taylor and McLennan (1985) adopted their niobium value from Shaw *et al*. (1976), and their tantalum value was derived by

assuming a Nb/Ta ratio of ~12 for the upper crust. The Plank and Langmuir niobium and tantalum values are similar to those derived from the surface-sampling studies of Condie (1993), Gao *et al*. (1998a), and Borodin (1998) and from more recent evaluations of these elements in shales, loess and other terrigenous sedimentary rocks (Barth *et al*., 2000; Gallet *et al*., 1998; McLennan, 2001b). All of these estimates range between 10 ppm and 14 ppm niobium and 0.74 ppm to 1.0 ppm tantalum, an overall variation of ~30%. Thus, niobium and tantalum concentrations now appear to be nearly as well constrained as the REE in the upper continental crust.

Plank and Langmuir (1998) also suggested, from their analyses of marine sediments, increasing the upper crustal TiO_2 values by ~40% (from 0.5 wt. % to 0.76 wt. %). Thus the TiO_2 content of the upper-continental crust probably lies between 0.55 wt.% and 0.76 wt.%, a difference of ~30%.

Of the remaining insoluble elements, recent evaluation of *zirconium* and *hafnium* concentrations derived from terrigenous sediment (McLennan, 2001b) show no significant differences with Taylor and McLennan's estimates, whose upper crustal zirconium value derives from the *Handbook of Geochemistry* (Wedepohl, 1969–1978), with hafnium determined from an assumed Zr/Hf ratio of 33. These values lie within ~20% of the surface-exposure averages (Table 2, Figure 3).

For the insoluble transition metals *chromium*, *cobalt*, and *nickel*, McLennan's (2001b) recent evaluation suggests approximate factor of 2 increases in average upper crustal values over those of Taylor and McLennan (1985). Taylor and McLennan's (1985) values were taken from a variety of sources (see Table 1 of Taylor and McLennan, 1981) and are similar to the Canadian Shield averages, which appear to represent a more felsic upper-crust composition, as discussed above. Even after eliminating these lower values, 30–40% variation exists for chromium, cobalt, and nickel between different estimates (Table 2 and Figure 3), and the upper crustal concentrations of these elements remains poorly constrained relative to REE.

McLennan (2001b) evaluated the upper crustal *lead* concentration from sediment averages and suggested a slight (~15%) downward revision (17 ppm) from the value of Taylor and McLennan (1985), whose value derives from a study by Heinrichs *et al*. (1980). McLennan's value is identical to that of surface averages (Table 2) and collectively these should be considered as a robust estimate for the lead content of the upper crust. For the remaining insoluble elements—*beryllium*, *copper*, *zinc*, *gallium*, *germanium*, *indium*, and *tin*—no newer data are available for terrigenous sediment averages. Estimates for some elements (e.g., zinc, gallium, germanium, and indium) vary by only ~20–30% between different studies, but others (beryllium, copper, and tin) vary by a factor of 2 or more (Table 2 and Figure 3).

It may also be possible to derive average upper crustal abundances of elements that have intermediate solubilities (e.g., vanadium, arsenic, silver, cadmium, antimony, caesium, barium, tungsten, and bismuth) using their concentrations in fine-grained sedimentary rocks, if they show significant correlations with lanthanum. Using this method McLennan (2001b) derived estimates of the upper crustal composition for *barium* (550 ppm) and *vanadium* (107 ppm). McLennan's barium value does not differ from that of Taylor and McLennan (1985), which derives from the *Handbook of Geochemistry* (Wedepohl, 1969–1978). This value is ~10% to a factor of 2 lower than the shield estimates; 630–700 ppm seems to be the most common estimate for barium from surface exposures. McLennan's vanadium estimate is ~50% higher than that of Taylor and McLennan (1985), which was derived from a 50 : 50 mixture of basalt : tonalite (Taylor and McLennan, 1981) and is similar to the Canadian Shield averages (Table 2). The revised vanadium value is similar to the surface-exposure averages from eastern China (Gao *et al*., 1998a) and Condie's (1993) global average.

Several studies have used data for sedimentary rocks to derive the concentration of *caesium* in the upper crust. McDonough *et al*. (1992) found that a variety of sediments and sedimentary rocks (including loess) have an Rb/Cs ratio of 19 (± 11, 1σ), which is lower than the value of 30 in Taylor and McLennan's (1985) upper crust. Using this ratio and assuming a rubidium content of 110 ppm (from Shaw *et al*., 1986; Shaw *et al*., 1976; Taylor and McLennan, 1981), led them to an upper crustal caesium concentration of ~6 ppm. Data for marine sediments compiled by Plank and Langmuir (1998) also support a lower Rb/Cs ratio of the upper crust. Using the observed Rb/Cs ratio of 15 and a rubidium concentration of 112 ppm, they derived an upper crustal caesium concentration of 7.8 ppm. Although caesium data show only a poor correlation with lanthanum, the apparent La/Cs ratio of sediments led McLennan (2001b) to a revised caesium estimate of 4.6 ppm, which yields an Rb/Cs ratio of 24. Very few data exist for caesium from shield composites. Gao *et al*. determined a value of 3.6 ppm caesium, which is very similar to the estimate of Taylor and McLennan (1985). However, the Gao *et al*. rubidium estimate (83 ppm) is lower than Taylor and McLennan's (112 ppm), leading to an Rb/Cs ratio of 23 in the upper crust of eastern China. Caesium concentrations in all estimates vary by up to 70% and there thus appears to be substantial uncertainty in the upper crust's caesium

concentration. Further evidence for the caesium content of the upper continental crust is derived from loess (see next section).

The upper crustal abundances of *arsenic*, *antimony*, and *tungsten* were determined by Sims *et al*. (1990), based on measurements of these elements in loess and shales. They find As/Ce to be rather constant at 0.08, leading to an arsenic content of 5.1 ± 1 ppm. In a similar fashion they estimate the upper crustal antimony content to be 0.45 ± 0.08 ppm and tungsten to be 3.3 ± 1.1 ppm. The antimony and arsenic values are factors of 2 and 3 higher, respectively, than the values given by Taylor and McLennan (1985), and the tungsten contents are a factor of 2 lower than Taylor and McLennan's (1985), which were adopted from the *Handbook of Geochemistry* (Wedepohl, 1969–1978). For all three elements, the Sims *et al*. estimates lie within uncertainty of the values given by Gao *et al*. (1998a) for the upper crust of eastern China, and these new estimates can thus be considered as representative of the upper crust to within ~30% uncertainty.

For the remaining moderately soluble elements *silver*, *cadmium*, and *bismuth*, there are no data for sedimentary composites. Taylor and McLennan (1985) adopted values from Heinrichs *et al*. (1980) for cadmium and bismuth and from the *Handbook of Geochemistry* (Wedepohl, 1969–1978) for silver. The only other data come from the study of Gao *et al*. (1998a). So essentially there are only two studies that address the concentrations of these elements in the upper crust: Gao *et al*. (1998a) and Wedepohl (1995) (which incorporates data from the *Handbook of Geochemistry* and Heinrichs *et al*. (1980)). For silver and cadmium, the two estimates converge: silver is identical and cadmium varies by 25% between Gao *et al*. and Wedepohl *et al*. estimates. In contrast, bismuth shows a factor of 2 of variation, with the Gao *et al*. estimates being higher.

3.01.2.2.2 Glacial deposits and loess

The concept of analyzing glacial deposits in order to determine average upper crustal composition originated with Goldschmidt (1933, 1958). The main attraction of this approach is that glaciers mechanically erode the rock types that they traverse, giving rise to finely comminuted sediments that represent averages of the bedrock lithologies. Because the timescale between erosion and sedimentation is short, glacial sediments experience little chemical weathering associated with their transport and deposition. In support of this methodology for determining upper crust composition, Goldschmidt noted that the major-element composition of composite glacial loams from Norway (analysed by Hougen *et al*., 1925, as cited in Goldschmidt, 1933, 1958), which sample $\sim 2 \times 10^5$ km^2 of Norwegian upper crust, compares favorably with the average igneous-rock composition determined by Clarke and Washington (1924) (Table 1). It would take another fifty years before geochemists returned to this method of determining upper crustal composition.

More recent studies using glacial deposits to derive average upper-crust composition have focused on the chemical composition of loess—fine-grained eolian sediment derived from glacial outwash plains (Taylor *et al*., 1983; Gallet *et al*., 1998; Peucker-Ehrenbrink and Jahn, 2001; Hattori *et al*., 2003). This can be accomplished in two ways: either using the average composition of loess as representative of the upper continental crust or, if an element correlates with an insoluble element such as lanthanum whose upper concentration is well established, using the average X/La ratio of loess (where "X" is the element of interest), and assuming an upper crustal lanthanum value to determine the concentration of "X" (e.g., McLennan, 2001b). In this and subsequent discussion of loess, we derive upper crustal concentrations for particular elements using this method and assuming an upper crustal lanthanum value of 31 ppm, and compare these to previous estimates for these elements. The quoted uncertainty reflects 1σ on that ratio.

Loess is rich in SiO_2 (most carbonate-free loess has 73 wt.% to 80 wt.% SiO_2 (Taylor *et al*., 1983; Gallet *et al*., 1998), which probably reflects both the preferential eolian transport of quartz into loess and sedimentary recycling processes. This enrichment causes other elemental concentrations to be diluted. In addition, some other elements may be similarly fractionated during eolian processing. For example, loess shows anomalously high concentrations of zirconium and hafnium (Taylor *et al*., 1983; Barth *et al*., 2000), which, like the SiO_2 excess, have been attributed to size sorting through eolian concentration of zircon (Taylor *et al*., 1983). Thus, loess Zr/La and Hf/La are enriched relative to the upper continental crust and cannot be used to derive upper crustal zirconium and hafnium concentrations. In addition, a recent study of rhenium and osmium in loess suggests that osmium contents are enhanced in loess compared to its source regions (Hattori *et al*., 2003). This is explained by Hattori *et al*. (2003) as being due to preferential sampling of the fine sediment fraction by the wind, which may be enriched in mafic minerals that are soft and hence more easily ground to finer, transportable particle sizes. Mafic-mineral enhancement could give rise to similar fractionations between lanthanum and elements that are found primarily in mafic minerals (e.g., nickel, vanadium, scandium, chromium, cobalt, manganese, etc.). In such cases

neither averages nor La/X ratios can be used to determine a reliable estimate of upper crustal composition. However, it is not apparent that eolian processing has significantly fractionated incompatible elements from lanthanum (e.g., barium, strontium, potassium, rubidium, niobium, thorium, etc.) that are not hosted primarily in mafic minerals. Indeed, the close correspondence of the thorium content of the upper crust derived from loess La–Th correlations (10.5 ± 1 ppm; Figure 6) to that deduced from shales (10.7 ppm, Taylor and McLennan, 1985) suggests that upper crustal concentrations of these elements derived from loess La–X correlations are not significantly affected by eolian processing.

Taylor *et al*. (1983), and later Gallet *et al*. (1998), determined the trace-element composition of a variety of loess samples from around the world and found that their REE patterns are remarkably constant and similar to that of average shales (see previous section and Figure 5). Likewise, niobium, tantalum, and thorium show strong positive correlations with the REE (Figure 6; Barth *et al*., 2000; Gallet *et al*., 1998). Thus, it appears that loess provides a robust estimate of average upper crustal composition for insoluble, incompatible trace elements.

Because loess is glacially derived, weathering effects are significantly reduced compared to shales (Taylor *et al*., 1983), raising the possibility that loess may provide robust upper crustal estimates for the more soluble trace elements. However, examination of the major-element compositions of loess shows that all bear the signature of chemical weathering (Gallet *et al*., 1998). Gallet *et al*. attributed this to derivation of

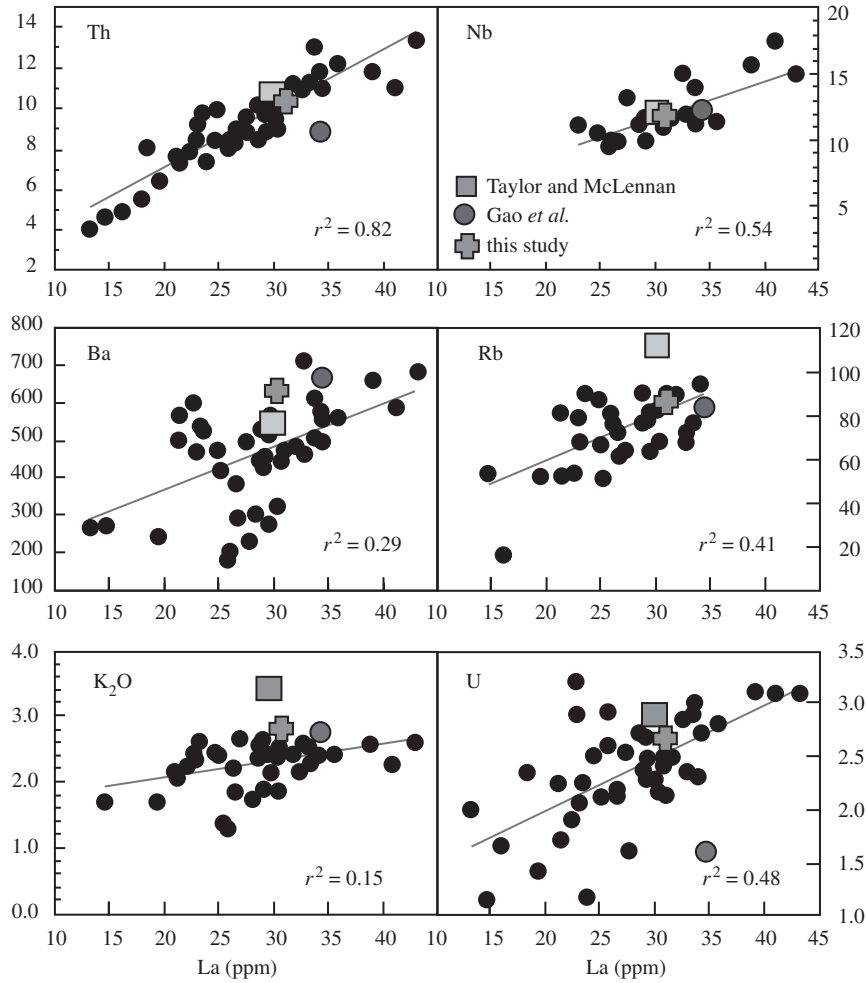

Figure 6 Lanthanum versus moderately to highly soluble incompatible trace elements in loess. Although loess is derived in part from weathered source regions, the positive correlations suggest that weathering has not completely obliterated the original, upper crustal mixing trends. Lines represent linear fit to data. Various models for the average upper crustal composition are superimposed (Taylor and McLennan, 1995, as modified by McLennan, 2001b; Gao *et al*., 1998a and this study—Table 3) (sources Taylor *et al*., 1983; Gallet *et al.,* 1998; Barth *et al*., 2000; Jahn *et al*., 2001; Peucker-Ehernbrink and Jahn, 2001).

loess particles from rocks that had previously experienced sedimentary differentiation. Likewise, Peucker-Ehernbrink and Jahn (2001) noted a positive correlation between $^{87}Rb/^{86}Sr$ and $^{87}Sr/^{86}Sr$ in loess, indicating that the weathering-induced fractionation is an ancient feature, and therefore inherited from the glacially eroded bedrocks. Even so, the degree of weathering in loess, as measured by the "chemical index of alteration" (CIA = molar $Al_2O_3/(Al_2O_3 + CaO + Na_2O + K_2O)$ Nesbit and Young (1984)), is small relative to that seen in shales (Gallet *et al*., 1998), and it is likely that loess would provide a better average upper crustal estimate for moderately soluble trace elements (e.g., arsenic, silver, cadmium, antimony, caesium, barium, tungsten, and bismuth) than shales. Unfortunately, few measurements of these elements in loess are available (Barth *et al*., 2000; Gallet *et al*., 1998; Jahn *et al*., 2001; Taylor *et al*., 1983). Barium data show a scattered, positive correlation with lanthanum, yielding an upper crustal average of 510 ± 139 ppm (Figure 6). This value of barium concentration is similar to the one adopted by Taylor and McLennan (1985) and is within the uncertainty of all the other estimates save those of the Canadian Shield, which are significantly higher (Table 2). Caesium also shows a positive, scattered correlation with lanthanum, yielding an uncertain upper crustal caesium content of 4.8 ± 1.6 ppm, which is similar to that recently suggested by McLennan (2001b). However, caesium shows a better correlation with rubidium (Figure 7), defining an Rb/Cs ratio of ~17 in loess. Thus, if the upper crustal rubidium concentration can be determined, better constraints on the caesium content can be derived.

The highly soluble elements (lithium, potassium, rubidium, strontium, and uranium) show variable degrees of correlation with lanthanum in loess. Strontium shows no correlation with lanthanum, which is likely due to variable amounts of carbonate in the loess samples (Taylor *et al*., 1983). Teng *et al*. (2003) recently reported lithium contents and isotopic compositions of shales and loess. Lithium contents of loess show no correlation with lanthanum, but fall within a limited range of compositions (17–41 ppm), yielding an average of 29 ± 10 ppm ($n = 14$). A similar value is derived using the correlation observed between lithium and niobium in shales. Thus, Teng *et al*. (2002) estimated the upper crustal lithium content at 31 ± 10 ppm, which is within error of previous estimates (Shaw *et al*., 1976; Taylor and McLennan, 1985; Gao *et al*., 1998a).

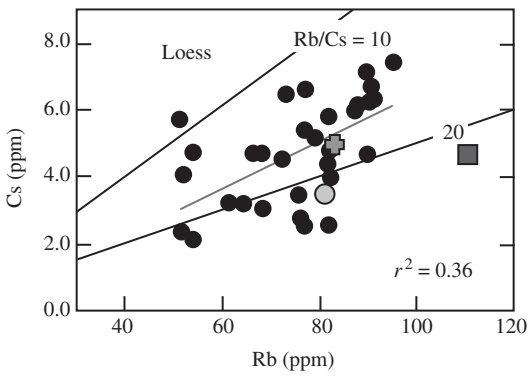

Figure 7 Rubidium versus caesium concentrations in loess samples. Short line is linear regression of data, thin, labeled lines represent constant Rb/Cs ratios. Symbols for crustal models and data sources as in Figure 6.

Potassium and rubidium show scattered, positive correlations with lanthanum (the Rb–La correlation is better, and the K–La is worse than the Ba–La correlation) (Figure 6). These correlations yield an upper crustal rubidium concentration of 84 ± 17 ppm. This rubidium value is identical to those derived from surface sampling by Eade and Fahrig (1973) , Condie (1993), and Gao *et al*. (1998a), but is lower than the widely used value of Shaw *et al*. (1976) at 110 ppm. The latter was adopted by both Taylor and McLennan (1985) and Wedepohl (1995) for their upper crustal estimates. The weak K–La correlation yields an upper crustal K_2O value of 2.4 ± 0.5 wt.%. This is within error of the surface-exposure averages of Fahrig and Eade (1968), Condie (1993), and Gao *et al*. (1998a), but is lower than the Shaw *et al*. surface averages of the Canadian shield (Shaw *et al*., 1967), values for the Russian platform and the value adopted by Taylor and McLennan (1985) based on K/U and Th/U ratios. The loess-derived K/Rb ratio is 238, which is similar to the "well established" upper crustal K/Rb ratio of 250 (Taylor and McLennan, 1985). Because both potassium and rubidium are highly soluble elements, and loess shows evidence for some weathering, the potassium and rubidium contents derived from loess are best viewed as minimum values for the upper crust.

Uranium shows a reasonable correlation with lanthanum (Figure 6), which yields an upper crustal uranium content of 2.7 ± 0.6 ppm. This value is within error of the averages derived from surface exposures, except for the value of Gao *et al*. (1998a) and Eade and Fahrig (1973), which are distinctly lower. The loess-derived K/U ratio of 7,400 is lower than that assumed for the upper crust of 10,000 (Taylor and McLennan, 1985), and may reflect some potassium loss due to weathering, as discussed above.

Peucker-Ehrenbrink and Jahn (2001) analyzed loess in order to determine the concentrations of the platinum-group element (PGE) in the upper

continental crust. To do this they examined PGE-major-element trends and used previously determined major-element compositions of the upper continental crust to infer the PGE concentrations (Table 2). Of the elements analyzed (ruthenium, palladium, osmium, iridium, and platinum), they found positive correlations for ruthenium, palladium, osmium, and iridium with major and trace elements for which upper crustal values had previously been established, leading to suggested upper crustal abundances of 340 ppt, 520 ppt, 31 ppt, and 22 ppt, respectively. They found no correlation between platinum contents and other elements, and so they simply used the average loess platinum content (510 ppt) as representative of the upper continental crust. We have estimated uncertainty on these values (shown in Table 2) by using the 95% confidence limit on the correlations published by Peucker-Ehrenbrink and Jahn (2001) and, for platinum, the standard deviation of the mean (Table 3). Recently, Hattori *et al*. (2003) suggested that preferential sampling of mafic minerals in loess may lead to enhancement of PGE and thus, loess-derived estimates may represent maximum concentrations for the upper crust. Based on samples of glacially derived desert sands and glacial moraines, Hattori *et al*. (2003) estimated an upper crustal osmium abundance of ~10 ppt.

Prior to these studies, few estimates were available for the PGE content of the upper continental crust. Peucker-Ehrenbrink and Jahn's loess-derived palladium value is similar to the value published by Taylor and McLennan (1985), which derives from the *Handbook of Geochemistry* (S. R. Taylor, personal communication), but is a factor of 3 smaller than that determined by Gao *et al*. (1998a) for the upper crust of eastern China. Peucker-Ehrenbrink and Jahn's (2001) loess-derived osmium abundance is ~65% lower than the estimate of Esser and Turekian (1993), which Peucker-Ehrenbrink and Jahn attribute to the hydrogenous uptake of osmium by the riverine sediments used in that study. Furthermore, the desert-sand and glacial moraine-derived osmium value of Hattori *et al*. (2003) is a factor of 3 lower than the estimate of Peucker-Ehrenbrink and Jahn (2001). Peucker-Ehrenbrink and Jahn's (2001) loess-derived iridium content is the same as that published for the Canadian Shield by Shaw *et al*. (1976). Thus, the upper crustal concentration of some PGE may be reasonably well constrained (e.g., palladium and iridium), while considerable uncertainty remains for others (e.g., platinum and osmium).

Rhenium is a highly soluble element that is easily leached during weathering, so the rhenium abundances of loess cannot be used directly to infer its upper crustal abundance. Following Esser and Turekian (1993), Peucker-Ehrenbrink and Jahn (2001) used the average $^{187}Os/^{188}Os$ ratio, osmium concentration, and average neodymium-model age of the crust to calculate the rhenium content of the upper continental crust. Their value (198 ppt) is about half that reported in Taylor and McLennan (1985) and calculated by Esser and Turekian (1993), who used the higher osmium abundance in their calculation. Using a similar methodology and osmium-isotopic composition, and the lower osmium abundance determined for glacially derived desert sands, Hattori *et al*. (2003) determined an upper crustal $^{187}Re/^{188}Os$ ratio of 35, which (assuming an average neodymium model age of 2.2 Ga for the crust) corresponds to a rhenium content of 74 ppt, about a third of the concentration determined by Peucker-Ehrenbrink and Jahn from loess data. Sun *et al*. (2003) used the rhenium contents of undegassed arc lavas to estimate the rhenium content of the bulk continental crust, assuming that the crust grows primarily by arc accretion. Their value of 2.0 ± 0.1 ppb is over an order of magnitude higher than that estimated by Peucker-Ehrenbrink and Jahn (2001) and Hattori *et al*. (2003) and is ~5 times higher than the Esser and Turekian (1993) and Taylor and McLennan (1985) values. Because rhenium is a moderately incompatible element, the rhenium concentration of the upper crust should be comparable to or higher than the bulk crust value (similar to ytterbium). However, this extreme rhenium concentration would require an order of magnitude higher osmium concentration in the crust or an extremely radiogenic crust composition, neither of which are consistent with any current estimates. Sun *et al*. (2003) suggest that rhenium may be lost from the continents by either rhenium degassing during arc volcanism or continental rhenium deposition into anoxoic sediments that are recycled into the mantle. Thus the value of 2 ppb rhenium is a maximum value for the upper continental crust and our knowledge of the rhenium content of the upper crust remains uncertain.

3.01.2.3 An Average Upper-crustal Composition

In Table 3 we present our best estimate for the chemical composition of the upper continental crust. The footnote provides detailed information on how the value for each element was derived. In general, major-element values represent averages of the different surface-exposure studies, and errors represent one standard deviation of the mean. Because two independent studies are available for the Canadian Shield, and because it appears the Canadian Shield has lower abundances of mafic lithologies and higher abundances of sodium-rich tonalitic–trondhjemitic granitic gneisses compared to other areas (see Section 3.01.2.1),

Table 3 Recommended composition of the upper continental crust. Major elements in weight percent.

Element	*Units*	*Upper crust*	*1 Sigma*	*%*	*Source*[a]	*Element*	*Units*	*Upper crust*	*1 Sigma*	*%*	*Source*[a]
SiO_2	wt.%	66.6	1.18	2	1	Ag	ng g^{-1}	53	3	5	4
TiO_2	”	0.64	0.08	13	2	Cd	μg g^{-1}	0.09	0.01	15	4
Al_2O_3	”	15.4	0.75	5	1	In	”	0.056	0.008	14	4
FeO_T	”	5.04	0.53	10	1	Sn	”	2.1	0.5	26	14
MnO	”	0.10	0.01	13	1	Sb	”	0.4	0.1	28	12
MgO	”	2.48	0.35	14	1	I	”	1.4		50	5
CaO	”	3.59	0.20	6	1	Cs	”	4.9	1.5	31	15
Na_2O	”	3.27	0.48	15	1	Ba	”	628	83	13	16
K_2O	”	2.80	0.23	8	3	La	”	31	3	9	4
P_2O_5	”	0.15	0.02	15	1	Ce	”	63	4	6	4
Li	μg g^{-1}	24	5	21	11	Pr	”	7.1			4
Be	”	2.1	0.9	41	4	Nd	”	27	2	8	4
B	”	17	8	50	4	Sm	”	4.7	0.3	6	4
N	”	83			5	Eu	”	1.0	0.1	14	4
F	”	557	56	10	4	Gd	”	4.0	0.3	7	4
S	”	62	33	53	4	Tb	”	0.7	0.1	21	4
Cl	”	370	382	103	4	Dy	”	3.9			17
Sc	”	14.0	0.9	6	6	Ho	”	0.83			17
V	”	97	11	11	6	Er	”	2.3			4
Cr	”	92	17	19	6	Tm	”	0.30			17
Co	”	17.3	0.6	3	6	Yb	”	1.96	0.4	18	4
Ni	”	47	11	24	6	Lu	”	0.31	0.05	17	4
Cu	”	28	4	14	7	Hf	”	5.3	0.7	14	4
Zn	”	67	6	9	7	Ta	”	0.9	0.1	13	11
Ga	”	17.5	0.7	4	8	W	”	1.9	1	54	18
Ge	”	1.4	0.1	9	4	Re	ng g^{-1}	0.198			13
As	”	4.8	0.5	10	9	Os	”	0.031	0.009	29	13
Se	”	0.09	0.05	54	4	Ir	”	0.022	0.007	32	13
Br	”	1.6			5	Pt	”	0.5	0.5	95	13
Rb	”	84	17	20	10	Au	”	1.5	0.4	26	4
Sr	”	320	46	14	4	Hg	μg g^{-1}	0.05	0.04	76	4
Y	”	21	2	11	4	Tl	”	0.9	0.5	57	4
Zr	”	193	28	14	4	Pb	”	17	0.5	3	4
Nb	”	12	1	12	11	Bi	”	0.16	0.06	38	19
Mo	”	1.1	0.3	28	12	Th	”	10.5	1.0	10	20
Ru	ng g^{-1}	0.34	0.02	6	13	U	”	2.7	0.6	21	20
Pd	”	0.52	0.02	3	13		”				

[a] Sources: (1) Average of all surface exposure data from Table 1, excluding Shaw *et al*. (1967), which is replicated by Fahrig and Eade (1968). (2) As (1) above, but including sediment-derived data from Plank and Langmuir (1998) and McLennan (2001b). (3) As (1) above, but also including K_2O value derived from loess (see text). (4) Average of all values in Table 2, excluding Wedepohl (1995) value or Taylor and McLennan (1985) value for Au, if it is derivitive from Shaw *et al*. (1976) and Taylor and McLennan (1985). (5) Wedepohl (1995). (6) Average of all surface composite data in Table 2, excluding Shaw *et al*. (1976), and including additional data from sediments (McLennan, 2001b). (7) Average of all surface composite data in Table 2, excluding Shaw *et al*. (1976), and including Taylor and McLennan (1985) values. (8) Average of all surface composite data in Table 2, excluding Shaw *et al*. (1976) due to their fractionated Ga/Al ratio. (9) Average of sedimentary data from Table 2 (Sims *et al*., 1990) and Gao *et al*. (1998a) surface averages. (10) Dervied from La/Rb correlation in loess (see text). Value is identical to surface exposure data except for the Shaw *et al*. (1976) values. Data from Handbook of Geochemistry are about a factor of 2 lower than the latter and are not included in the average. (11) Average of all surface exposure data in Table 2 (minus Shaw *et al*. (1976), values) plus data from sediments and loess (Plank and Langmuir, 1998; Barth *et al*., 2000; McLennan, 2001b; Teng *et al*., 2003). (12) Average of all data in Table 2, excluding Taylor and McLennan (1985), which derive from same source as Wedephol's. (13) From Peucker-Ehrenbrink and Jahn (2001); see text for origin of error estimates. (14) Average of all data in Table 2, excluding Taylor and McLennan (1985), which is a factor of two higher than all other estimates. (15) Derived from Rb/Cs = 17 and upper crustal Rb value (see text). (16) Average of all data in Table 2, excluding the Shaw *et al*. (1976) and including additional data from loess (see text). (17) Value interpolated from REE pattern. (18) Average of all values in Table 2, plus correlation from Newsom *et al*. (1996), assuming W/Th = 0.2 (19) Average of all values in Table 2, excluding the Shaw *et al*. (1976) value, which is a factor of 5 lower than the others. (20) From loess correlations with La (see text). Both values are within error of the average of all surface exposure data and other sedimentary data (Taylor and McLennan, 1985; McLennan, 2001b).

we include only values from one of these studies—the Fahrig and Eade (1968) study, which encompasses a greater number of samples compared to that of Shaw *et al*. (1967). We also incorporate TiO_2 values derived from recent sedimentary studies (McLennan, 2001b; Plank and Langmuir, 1998) and the K_2O value from loess (Section 3.01.2.2) into the upper crustal averages (note that including the latter value in the average does not significantly change it). The standard deviation for most major-element averages is 10% or less. Only the ferromagnesian elements (iron, manganese, magnesium, and titanium), Na_2O, and P_2O_5 vary by up to 15%.

The trace-element abundances shown in Table 3 derive from different methods depending on their solubility. For most insoluble elements (see Section 3.01.2.2 and Figure 4 for definitions of solubility), we average the surface composites in addition to sediment or loess-derived estimates to derive the upper crustal composition. The uncertainty reported represents 1σ from the mean of all estimates. For moderately and highly soluble elements, we use the data derived from loess, if the elements show correlations with lanthanum ($r^2 > 0.4$), to infer their concentrations. In this case, the error represents the SD of the X/La ratio (where X is the element of interest). For elements that show no or only a poor correlation with lanthanum in loess and sediments (e.g., K_2O, Li, Ba, and Sr), we use the average of surface composites and sedimentary data (if some correlations exist with lanthanum) to derive an average. In most cases, the loess or sediment-derived values are within error of the surface-composite averages and these are noted in the footnote. Caesium is a special case. The loess caesium data show a poor correlation with lanthanum, but good correlation with rubidium. We thus use the observed Rb/Cs ratio of 17 (which is similar to the previous determination of this ratio in sedimentary rocks (McDonough *et al*., 1992)) and the upper crustal rubidium concentration of 84 ppm to derive the caesium concentration of 4.9 ppm in the upper crust. The error on this estimate derives from the standard deviation of the Rb/Cs ratio. For some elements, only single estimates are available (e.g., bromine, nitrogen, iodine), and these are adopted as reported. The uncertainty of these estimates is likely to be very high, but there is no way to estimate uncertainty quantitatively with such few data. Remarkably, the SD on a large number of trace elements is below 20%, and the concentrations of a few (flourine, scandium, vanadium, cobalt, zinc, gallium, germanium, arsenic, yttrium, niobium, LREEs, tantalum, lead, and thorium) would appear to be known within ~10% (Table 3). However, in a number of these cases (e.g., flourine, cobalt, gallium, germanium, and arsenic), the small uncertainties undoubtedly reflect the fact that there have been few independent estimates made of the upper crust composition for these elements. It is likely that the true uncertainty for these elements is considerably greater than expressed in Table 3.

The upper crustal composition in Table 3 has many similarities to the widely used estimate of Taylor and McLennan (1985, with recent revision by McLennan (2001b)), but also some notable differences (Figure 8). Most of the elements that vary by more than 20% from the estimate of Taylor and McLennan are elements for which new data are recently available and few data exist overall (i.e., beryllium, arsenic, selenium, molybdenum, tin, antimony, rhenium, osmium, iridium, thallium, and bismuth). However, a number of estimates exist for K_2O, P_2O_5, and rubidium contents of the upper crust and our estimates are significantly lower (by 20–40%) than Taylor and McLennan's upper crust. The difference in P_2O_5 may simply be due to rounding errors. Taylor and McLennan (1985) report P_2O_5 of 0.2 wt.% versus 0.15 wt.% in our and other estimates of the upper crust—Tables 2 and 3). Taylor and McLennan (1985) derived their upper crustal K_2O indirectly from thorium abundances by assuming $Th/U = 3.8$ and $K/U = 10{,}000$. The resulting K_2O value is the highest of any of the estimates

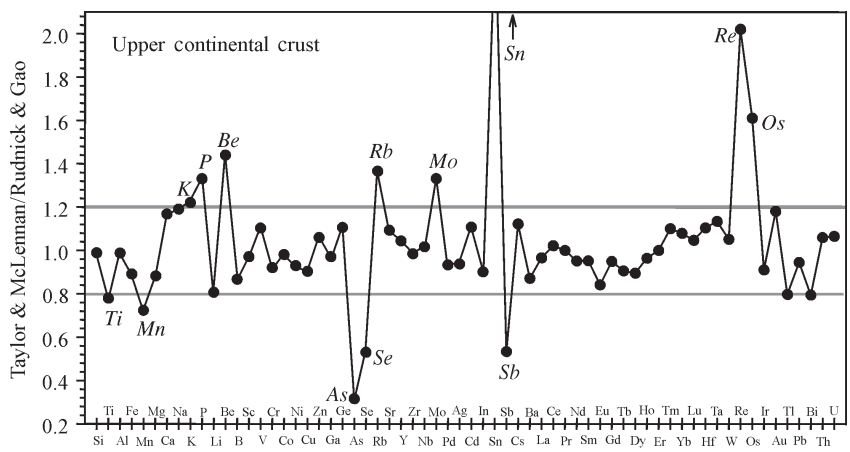

Figure 8 Plot of upper crustal compositional estimate of Taylor and McLennan (1995) (updated with values from McLennan, 2001b), divided by recommended values from this study. Horizontal lines mark 20% variation. Most elements fall within the ±20% bounds; elements falling beyond these bounds are labeled. Of the elements that differ by over 20%, potassium and rubidium are probably the most significant, since these elements are commonly analyzed to high precision in crustal rocks.

(Table 2 and Figure 2). Likewise, Taylor and McLennan's rubidium value was determined from their K_2O content, assuming a K/Rb ratio of the upper crust of 250. Their rubidium concentration matches the Canadian Shield value of Shaw *et al*. (1976), but is higher than all other surface-exposure studies, including Fahrig and Eade's Canadian Shield estimate (Table 2 and Figure 3). In contrast, the remaining surface-exposure studies match the rubidium value we derived from the loess Rb–La correlation (Figure 6). We conclude that the upper crust may have lower potassium and rubidium contents than estimated by Taylor and McLennan (1985). This finding has implications for total crustal heat production (see Section 3.01.4 and Chapter 3.02).

3.01.3 THE DEEP CRUST

The deep continental crust is far less accessible than the upper crust and consequently, estimates of its composition carry a greater uncertainty. Compared to the upper crust, the earliest estimates of the composition of the deep crust are relatively recent (i.e., 1950s and later) and derive from both seismological and geological studies.

On the basis of observed isostatic equilibrium of the continents and a felsic upper crust composition, Poldervaart (1955) suggested a two-layer crust with granodioritic upper crust underlain by a basaltic lower crust. The topic of deep crustal composition doesn't seem to have been considered again until ~20 years later, when a series of works in the 1970 s and 1980 s made significant headway into the nature of the deep continental crust. On the basis of surface heat-flow, geochemical studies of high-grade metamorphic rocks and seismological data, Heier (1973) proposed that the deep crust is composed of granulite-facies rocks that are depleted in heat-producing elements. A similar conclusion was reached by Holland and Lambert (1972) based on their studies of the Lewisian complex of Scotland. Smithson (1978) used seismic reflections and velocities to derive both structure and composition of the deep crust. He divided the crust into three, heterogeneous regions: (i) an upper crust composed of supracrustal metamorphic rocks intruded by granites, (ii) a migmatitic middle crust and (iii) a lower crust composed of a heterogenous mixture of igneous and metamorphic rocks ranging in composition from granite to gabbro, with an average intermediate (dioritic) composition. This three-layer model of the crust survives today in most seismologically based studies. Weaver and Tarney (1980, 1981, 1984) derived a felsic and intermediate composition for the Archean middle and lower crust, respectively, based on studies of amphibolite to granulite-facies rocks exposed in the Lewisian complex, Scotland. R. W. Kay and S. M. Kay (1981) were one of the first to stress the importance of xenolith studies to unravelling deep-crustal composition. They highlighted the heterogeneous nature of the deep crust and suggested its composition should vary depending on tectonic setting, cautioning against the use of singular cross sections or deep-crustal exposures to derive global models. Taylor and McLennan (1985) considered the lower crust to be the portion of the crust from 10 km depth to the Moho. Their "lower crust" thus includes both middle and lower crust, as used here (see Section 3.01.3.1). Taylor and McLennan's (1985) lower-crust composition was derived by subtracting the upper crust from their total-crust composition (see Section 3.01.4). The Taylor and McLennan (1985) lower crust is thus not based on observed lower crustal rock compositions, but rather on models of upper- and total-crust compositions and assumptions about the origin of surface heat flow.

More recent attempts to define deep crust composition have relied upon linking geophysical data (principally seismic velocities) to deep crustal lithologies and their associated compositions to derive the bulk composition of the deep crust as a function of tectonic setting (Christensen and Mooney, 1995; Rudnick and Fountain, 1995; Wedepohl, 1995; Gao *et al*., 1998a,b). Despite the attendant large uncertainties in deriving composition from velocity (Rudnick and Fountain, 1995; Brittan and Warner, 1996, 1997; Behn and Kelemen, 2003) and the lack of thorough geochemical sampling of the deep crust in many regions, these efforts nevertheless provide the best direct estimates of present-day deep crustal composition.

In this section we examine the composition of the deep crust by first defining its structure and lithology and the methods employed to determine deep crust composition. We then examine observations on middle and lower crustal samples, average seismic velocities and the resulting models of deep crust composition.

3.01.3.1 Definitions

Following recent compilations of the seismic-velocity structure of the continental crust, we divide the deep crust into middle and lower crust (Holbrook *et al*., 1992; Christensen and Mooney, 1995; Rudnick and Fountain, 1995). Holbrook *et al*. (1992) defined the middle crust as: (i) the middle-third, where the velocity structure suggests a natural division of the crust into thirds; (ii) the region beneath the upper crust and above a Conrad discontinuity, if there is a layer beneath the Conrad; and (iii) the region immediately beneath the Conrad if there are two distinct velocity layers beneath a Conrad discontinuity.

The lower crust is thus the layer beneath the middle crust and above the Moho.

For a ~40 km thick average global continental crust (Christensen and Mooney, 1995; Rudnick and Fountain, 1995), the middle crust is 11 km thick and ranges in depth from 12 km, at the top, to 23 km at the bottom (Gao *et al.* (1998b) based on the compilations of data for crustal structure in various tectonic settings by Rudnick and Fountain (1995)). The average lower crust thus begins at 23 km depth and is 17 km thick. However, the depth and thickness of both middle and lower crust vary from setting to setting. In fore-arcs, active rifts, and rifted margins, the crust is generally thinner: middle crust extends from 8 km to 17 km depth and lower crust from 17 km to 27 km depth. In Mesozoic–Cenozoic orogenic belts the crust is thicker and middle crust extends from 16 km to 27 km depth and the lower crust from 27 km to 51 km depth (Rudnick and Fountain, 1995).

3.01.3.2 Metamorphism and Lithologies

Studies of exposed crustal cross-sections and xenoliths indicate that the middle crust is dominated by rocks metamorphosed at amphibolite facies to lower granulite facies, while the lower crust consists mainly of granulite facies rocks (Fountain *et al.*, 1990a; Fountain and Salisbury, 1981; Mengel *et al.*, 1991; Weber *et al.*, 2002). However, exceptions to these generalities do occur. For thin crust in rifted areas, greenschist-facies and amphibolite-facies rocks may predominate in the middle and lower crust, respectively. In overthickened Mesozic and Cenozoic orogenic belts (e.g., Alps, Andes, Tibet, and Himalyas), and paleo-orogenic belts that now have normal crustal thicknesses (e.g., Appalachains, Adirondacks, Variscan belt), granulite-facies and eclogite-facies rocks may be important constituents of the middle and lower crust (Leech, 2001; LePichon *et al.*, 1997; Lombardo and Rolfo, 2000). In contrast, amphibolite-facies lithologies may be present in the deep crust of continental arcs (Aoki, 1971; Miller and Christensen, 1994; Weber *et al.*, 2002), where hydrous fluids are fluxed from the subducting slab and the water contents of underplating magmas are high.

Lithologically, both middle and lower crust are highly heterogeneous, as seen in surface exposures of high-grade metamorphic rocks, crustal cross-sections, and deep-crustal xenolith suites. However, there is a general tendency for the middle crust to have a higher proportion of evolved rock compositions (as observed in cross-sections and granulite-facies terranes) while the lower crust has a higher proportion of mafic rock types (as observed in xenolith suites (Bohlen and Mezger, 1989)). Metasedimentary lithologies are often present, albeit in small proportions. The exact proportions of felsic to mafic lithologies in the deep crust varies from place to place and can only be established through the study of crustal cross-sections or inferred from seismic velocity profiles of the crust (Christensen and Mooney, 1995; Rudnick and Fountain, 1995; Wedepohl, 1995; Gao *et al.*, 1998b).

3.01.3.3 Methodology

There are three approaches to derive the composition of the deep crust (see Rudnick and Fountain (1995) for a review).

(i) *By studying samples derived from the deep crust*. These occur as surface outcrops of high-grade metamorphic terranes (e.g., Bohlen and Mezger, 1989; Harley, 1989), tectonically uplifted crustal cross-sections (e.g., Fountain and Salisbury, 1981; Percival *et al.*, 1992), and as deep-crustal xenoliths carried in volcanic pipes (Rudnick, 1992; Downes, 1993).

(ii) *By correlating seismic velocities with rock lithologies* (Christensen and Mooney, 1995; Rudnick and Fountain, 1995; Wedepohl, 1995, Gao *et al.*, 1998a,b).

(iii) From surface heat-flow measurements (see Chapter 3.02).

As pointed out by Jaupart and Mareschal (see Chapter 3.02), surface heat flow is the only geophysical parameter that is a direct function of crustal composition. In general, however, heat flow provides only very broad constraints on deep-crust composition due to the ambiguity involved in distinguishing the amount of surface heat flow arising from crustal radioactivity versus the Moho heat flux (see Chapter 3.02); Rudnick *et al.*, 1998). Most models of the deep-crust composition fall within these broad constraints. The exception is the global model of Wedepohl, 1995, which produces more heat than the average surface heat flow in the continents, thereby allowing no mantle heat flux into the base of the crust (Rudnick *et al.*, 1998). In addition, the regional model of Gao *et al.* (1998a) for eastern China produces too much heat to be globally representative of the continental crust composition (see discussion in Rudnick *et al.* (1998) and Jaupart and Mareschal (Chapter 3.02)). However, the Gao *et al.* composition may be representative of the continental crust of eastern China, where the crust is relatively thin (30–35 km) and the heat flow is high (>60 mW m^{-2}). In the remaining discussion of deep-crust composition, we rely most heavily on methods (i)–(ii), above, but return to the question of heat flow when considering the bulk crust composition in Section 3.01.4.

In addition to mineralogy, which is in turn a function of bulk composition and metamorphic

grade, factors affecting the seismic velocities of the continental crust include temperature, pressure, and the presence or absence of volatiles, fractures, and mineralogical anisotropy. It is generally assumed that cracks and fractures are closed under the ambient confining pressures of the middle to lower crust (0.4–1.2 GPa). In addition, although evidence for volatile transport is present in many rocks derived from the deep crust (see Chapters 3.06 and 3.09), the low density of these fluids allows for their escape to the upper crust shortly after their formation. Hence, most studies assume the deep crust does not, in general, contain an ambient, free volatile phase (Yardley, 1986).

Some minerals are particularly anisotropic with respect to seismic-wave speeds (e.g., olivine, sillimanite, mica (Christensen, 1982)), which can lead to pronounced seismic anisotropy in rocks if these minerals are crystallographically aligned through deformational processes (Meltzer and Christensen, 2001). This, in turn, could lead to over- or underestimation of representative seismic velocities of the deep crust if deformed rocks with such anisotropic minerals occur there. Olivine is not commonly stable in the deep crust, but other strongly anisotropic minerals are (e.g., mica, which is predominantly stable in the middle crust, and sillimanite, which is found in metapelitic rocks in the middle-to-lower crust). Some of the largest seismic anisotropies have been recorded in mica schists and gneisses, which can have average anisotropies over 10% (Christensen and Mooney, 1995; Meltzer and Christensen, 2001). Amphibole is also anisotropic and the average anisotropies for amphibolite are also ~10% (Christensen and Mooney, 1995; Kern *et al*., 1996). In general, anisotropy is expected to be highest in metapelitic rocks and amphibolites, which contain the highest proportions of anisotropic minerals. These lithologies appear to be subordinate in middle-crustal sections and outcrops (described in the next section) compared to felsic gneisses, which typically have low anisotropies (<5%). In contrast, studies of xenoliths show metapelite to be a common lithology in the lower crust, albeit proportionally minor, and amphibolite may be important in some regions (Section 3.01.3.5.1). Thus, seismic anisotropy could be especially important in regions having large amounts of metasedimentary rocks (e.g., accretionary wedges) and amphibolite (arc crust?) in the deep crust, but is less likely to be important in crust dominated by felsic metaigneous rocks or mafic granulites.

Changes in *P*-wave velocity of a rock as a function of temperature and pressure are generally assumed to be on the order of -4×10^{-4} km s^{-1} °C^{-1} and 2×10^{-4} km s^{-1} MPa^{-1} (see Rudnick and Fountain (1995 and references therein). Because most laboratory measurements of ultrasonic velocities are carried out at confining pressures of 0.6–1.0 GPa, no pressure correction needs to be made in order to compare field and laboratory-based velocity measurements. However, temperature influence on seismic-wave speeds can be significant, especially when comparing laboratory data collected at room temperature to field-based measurements in areas of high heat flow (e.g., rifts, arcs, extentional settings). The decrease in compressional wave velocities in the deep crust under these high geotherms can be as much as 0.3 km s^{-1} (see Rudnick and Fountain, 1995, figure 1). For these reasons, Rudnick and Fountain (1995) used regional surface heat flow and assumed a conductive geothermal gradient, to correct the field-based velocities to room-temperature conditions. In this way, direct comparisons can be made between velocity profiles and ultrasonic velocities of lower-crustal rock types measured in the laboratory. Another benefit of this correction is that deep-crustal velocities from areas with grossly different geotherms can be considered directly in light of possible lithologic variations. In subsequent sections we quote deep-crustal velocities corrected to room-temperature conditions as "temperature-corrected velocities."

3.01.3.4 The Middle Crust

3.01.3.4.1 Samples

The best evidence for the compositional makeup of the middle crust comes from studies of high-grade metamorphic terranes and crustal cross-sections. There are far fewer studies of amphibolite-facies xenoliths derived from mid-crustal depths (Grapes, 1986; Leeman *et al*., 1985; Mattie *et al*., 1997; Mengel *et al*., 1991; Weber *et al*., 2002) compared to their granulite-facies counterparts. This may be due to the fact that it can be difficult to distinguish such xenoliths from the exposed or near-surface amphibolite-facies country rocks through which the xenolith-bearing volcanic rocks erupted. For this reason, xenolith studies have not been employed to any large extent in understanding the composition of the middle crust, and most information about the middle crust comes from studies of high-grade terranes, crustal cross-sections, and seismic profiles.

Interpreting the origin of granulite-facies terranes and hence their significance towards determining deep-crustal composition depends on unraveling their pressure–temperature–time history (see Chapters 3.07 and 3.08). Those showing evidence for a "clockwise" *P*–*T* path (i.e., heating during decompression) are often interpreted as having been only transiently in the lower crust; they represent upper crustal

assemblages that passed through high $P-T$ conditions on their way back to the surface during continent-scale collisional orogeny. In contrast, granulite terrains showing evidence for isobaric cooling can have extended lower-crustal histories, and thus may shed light on deep-crustal composition (see discussion in Rudnick and Fountain (1995)). Bohlen and Mezger (1989) pointed out that isobarically cooled granulite-facies terranes show evidence of equilibration at relatively low pressures (i.e., $\leq$0.6–0.8 GPa), corresponding to mid-crustal depths ($\leq$25 km). Although a number of high-pressure and even ultra-high-pressure metamorphic belts (Chapter 3.09) have been recognized since their study, it remains true that the majority of isobarically cooled granulite-facies terranes show only moderate equilibration depths and, therefore, may provide evidence regarding the composition of the middle crust.

Although lithologically diverse, the average composition of rocks analyzed from granulite terrains is evolved (Rudnick and Presper, 1990), with median compositions corresponding to granodiorite/dacite (64–66 wt.% SiO_2, 4.1–5.2 wt.% $Na_2O + K_2O$, based on classification of Le Bas and Streckeisen (1991)). Rudnick and Fountain (1995) suggested that isobarically cooled granulite terrains have a higher proportion of mafic lithologies than granulites having clockwise $P-T$ paths. However, the median composition of rocks analyzed from isobarically cooled terranes is indistinguishable (62 wt.% SiO_2, 4.6 wt.% $Na_2O + K_2O$) from the median composition of the entire granulite-terrane population given in Rudnick and Presper (1990). Collectively, these data point to a chemically evolved mid-crustal composition.

Observations from crustal cross-sections also point to an evolved mid-crust composition (Table 4). Most of these cross-sections have been exposed by compressional uplift due to thrust faulting (e.g., Kapuskasing, Ivrea, Kohistan, and Musgrave). Other proposed origins for the uplift include wide, oblique transitions (Pikwitonei), impactogenesis (Vredefort), and transpression (Sierra Nevada) (Percival *et al*., 1992). In nearly all these sections, sampling depth ranges from upper to middle crust; only a few (e.g., Vredefort, Ivrea, Kohistan) appear to penetrate into the lower crust. In the following paragraphs we review the insights into middle (and lower) crust lithologies gained from the studies of these crustal cross-sections.

The Vredefort dome represents a unique, upturned section through ~36 km of crust of the Kaapvaal craton, possibly exposing a paleo-Moho at its base (Hart *et al*., 1981, 1990; Tredoux *et al*., 1999; Moser *et al*., 2001). The origin of this structure is debated, but one likely scenario is that it was produced by crustal rebound following meteorite impact. The shallowest section of basement (corresponding to original depths of 10–18 km depth) is composed of amphibolite-facies rocks consisting of granitic gneiss (the outer granite gneiss). The underlying granulite-facies rocks (original depths of 18–36 km) are composed of charnockites and leucogranofels with ~10% mafic and ultramafic granulites (the Inlandsee Leucogranofels terrain). The mid-crust, as defined here, is thus composed of amphibolite-facies felsic gneisses in fault contact with underlying charnockites and mixed felsic granulites and mafic/ultramafic granulites (Hart *et al*., 1990). The lower crust, which is only partially exposed, consists of mixed felsic and mafic/ultramafic granulites, with the proportion of mafic rocks increasing with depth. The mantle beneath the proposed paleo-Moho, as revealed by borehole drilling, is dominated by 3.3–3.5 Ga serpentinized amphibole-bearing harzburgite (Tredoux *et al*., 1999).

The Kapuskasing Structural Zone represents an exposed middle-to-lower crustal section through a greenstone belt of the Archean Canadian Shield, where the middle crust is represented by the amphibolite-facies Wawa gneiss dome and lower granulite-facies litihologies along the Kapuskasing uplift. Altogether, ~25 km of crust are exposed out of a total crustal thickness of 43 km (Fountain *et al*., 1990b; Percival and Card, 1983). The Wawa gneiss dome is dominated by tonalite–granodiorite gneisses and their igneous equivalents (87%), but also contains small amounts of paragneiss (5%) and mafic gneiss and intrusives (8%) (Burke and Fountain, 1990; Fountain *et al*., 1990b; Shaw *et al*., 1994). The slightly deeper-level Kapuskasing Structural Zone has a greater proportion of paragneisses and mafic lithologies. It contains 35% mafic or anorthositic gneisses, 25% dioritic gneisses, 20% paragneiss, and only 20% tonalite gneisses.

Like the high-grade rocks of the Kapusksasing Structural Zone, those in the Pikwitonei crustal cross-section represent high-grade equivalents of granite–gneiss–greenstone successions (Fountain and Salisbury, 1981; Percival *et al*., 1992). Approximately 25 km of upper-to-middle crust is exposed in this section out of a total-crustal thickness of 37 km (Fountain *et al*., 1990b). Both amphibolite- and granulite-facies rocks are dominated by tonalitic gneiss with minor mafic gneiss, and metasedimentary rocks.

The Wutai–Jining Zone is suggested to be an exposed cross-section through the Archean North China craton (Kern *et al*., 1996). Rocks from this exposure equilibrated at depths of up to ~30 km, thus sampling middle and uppermost lower crust, but leaving the lowermost 10 km of crust unexposed (Kern *et al*., 1996). Like the previously described cross-sections, felsic gneisses dominate

Table 4 Chemical and petrological composition of crustal cross-sections.

	Reference[a]	*Age*	*Setting, (uplift origin)*[b]	*Current crustal thickness* (km)	*Maximum depth* (km)	*Middle crust lithologies*	*Lower crust lithologies*
Archean							
Vredefort Dome	1–3	2.6–3.6 Ga	Kaapvaal craton, (3)	36	36 (w/paleo Moho)	Amphibolite-facies granitic gneiss	Granulite-facies charnockites, leucogranofels, mafic, and ultramafic granulites
Kapuskasing Uplift	4–5	2.5–2.7 Ga	Superior craton, (1)	43	25	*Amphibolite-facies* *87% felsic* 8% mafic-intermediate 5% metasediment	*Lower granulite-facies* *35% mafic/anorthositic* 25% diorite 20% metasediments 20% felsic
Pikwitonei granulite domain	6–9	2.5–3.1 Ga	Superior craton, (2)	37	25	*Amphibolite-lower granulite facies.* Dominately tonalite gneiss, minor mafic gneisses, quartzites, anorthosites.	*Granulite-facies*. Predominantly silicic to intermediate gneiss, with minor paragneiss, mafic-ultramafic bodies and anorthosites
Wutai-Jining zone	10	2.5–2.8 Ga	North China Craton, (2)	40	30	*Amphibolite-lower granuilte facies.* *89% tonalitic-trondhjemitic-granodioritic-granitic gneiss* 8% amphibolite and mafic granulite 3% metapelite	*Granulite-facies.* *54% tonalitic-trondhjemitic-granodioritic-granitic gneiss* 32% mafic granulite 6% metapelite 8% metasandstone
Proterozoic							
Musgrave ranges	6, 8, 11	1.1–2.0 Ga	Central Australia, (1)	40	Unknown	Quartzofeldspathic gneiss, amphibolite, metapelite, marble, calc-silicate gneiss	Silicic to intermediate gneiss, mafic granulite, layered mafic-ultramafic intrusions
S. Norway	12–13	1.5–2.0 Ga	Baltic Shield, (2)	35	Unknown	Quartzofeldspathic gneiss, amphibolite, metasediments	Felsic granulite, mafic granulite, metasediments
Phanerozoic							
Ivrea-Verbano zone	14–17	Permian	Alps, (1)	35	30	*Amphibolite-facies.* felsic gneiss, amphibolite, metapelite (kinzigite), marble	*Granulite facies.* mafic intrusives and ultramafic cumulates, resistic metapelite (stronalite), diorite
Sierra Nevada, California	8, 18–20	Cretaceous	Continental arc, (4)	27–43	30	Mafic to felsic gneiss, amphibolite, diorite–tonalite	Granofels, mafic granulite, graphite-bearing metasediments
Kohistan, Pakistan	8, 21	Late Jurassic-Eocene	Oceanic arc, (1)	Unknown	45	Diroite, metadiorite, gabbronorite	Amphibolite, metagabbro, gabbronorite, garnet gabbro, garnet hornblendite, websterite
Talkeetna, Alaska	22–23	Jurassic	Oceanic arc, (1)	25–35	13	Gabbro, tonalite, diorite	Garnet gabbro, amphibole gabbro, dunite, wehrlite, pyroxenite

[a] References: 1. Hart *et al.* 1990, 2. Tredoux *et al.*, 1999, 3. Moser *et al.*, 2001, 4. Fountain *et al.*, 1990a, 5. Shaw *et al.*, 1994, 6. Fountain and Salisbury, 1981, 7. Fountain *et al.*, 1987, 8. Percival *et al.*, 1992, 9. Fountain and Salisbury 1995, 10. Kern *et al.*, 1996, 11. Clitheroe *et al.*, 2000, 12. Pinet and Jaupart, 1987, 13. Alirezaei and Cameron, 2002, 14. Mehnert, 1975, 15. Fountain, 1976, 16. Voshage *et al.*, 1990, 17. Mayer *et al.*, 2000, 18. Ross, 1985, 19. Saleeby, 1990, 20. Ducea, 2001, 21. Miller and Christensen, 1994, 22. Pearcy *et al.*, 1990, 23. see Chapter 3.18. [b] The different mechanisms responsible for uplift of these crustal cross sections include (1) compressional uplifts along thrust faults, (2) wide, oblique transitions, which are also compressional in origin, but over wide transitions, with no one thrust fault obviously responsible for their uplift, (3) meteorite impact, and (4) transpressional uplifts, which are vertical uplifts along a transcurrent faults (Percival *et al.*, 1992).

the middle crust; tonalitic–trondhjemitic–granodioritc, and granitic gneisses comprise 89% of the dominant amphibolite to granulite-facies Henshan-Fuping terrains, the remaining lithologies are amphibolite-mafic granulite (8%) and metapelite (3%). Tonalitic–trondhjemitic–granodioritc and granitic gneiss (54%) are less significant but still dominant in the lower-crustal Jining terrain.

The Musgrave Range (Fountain and Salisbury, 1981; Percival *et al*., 1992) and the Bamble Sector of southern Norway (Pinet and Jaupart, 1987; Alirezaei and Cameron, 2002)) represent two crustal sections through Proterozoic crust of central Australia and the Baltic Shield, respectively. In both sections, the middle crust is dominated by quartzofeldspathic gneiss. The lower crust consists of silicic to intermediate gneiss, felsic granulite, and mafic granulite with layered mafic and ultramafic intrusions being important lithological components in the Musgrave Range and metasediments being important in the lower crust of southern Norway.

The Ivrea–Verbano Zone in the southern Alps of Italy was the first to be proposed as an exposed deep-crustal section by Berckhemer (1969) and has subsequently been the focus of extensive geological, geochemical, and geophysical studies (e.g., Mehnert, 1975; Fountain, 1976; Dostal and Capedri, 1979; Voshage *et al*., 1990; Quick *et al*., 1995). The Paleozoic rocks of the Ivrea zone are unusual when compared with Precambrian granulite outcrops because they contain a large proportion of mafic lithologies and, as such, closely resemble granulite xenoliths in composition (Rudnick, 1990b). Amphibolite-facies rocks of the middle crust consist of felsic gneiss, amphibolite, metapelite (kinzigite), and marble, whereas the lower crustal section comprises mafic granulite and diorite, which formed by intrusion and subsequent fractionation of basaltic melts that partially melted the surrounding metasediments (now resistic stronalite) (Mehnert, 1975; Dostal and Capedri, 1979; Fountain *et al*., 1976; Voshage *et al*., 1990). Detailed mapping by Quick *et al*. (1995) demonstrated that mantle peridotites in the southern Ivrea Zone are lenses that were tectonically interfingered with metasedimentary rocks prior to intrusion of the gabbroic complex and the present exposures reside an unknown distance above the pre-Alpine contiguous mantle. Thus reference to the section as a complete crust–mantle transition could be misleading. Altogether, the exposed rocks represent ~30 km of crust with ~5 km lowermost crust remaining unexposed (Fountain *et al*., 1990a). The similarity in isotope composition and age between the Ivrea zone cumulates and Hercynian granites in the upper crust led Voshage *et al*. (1990) to speculate that these granites were derived from lower-crustal magma chambers similar to those in the Ivrea Zone, suggesting that basaltic underplating may be important in the formation and modification of the lower continental crust (Rudnick, 1990a).

Three sections through Mesozoic arcs show contrasting bulk compositions, depending on their settings (continental versus oceanic). In the southern Sierra Nevada, a tilted section exposes the deeper reaches of the Sierra Nevada batholith, which is part of a continental arc formed during the Mesozoic. This section is dominated by arc-related granitoids to depths of ~30 km, which have a tonalitic bulk chemistry (Ducea and Saleeby, 1996; Ducea, 2001). At the deepest structural levels, the mafic Tehachapi Complex comprises mafic and felsic gneiss, amphibolite, diorite, tonalite, granulite, and rare metasediments (Percival *et al*., 1992; Ross, 1985). In contrast, two sections through accreted intraoceanic arcs have considerably more mafic middle-crust compositions. In the Jurassic Talkeetna section of southeastern Alaska, the middle crust comprises gabbro and tonalite (4.5 km), which is underlain by variably deformed garnet gabbro and gabbro with cumulate dunite, wehrlite, and pyroxenite (2.2 km) in the lower crust (Pearcy *et al*., 1990; see Chapter 3.18). The upper, middle, and lower crustal units are estimated to have an average SiO_2 of 57%, 52%, and 44–45%, respectively. The Late Jurassic–Eocene Kohistan arc of Pakistan represents a 45 km thick reconstructed crustal column through a deformed, intruded intraoceanic arc sequence exposed in the Himalayan collision zone (Miller and Christensen, 1994). The depth interval from 10 km to 18 km is dominated by diorite and metadiorite. Rocks below this level, from ~18 km to the Moho, are dominated by metamorphosed mafic to ultramafic rocks from a series of layered mafic intrusions.

In summary, exposed amphibolite- to granulite-facies terranes and middle crustal cross-sections contain a wide variety of lithologies, including metasedimentary rocks, but they are dominated by igneous and metamorphic rocks of the diorite–tonalite–trondhjemite–granodiorite (DTTG), and granite suites. This is true not only for Precambrian shields but also for Phanerozoic crust and continental arcs, as documented in the crustal cross-sections described above. However, intraoceanic arcs may contain substantially greater proportions of mafic rocks in the middle and lower crust, as illustrated by the Kohistan and Talkeetna arc sections (Pearcy *et al*., 1990; Miller and Christensen, 1994; see Chapter 3.18).

3.01.3.4.2 Seismological evidence

The samples described above provide evidence of the lithologies likely to be present in the middle

crust. By definition, however, these samples no longer reside in the middle crust and additional information is required in order to determine the composition of the present-day middle crust. For this, we turn to seismological data for continental crust from a variety of tectonic settings.

Except for active rifts and some intra-oceanic island arcs, which exhibit the highest middle-crust *P*-wave velocities (6.7 ± 0.3 km s^{-1} (Rudnick and Fountain, 1995) and 6.8 ± 0.2 km s^{-1} (data from Holbrook *et al*., 1992) corrected to room temperature), other continental tectonic units have room-temperature middle-crustal *P*-wave velocities between 6.4 km s^{-1} and 6.6 km s^{-1} (Rudnick and Fountain, 1995). This range overlaps the average velocity of *in situ* middle crust, which was determined by Christensen and Mooney (1995) to be from 6.3 km s^{-1} to 6.6 ± 0.3 km s^{-1}, with an average of 6.5 ± 0.2 km s^{-1} over the depth range of 15–25 km. When corrected for temperature (an increase of 0.1–0.2 km s^{-1}, depending on the regional geotherm), these average middle-crustal velocities are similar to the room-temperature velocities considered by Rudnick and Fountain (1995). Thus, the middle crust has average, room-temperature-corrected velocity between 6.4 km s^{-1} and 6.7 km s^{-1}.

Amphibolite-facies felsic gneisses have room temperature *P*-wave velocities of 6.4 ± 0.1 km s^{-1} (Rudnick and Fountain, 1995). This compares well with the room-temperature velocity of average biotite (tonalite) gneiss at 6.32 ± 0.17 km s^{-1} (20 km depth; Christensen and Mooney, 1995). Granitic gneiss has a slightly lower velocity (6.25 ± 0.11 km s^{-1}; Christensen and Mooney (1995)), but is within uncertainty of the tonalite. A mixture of such gneisses with 0–30% amphibolite or mafic gneiss of the same metamorphic grade ($Vp = 7.0$ km s^{-1}; Rudnick and Fountain, 1995, Christensen and Mooney, 1995) yields *P*-wave velocities in the range observed for most middle crust. The above seismic data are thus consistent with the observations from granulite terranes and crustal cross-sections, and suggest that the middle crust is dominated by felsic gneisses.

3.01.3.4.3 Middle-crust composition

Compared to other regions of the crust (upper, lower, and bulk), few estimates have been made of the composition of the middle crust (Table 5, and Figures 9 and 10). Moreover, these estimates provide data for a far more limited number of elements, and large differences exist between different estimates. The estimates of Weaver and Tarney (1984), Shaw *et al*. (1994) and Gao *et al*. (1998a) are based on surface sampling of amphibolite-facies rocks in the Lewisian Complex, the Canadian Shield, and Eastern China, respectively. Rudnick and Fountain (1995) modeled the middle crust as 45% intermediate amphibolite-facies gneisses, 45% mixed amphibolite and felsic amphibolite-facies gneisses, and 10% metapelite. This mixture is very similar to that of Christensen and Mooney (1995), who proposed a middle crust of 50% tonalitic gneiss, 35% amphibolite, and 15% granitic gneiss. Unfortunately, compositional data are not available for Christensen and Mooney's samples and so the chemical composition of their middle crust cannot be calculated.

The estimates of Rudnick and Fountain (1995) and Gao *et al*. (1998a) show a broad similarity, although the latter is more evolved, having higher SiO_2, K_2O, barium, lithium, zirconium, and LREEs and La_N/Yb_N and lower total FeO, scandium, vanadium, chromium, and cobalt with a significant negative europium anomaly (Figures 9 and 10). These differences are expected, based on the slightly higher compressional velocity of Rudnick and Fountain's global middle crust compared to that of Eastern China (6.6 km s^{-1} versus 6.4 km s^{-1}; Gao *et al*., 1998b). The consistency is surprising considering that the two estimates are based on different sample bases and different approaches, one global and the other regional.

The middle-crustal compositions of Weaver and Tarney (1984) and Shaw *et al*. (1994) deviate from the above estimates by being markedly higher in SiO_2 and lower in TiO_2, FeO, MgO, and CaO. Moreover, these middle-crust compositions are more felsic (based on the above elements) than all estimates of the upper-continental crust composition given in Table 1. Thus, it is unlikely that the Weaver and Tarney (1984) and Shaw *et al*. (1994) compositions are representative of the global average middle crust, as both heat flow and seismic observations require that the crust becomes more mafic with depth. It should be noted, however, that heat production for Shaw's middle-crust composition is indistinguishable from those of Rudnick and Fountain (1995) and Gao *et al*. (1998a) at ~1.0 μW m^{-3}, due largely to the very high K/Th and K/U of Shaw *et al*. estimate. The middle crust of Weaver and Tarney (1984) has significantly higher heat production, at 1.4 μW m^{-3}.

Generally speaking, it would be best to derive the middle-crust composition from observed seismic-wave speeds and chemical analyses of amphibolite-facies rocks. However, few such data sets exist. Only two studies attempt to define the global average seismic-wave speeds for the middle crust (Christensen and Mooney, 1995; Rudnick and Fountain, 1995) and neither provides chemical data for amphibolite facies samples. Rudnick and Fountain used compiled chemical

Table 5 Compositional estimates of the middle continental crust. Major elements in weight percent. Trace element concentration units the same as in Table 2.

	1 *Weaver and Tarney (1984)*	*2* *Shaw et al. (1994)*	*3* *Rudnick and Fountain (1995)*	*4* *Gao et al.* (1998a)	*5* *This study*[a]	*1 Sigma*[a]	*%*
SiO_2	68.1	69.4	62.4	64.6	63.5	2	2
TiO_2	0.31	0.33	0.72	0.67	0.69	0.04	6
Al_2O_3	16.33	16.21	15.96	14.08	15.0	1	9
FeO_T[b]	3.27	2.72	6.59	5.45	6.02	0.8	13
MnO	0.04	0.03	0.10	0.11	0.10	0.00	2
MgO	1.43	1.27	3.50	3.67	3.59	0.1	3
CaO	3.27	2.96	5.25	5.24	5.25	0.01	0
Na_2O	5.00	3.55	3.30	3.48	3.39	0.1	4
K_2O	2.14	3.36	2.07	2.52	2.30	0.3	14
P_2O_5	0.14	0.15	0.10	0.19	0.15	0.06	43
Mg#	43.8	45.5	48.6	54.5	51.5		
Li		20.5	7	16	12	6	55
Be				2.29	2.29		
B		3.2		17	17		
N							
F				524	524		
S				20	20		
Cl				182	182		
Sc		5.4	22	15	19	5	27
V		46	118	95	107	16	15
Cr	32	43	83	69	76	10	13
Co		30	25	18	22	5	23
Ni	20	18	33	34	33.5	0.7	2
Cu		8	20	32	26	8	33
Zn		50	70	69	69.5	0.7	1
Ga			17	18	17.5	0.7	4
Ge				1.13	1.13		
As				3.1	3.1		
Se				0.064	0.064		
Br							
Rb	74	92	62	67	65	4	5
Sr	580	465[c]	281	283	282	1	1
Y	9	16	22	17.0	20	4	18
Zr	193	129	125	173	149	34	23
Nb	6	8.7	8	11	10	2	22
Mo		0.3		0.60	0.60		
Ru							
Pd				0.76	0.76		
Ag				48	48		
Cd				0.061	0.061		
In							
Sn				1.30	1.30		
Sb				0.28	0.28		
I							
Cs		0.98	2.4	1.96	2.2	0.3	14
Ba	713	1376	402	661	532	183	34
La	36	22.9	17	30.8	24	10	41
Ce	69	42.1	45	60.3	53	11	21
Pr			5.8		5.8		
Nd	30	18.3	24	26.2	25	2	6
Sm	4.4	2.8	4.4	4.74	4.6	0.2	5
Eu	1.09	0.78	1.5	1.20	1.4	0.2	16
Gd		2.11	4.0		4.0		
Tb	0.41	0.28	0.58	0.76	0.7	0.1	19
Dy		1.54	3.8		3.8		
Ho			0.82		0.82		

(continued)

Table 5 (continued).

	1 *Weaver and Tarney (1984)*	*2* *Shaw et al. (1994)*	*3* *Rudnick and Fountain (1995)*	*4* *Gao et al.* (1998a)	*5* *This study*[a]	*1 Sigma*[a]	*%*
Er			2.3		2.3		
Tm	0.14				0.32		
Yb	0.76	0.63	2.3	2.17	2.2	0.09	4
Lu	0.1	0.12	0.41	0.32	0.4	0.06	17
Hf	3.8	3.3	4.0	4.79	4.4	0.6	13
Ta		1.8	0.6	0.55	0.6	0.04	6
W				0.60	0.60		
Re							
Os							
Ir							
Pt				0.85	0.85		
Au				0.66	0.66		
Hg				0.0079	0.0079		
Tl				0.27	0.27		
Pb	22	9.0	15.3	15	15.2	0.2	1
Bi				0.17	0.17		
Th	8.4	6.4	6.1	6.84	6.5	0.5	8
U	2.2	0.9	1.6	1.02	1.3	0.4	31

Units for trace elements are the same as in Table 2. Major elements recast to 100% anhydrous.
[a] Averages and standard deviations of middle crustal composition by Rudnick and Fountain (1995) and Gao *et al*. (1998a), or from either of these two studies if data from the other one are unavailable. [b] Total Fe as FeO. [c] Recalculated from original data given by Shaw *et al*. (1994; Table 4), due to a typographical error in the published table. Mg# = molar $100 \times Mg/(Mg + Fe_{tot})$.

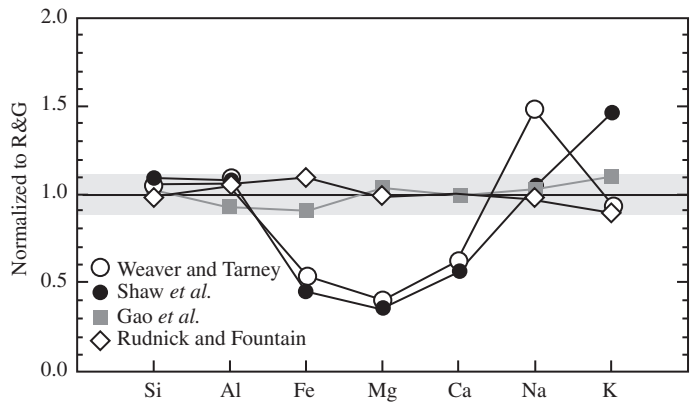

Figure 9 Comparison of the major-element composition of the middle continental crust as determined by sampling of surface exposures (Shaw *et al*., 1994; Weaver and Tarney, 1984) and inferred from middle-crustal seismic velocities combined with surface and xenolith samples (Rudnick and Fountain, 1995; Gao *et al*., 1998a). All values normalized to the new composition provided in Table 5 ("R&G"), which is an average between the values of Gao *et al*. (1998a) and Rudnick and Fountain (1995). Gray shaded field represents ±10% variation from this value.

data for granulite-facies rocks and inferred the concentrations of fluid-mobile elements (e.g., rubidium, uranium) of their amphibolite facies counterparts, while Christensen and Mooney (1995) did not publish their chemical data for the amphibolite-facies rocks they studied. For this reason, we have chosen to estimate the middle-crust composition by averaging the estimates of Rudnick and Fountain (1995) and Gao *et al*. (1998a) (Table 5), where corresponding data are available. Although the latter study is regional in nature, its similarity to the global model of Rudnick and Fountain (1995) suggests that it is not anomalous from a global perspective (unlike the lower crust of Eastern China as described in Section 3.01.3.5) and it provides additional estimates for little-measured trace elements.

This middle crust has an intermediate composition with lower SiO_2 and K_2O concentrations and higher FeO, MgO, and CaO concentrations than average upper crust (Table 1), consistent with the geophysical evidence (cited above) of

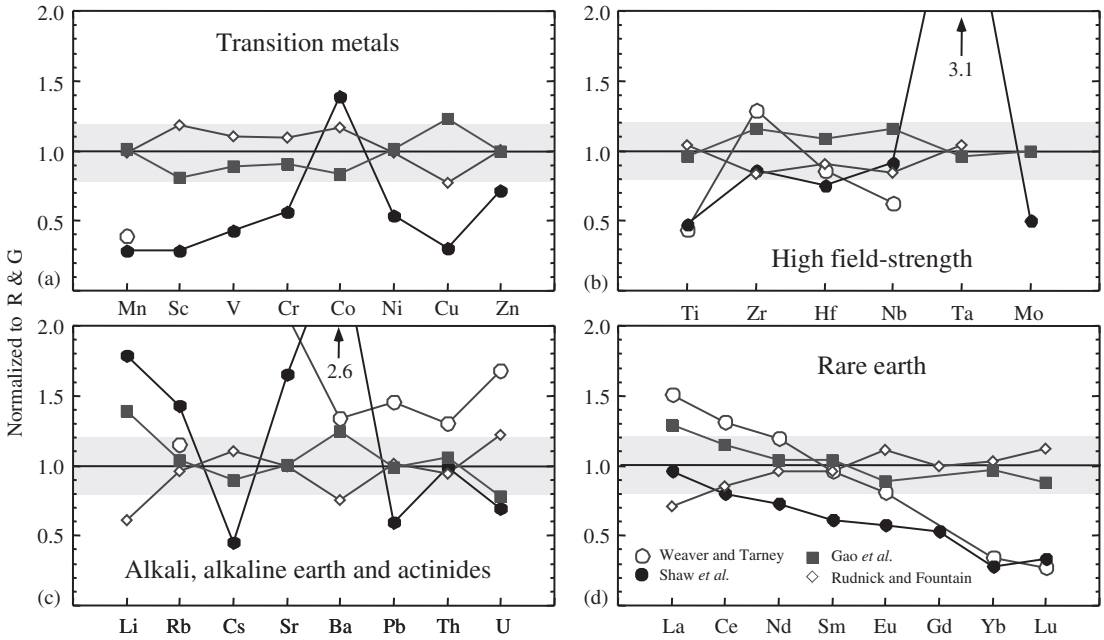

Figure 10 Comparison of the trace-element composition of the middle continental crust as determined by sampling of surface exposures (Shaw *et al*., 1994; Weaver and Tarney, 1984) and inferred from middle-crustal seismic velocities combined with surface and xenolith samples (Rudnick and Fountain, 1995; Gao *et al*., 1998a). All values normalized to the new composition provided in Table 5 ("R&G"), which is an average of the values of Gao *et al*. (1998a) and Rudnick and Fountain (1995). Gray shaded field represents ±20% variation from this value. (a) transition metals, (b) high-field strength elements, (c) alkali, alkaline earth and actinides, and (d) REEs.

a chemically stratified crust. Differences in trace-element concentrations between these two estimates are generally less than 30%, with the exceptions of P_2O_5, lithium, copper, barium, lanthanum, and uranium (Figure 10). The concentrations of these elements are considered to be less constrained. The middle crust is LREE enriched and exhibits the characteristic depletion of niobium relative to lanthanum and enrichment of lead relative to cerium seen in all other parts of the crust (Figure 11).

In summary, our knowledge of middle-crustal composition is limited by the small number of studies that have focused on the middle crust and the ambiguity in deriving chemical compositions from seismic velocities. Thus, the average composition given in Table 5 is poorly constrained for a large number of elements. Seismological and heat-flow data suggest an increase in seismic-wave speeds and a decrease in heat production with depth in the crust. Studies of crustal cross-sections show the middle crust to be dominated by felsic gneisses of tonalitic bulk composition. The average middle-crust composition given in Table 5 is consistent with these broad constraints and furthermore suggests that the middle crust contains significant concentrations of incompatible trace elements. However, the uncertainty on the middle-crust composition, particularly the trace elements, remains large.

3.01.3.5 The Lower Crust

3.01.3.5.1 Samples

Like the middle crust, the lower crust also contains a wide variety of lithologies, as revealed by granulite xenoliths, exposed high-pressure granulite terranes and crustal cross-sections. Metaigneous lithologies range from granite to gabbro, with a predominance of the latter in most lower crustal xenolith suites. Exceptions include xenolith suites from Argentina (Lucassen *et al*., 1999) and central Spain (Villaseca *et al*., 1999), where the xenoliths are dominated by intermediate to felsic granulites and the Massif Central (Leyreloup *et al*., 1977; Downes *et al*., 1990) and Hannuoba, China (Liu *et al*., 2001), where intermediate to felsic granulites comprise nearly half the population. Metapelites occur commonly in both terranes and xenoliths, but only rarely do other metasedimentary lithologies occur in xenolith suites; unique xenolith localities have been documented with meta-arenites (Upton *et al*., 1998) and quartzites (Hanchar *et al*., 1994), but so far marbles occur only in terranes. The reason for their absence in lower crustal xenolith suites is uncertain—they may be absent in the lower crust sampled by volcanoes, they may not survive transport in the hot magma, or they may simply have been overlooked by xenolith investigators.

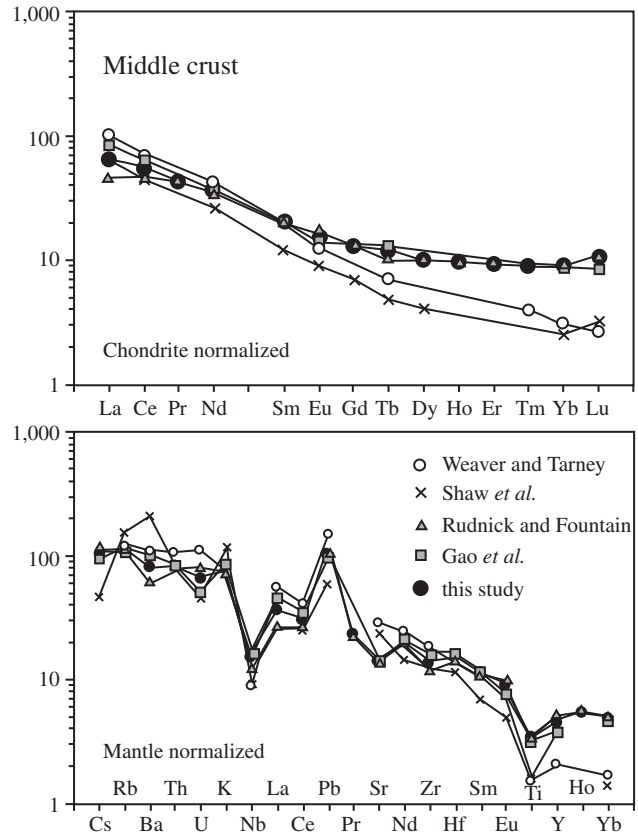

Figure 11 REE (upper) and multi-element plot (lower) of the compositions of the middle crust given in Table 5. Chondrite values from Taylor and McLennan (1985) and primitive mantle values from McDonough and Sun (1995).

These issues related to the representativeness of xenolith sampling are the reason why robust estimates of lower-crustal composition must rely on a grand averaging technique, such as using seismic velocities to infer composition.

Information on the lower crust derived from crustal cross-sections has been given in Section 3.01.3.4.1 and only the main points are summarized here. All crustal cross-sections show an increase in mafic lithologies with depth and most of those in which possible crust–mantle boundaries are exposed reveal a lower crust that is dominated by mafic compositions. For example, in the Ivrea Zone, Italy, the lower crust is dominated by mafic granulite formed from basaltic underplating of country rock metapelite (Voshage *et al*., 1990). The same is true for the Kohistan sequence, Pakistan (Miller and Christensen, 1994), although here metapelites are lacking. Although the crust–mantle boundary is not exposed in the Wutai-Jining terrain, the granulite-facies crust exposed in this cross-section has a more mafic composition than the rocks of the middle-crust section. Even in the Vredefort and Sierra Nevada cross-sections, which are dominated by granitic rocks throughout most of the crustal sections (Ducea, 2001; Hart *et al*., 1990), the deepest reaches of exposed crust are characterized by more mafic lithologies (Ross, 1985; Hart *et al*., 1990; Table 4).

There have been a number of studies of granulite-facies xenoliths since the reviews of Rudnick (1992) and Downes (1993) and a current tabulation of xenolith studies is provided in Table 6, which provides a summary of most lower crustal xenolith studies published through 2002. Perhaps most significant are the studies of lower-crustal xenoliths from Archean cratons, which had been largely lacking prior to 1992 (Kempton *et al*., 1995, 2001; Davis, 1997; Markwick and Downes, 2000; Schmitz and Bowring, 2000, 2003a,b; Downes *et al*., 2002). These studies reveal a great diversity in lower-crustal lithologies beneath Archean cratons, which appear to correlate with seismic structure of the crust.

Lower-crustal xenoliths from the Archean part of the Baltic (or Fennoscandian) Shield, like their post-Archean counterparts, are dominated by mafic lithologies (Kempton *et al*., 1995, 2001; Markwick and Downes, 2000; Hölttä *et al*., 2000). Most equilibrated at depths of 22–50 km and contain hydrous phases (amphibole ± biotite). Partial melting and restite development is evident in some migmatitic xenoliths, but cumulates are

Table 6 Geochemical and mineral chemical studies of lower crustal xenoliths.

Locality	*Host*	*Xenolith types*	*Types of analyses*	*Pipe age*	*Crust age*	*Age*	*References*
North America							
Nunivak Island, Alaska	AB	MG	ME, Min.	<5 Ma	Phanerozoic		Francis (1976)
Central Slave Province, Canada	K	MGG, FG, MG	U–Pb	50–70 Ma	Archean	2.5 Ga, 1.3 Ga (meta)	Davis (1997)
Kirkland Lake, Ontario, Superior craton	K	AN, MG	U–Pb	160 Ma	Archean	2.6–2.8 Ga, 2.4–2.5 Ga (meta)	Moser and Heaman (1997)
Ayer's cliff, Quebec	K	MG, PG	Min.	~100 Ma	Proterozoic		Trzcienski and Marchildon (1989)
Popes Harbour[a], Nova Scotia	K	MG, PG, FG	ME, TE, Min.	<400 Ma	Phanerozoic		Owen (1988), Eberz (1991)
Snake River Plains[a], Idaho	Evol. B	PG	Sr, Nd, Pb	<2 Ma	Archean	~2.8 Ga	Leeman *et al.* (1985, 1992)
Bearpaw Mts., Montana	K	MGG, MG, FG	ME, TE, O, U–Pb	45 Ma	Archean	~2.6 Ga	Collerson *et al.* (1989), Kempton and Harmon (1992), Moecher *et al.* (1994), Rudnick *et al.* (1999)
Simcoe Volcanic Field, Washington Cascades	AB	MG	FI	<1 Ma	Phanerozoic		Ertan and Leeman (1999)
Riley County, Kansas	K	MGG, EC	Min.	<230 Ma	Proterozoic		Meyer and Brookins (1976)
Central Sierra Nevada, California	AB	MGG, EC, FG, MP	ME, TE, Min., Sr, Nd, O, U–Pb	8–11 Ma	Proterozoic	180 Ma	Dodge *et al.* (1986, 1988), Domenick *et al.* (1983), Ducea and Saleeby (1996, 1998)
Colorado/Wyoming	K	MGG, MG	ME, Min.		Proterozoic		Bradley and McCallum (1984)
Mojave Desert, California	AB	MP, FG, IG, QZ, MGG	ME, TE, Min., Sr, Nd, Pb, U–Pb		Archean	~1,7 Ga	Hanchar *et al.* (1994)
Navajo Volcanic Field, Colorado Plateau	K	MGG, FG, AM, EC, MP	ME, TE, Min., Sr, Nd	25–30 Ma	Proterozoic	~1.8 Ga	Ehrenberg and Griffin (1979), Broadhurst (1986), Wendlandt *et al.* (1993, 1996), Mattie *et al.* (1997), Condie *et al.* (1999)
Camp Creek, Arizona	L	MGG, AM, EC	ME, TE, Min., Sr, Nd, Pb	23–27 Ma	Proterozoic	1.2–1.9 Ga	Esperanca *et al.* (1988)

(continued)

Table 6 (continued).

Locality	*Host*	*Xenolith types*	*Types of analyses*	*Pipe age*	*Crust age*	*Age*	*References*
Chino Valley, Arizona	L	MGG, AM	ME, TE, Min.	25 Ma	Proterozoic		Arculus and Smith (1979), Schulze and Helmstadt (1979), Arculus *et al.* (1988)
San Francisco Volcanic Field	AB	MG, IG	ME, TE, Min., Sr, Nd	<20 Ma	Proterozoic	~1.9 Ga	Chen and Arculus (1995)
Geronimo Volcanic Field, New Mexico	AB	MG, IG	ME, TE, Min., Sr, Nd, Pb, O	<3 Ma	Proterozoic	1.1–1.4 Ga	Kempton *et al.* (1990), Kempton and Harmon (1992)
Kilbourne Hole, New Mexico	AB	MG, AN, PG, FG	Min., ME, Sr, Nd, Pb, O, U–Pb	<1 Ma	Proterozoic	1.5 Ga	Padovani and Carter (1977), Davis and Grew (1977), James *et al.* (1980), Padovani *et al.* (1982), Reid *et al.* (1989), Leeman *et al.* (1992), Scherer *et al.* (1997).
Elephant Butte, New Mexico	AB	MG	Min., ME	<3 Ma	Proterozoic		Baldridge (1979)
Engle Basin, New Mexico	AB	MG	Min.	<3 Ma	Proterozoic		Warren *et al.* (1979)
West Texas	AB	MGG, IG, FG	ME, Sr, Nd, Pb, U–Pb	<40 Ma	Proterozoic	1.1 Ga	Cameron and Ward (1998)
Northern Mexico	AB	MG, PG, FG	ME, TE, Min., Sr, Nd, C, U–Pb	<25 Ma	Proterozoic	From 1 to 1400 Ma	Nimz *et al.* (1986), Ruiz *et al.* (1988a,b), Roberts and Ruiz (1989), Hayob *et al.* (1989), Rudnick and Cameron (1991), Cameron *et al.* (1992), Moecher *et al.* (1994), Smith *et al.* (1996), Scherer *et al.* (1997)
Central Mexico	AB	MG	ME, Min, Nd		Phanerozoic	1.5 Ga	Urrutia-Fucagauchi and Uribe-Cifuentes (1999)
San Luis Potosi, Central Mexico	AB	MG, MGG, IG	ME, TE, Min., Sr, Nd	<1 Ma	Proterozoic	~1.2 Ga	Schaaf *et al.* (1994)
South America							
Mercaderes, SW Columbia	AB	MG, MGG, IG, HB,	ME, TE, Min., Sr, Nd, Pb	<10 Ma	Phanerozoic		Weber *et al.* (2002)
Salta Rift, NW Argentina	AB	FG, MG	Min., ME, TE, Sr, Nd, Pb	Mesozoic	Proterozoic	~1.8 Ga	Lucassen *et al.* (1999)
Calbuco Volcano, Chile	AND	MG	ME, TE, Min., Sr, Nd	<1,000 yr	Paleozoic		Hickey-Vargas *et al.* (1995)
Pali Aike, Southern Chile	AB	MG	ME, Min., FI	<3 Ma	Phanerozoic		Selverstone and Stern (1983)

Europe							
Scotland, Northern Uplands	AB	MG, AN, IG, MP, MGG, HB	ME, TE, Min., Nd, Sr, U–Pb	~300 Ma	Archean/ Proterozoic	360 Ma, 1.8 Ga	van Breeman and Hawkesworth (1980), Upton *et al*. (1983), Halliday *et al*. (1984), Hunder *et al*. (1984), Upton *et al*. (1998, 2001)
Eastern Finland	K	MG, MGG, AM	ME, TE, Min., Nd, U–Pb	525 Ma	Archean	1.7–2.6 Ga	Hölttä *et al*. (2000)
Arkhangelsk Kimberlite, Baltic shield, Russia	K	MGG	ME, TE, Min., Sr, Nd	360 Ma	Archean	1.7–1.9 Ga	Markwick and Downes (2000)
Elovy island, Baltic shield, Russia	K	MGG, EC, FG, AM	ME, TE, Min., Sr, Nd, Pb, U–Pb	360–380 Ma	Archean	~1.8 Ga, 2.4–2.5 Ga	Kempton *et al*. (1995, 2001), Downes *et al*. (2002)
Belarus, Russia	K	MGG, EC, HB	ME, TE, Min., Sr, Nd	370 Ma			Markwick *et al*. (2001)
Pannonian basin, W. Hungary	AB	MG, MGG	ME, TE, Min., Sr, Nd, O	2–5 Ma	Phanerozoic		Embey-Isztin *et al*. (1990), Kempton *et al*. (1997), Embey-Isztin *et al*. (2003), Dobosi *et al*. (2003)
Kampernich, E. Eifel, Germany	AB	MGG, AM	ME, TE, Min., Sr, Nd, Hf, Pb, O	<1 Ma	Phanerozoic	1.5 Ga or ~450 Ma?	Okrusch *et al*. (1979), Stosch and Lugmair (1984), Rudnick and Goldstein (1990), Loock *et al*. (1990), Kempton and Harmon (1992), Sachs and Hansteen (2000)
Wehr Volcano[a], E. Eifel, Germany	AB	AM	ME, TE, Min.	<1 Ma	Phanerozoic		Worner *et al*. (1982), Grapes (1986)
N. Hessian Depression, Germany	AB	MGG, MG, PG, FG	ME, TE, Min., O	<50 Ma	Phanerozoic		Mengel and Wedepohl (1983), Mengel (1990)
Massif Central, France	AB	MGG, MG, PG, FG	ME, TE, Nd, Sr, Pb, O, C	<5 Ma	Phanerozoic	~350 Ma	Leyreloup *et al*. (1977), Dostal *et al*. (1980), Vidal and Postaire (1985), Downes and Leyreloup (1986), Kempton and Harmon (1992), Downes *et al*. (1991), Moecher *et al*. (1994)
Tallante, Spain	AB	PG	Min.	<20 Ma	Phanerozoic		Vielzeuf (1983)
Central Spain	K	IG, FG, MP	ME, TE, Min.	Early Mesozoic	Proterozoic		Villaseca *et al*. (1999)
Sardinia, Italy	AB	MG	Min.	~3 Ma	Phanerozoic		Rutter (1987)

(continued)

Table 6 (continued).

Locality	*Host*	*Xenolith types*	*Types of analyses*	*Pipe age*	*Crust age*	*Age*	*References*
Africa							
Hoggar, Algeria	AB	MG, AN, PG	ME, TE	<20 Ma	Proterozoic		Leyreloup *et al.* (1982)
Man Shield, Sierra Leone	K	MGG, AN, EC	ME, Min., U–Pb	90–120 Ma	Archean		Toft *et al.* (1989), Barth *et al.* (2002)
Lashaine, Tanzania	AB	MGG, EC, AN	ME, TE, Min., Sr, Nd, Pb, C	<20 Ma	Proterozoic		Dawson (1977), Jones *et al.* (1983), Cohen *et al.* (1984), Moecher *et al.* (1994)
Fort Portal, Uganda	AB	MGG, MG	Min., ME, TE	<3Ma	Proterozoic		Thomas and Nixon (1987)
Free State Kimberlites, Kaapvaal Craton, South Africa	K	PG	Min., U–Pb	90–140 Ma	Archean	~2.7 Ga (meta)	Dawson and Smith (1987), Dawson *et al.* (1997), Schmitz and Bowring (2003a,b)
Newlands Kimberlite, Kaapvaal Craton, South Africa	K	PG	U–Pb	114 Ma	Archean	~2.7 Ga	Schmitz and Bowring (2003a,b)
Lesotho, South Africa	K	MGG, MG, FG, MP, EC	ME, TE, Min., Sr, Nd, Pb, U–Pb	90–140 Ma	Proterozoic	1.4 Ga, 1.1–1.0 Ga (meta)	Davis (1977), Rogers and Hawkesworth (1982), Griffin *et al.*, 1979), Rogers (1977), van Calsteren *et al.* (1986), Huang *et al.* (1995), Schmitz and Bowring (2003a)
Orapa, Zimbabwe Craton, Botswana	K	MP	U–Pb	93 Ma	Proterozoic	2.0 Ga (meta), 1.24 Ga (meta)	Schmitz and Bowring (2003a)
Central Cape Province, Eastern Namaqualand, South Africa	K	MGG, AM	ME, TE, Min., Sr, Nd, Pb, U–Pb	90–140 Ma	Proterozoic	~1.1 Ga (meta)	van Calsteren *et al.* (1986), Pearson *et al.* (1995), Schmitz and Bowring (2000), Schmitz and Bowring (2003a)
Middle East							
Mt. Carmel, Israel	AB	MGG	Min.	~100 Ma	Phanerozoic		Esperanca and Garfunkel (1986), Mittlefehldt (1986)
Birket Ram, Israel	AB	MGG, Am	TE	10,000 yr	Phanerozoic		Mittlefehldt (1984)
Jordan	AB	MG	Min.	<2 Ma	Proterozoic		Nasir (1992), Nasir (1995)
Shamah volcanic fields, Syria	AB	MG					Nasir and Safarjalani (2000)

Asia							
Udachnaya, Siberia, Russia	K	MGG	Min.		Archean		Shatsky *et al*. (1990, 1983)
Tariat Depression, Central Mongolia	AB	MG, MGG, IG, AM	ME, TE, Min., Sr, Nd, Pb, O	<5 Ma	Proterozoic		Kempton and Harmon (1992), Kopylova *et al*. (1995), Stosch *et al*. (1995)
Hannuoba, North China Craton	AB	FG, IG, MG, MGG, AN, MP	ME, TE, Sr, Nd, Pb, U–Pb	14–27 Ma	Archean	~2.5, 1.9, 0.4, 0.22 Ga	Gao *et al*. (2000), Liu *et al*. (2001), Chen *et al*. (2001), Zhou *et al*. (2002)
Xinyang, North China craton	AB	MGG	ME, TE, Min.	Mesozoic	Archean		Zheng *et al*. (2003)
Penghu Islands, SE China	AB	MG					Lee *et al*. (1993)
Southeastern China	AB	MG, MGG, IG, FG	ME, TE, Min., Sr, Nd	<20Ma	Archean/ Proterozoic		Yu *et al*. (2003)
Ichinomegata, Japan	AND	AM	ME, TE, Min., Sr	10,000 yr	Phanerozoic		Kuno (1967), Aoki (1971), Zashu *et al*. (1980), Tanaka and Aoki (1981)
Deccan Traps, India	K	MG	ME, Min.				Dessai *et al*. (1999), Dessai and Vasseli (1999)
Tibetan plateau			Min.				Hacker *et al*. (2000)
Australia–New Zealand–Antarctica							
McBride Province, N. Queensland	AB	MGG, MG, PG, FG	ME, TE, Min., Sr, Nd, Pb, O, C, U–Pb	<3 Ma	Proterozoic	300 Ma and ~1.6 Ga	Kay and Kay (1983), Rudnick and Taylor (1987), Rudnick and Williams (1987), Stolz and Davies (1989), Stolz (1987), Rudnick (1990), Rudnick and Goldstein (1990), Kempton and Harmon (1992), Moecher *et al*. (1994)
Chudleigh Province, N. Queensland	AB	MGG, MG	ME, TE, Min., Sr, Nd, Pb, O	<1 Ma	Phanerozoic	<100 Ma	Kay and Kay (1983), Rudnick *et al*. (1986), Rudnick and Taylor (1991), O'Reilly *et al*. (1988), Rudnick and Goldstein (1990), Kempton and Harmon (1992)
Central Queensland	AB	MG, MGG	ME, TE, Min., Sr, Nd	≤50 Ma	Phanerozoic		Griffin *et al*. (1987), O'Reilly *et al*. (1988)
Gloucester, NSW	AB	MGG, MG	ME, TE, Sr, Nd	≤50 Ma	Phanerozoic		Griffin *et al*. (1986), O'Reilly *et al*. (1988)
Sydney Basin	AB	MG	ME, TE, Sr, Nd	≤50 Ma	Phanerozoic		Griffin *et al*. (1986), O'Reilly *et al*. (1988)
Boomi Creek, NSW	AB	MG	ME, TE, Min.	≤50 Ma	Phanerozoic		Wilkinson (1975), Wilkinson and Taylor (1980)

(continued)

Table 6 (continued).

Locality	*Host*	*Xenolith types*	*Types of analyses*	*Pipe age*	*Crust age*	*Age*	*References*
Delegate, NSW	AB	MG, MGG, FG, EC	ME, TE, Min., Sr, Nd, U–Pb	~140 Ma	Phanerozoic	400 Ma	Lovering and White, (1964, 1969), Griffin and O'Reilly (1986), O'Reilly *et al*. (1988), Arculus *et al*. (1988), Chen *et al*. (1998)
Jugiong, NSW	K	MG, MGG	Min.	<17 Ma	Phanerozoic		Arculus *et al*. (1988)
White Cliffs, NSW	K	MGG	Min.	~260 Ma	Proterozoic		Arculus *et al*. (1988)
Anakies, Victoria	AB	MG, MGG	ME, TE, Min., Sr, Nd	<2 Ma	Phanerozoic		Sutherland and Hollis (1982), Wass and Hollis (1983), O'Reilly *et al*. (1988)
El Alamein, South Australia	K	MGG, EC	ME, TE, Min.	~170 Ma	Proterozoic		Edwards *et al*. (1979), Arculus *et al*. (1988)
Calcutteroo, South Australia	K	MGG, FG, EC	ME, TE, Min., Sr, Nd, U–Pb	~170 Ma	Proterozoic	1.6–1.5 Ga, 780 Ma, 620 Ma, 330 Ma	McCulloch *et al*. (1982), Arculus *et al*. (1988), Chen *et al*. (1994)
Banks Penninsula, New Zealand	AB	MG	ME, TE, Min				Sewell *et al*. (1993)
Mt. Erebus Volcanic Field,	AB	MG, MGG	ME, TE, Min., Sr, O	<5 Ma	Phanerozoic/ Proterozoic		Kyle *et al*. (1987), Kalamarides *et al*. (1987), Berg *et al*. (1989)
Indian Ocean							
Kergulen Archipelago	AB	MG, SG	ME, Min.		Phanerozoic/ Proterozoic		McBirney and Aoki (1973), Gregoire *et al*. (1998, 1994)

Only papers in which data are reported are listed here.

Abbreviations

Host types: AB = alkali basaltic association; AND = andesite; K = kimberlitic association (including lamproites, minettes, kimberlites), Evol. B. = evolved basalt; L = latite.

Xenolith types: AM = amphibolite; AN = anorthosite; EC = elcogite; FG = felsic granuilte; HB = hornblendite; IG = intermediate granulite; MG = mafic granulite; MGG = mafic garnet granulite; MP = metapelite, PG = paragneiss, QZ = quartzite, SG = saphirine granulites.

Types of analyses: FI = fluid inclusions, ME = major element analyses; Min = mineral analyses; TE = trace element analyses; Sr = Sr isotope analyses; Nd = Nd isotope analyses; Pb = Pb isotope analyses, O = oxygen isotope analyses, C = carbon isotope analyses, U–Pb = U–Pb geochronology on accessory phases (zircon, rutile, titanite, etc.).

[a] Xenoliths from these localities are probably derived from mid-crustal levels based on either: equilibration pressures, lack of mantle derived xenoliths in the same hosts and/or chemically evolved character of the host.

absent (Kempton *et al*., 1995, 2001; Hölttä *et al*., 2000). A curious feature of these samples is the common occurrence of potassic phases (e.g., potassium feldspar, hornblende, biotite) in otherwise mafic granulites. These mafic xenoliths have been interpreted to represent gabbroic intrusions that underplated the Baltic Shield during the Paleoproterozoic flood-basalt event (2.4–2.5 Ga) and later experienced potassium-metasomatism coincident with partial melting at ~1.8 Ga, a major period of granitic magmatism in this region (Kempton *et al*., 2001; Downes *et al*., 2002). The dominately mafic compositions of these xenoliths is consistent with the thick layer of high-velocity ($\geq$7 km s^{-1}) material imaged beneath the Archean crust of the Baltic Shield (Luosto *et al*., 1989, 1990). The xenolith studies suggest that this layer formed during Paleoproterozoic basaltic underplating and is not part of the original Archean architecture of this Shield.

In contrast to the Baltic Shield, mafic granulites appear to be absent in lower-crustal xenolith suites from the Archean Kaapvaal craton, which are dominated by metapelite and unique ultra-high-temperature granulites of uncertain petrogenesis (Dawson *et al*., 1997; Dawson and Smith, 1987; Schmitz and Bowring, 2003a,b). These xenoliths derive from depths of $>$30 km and show evidence for multiple thermal metamorphic overprints starting with ultrahigh temperature metamorphism at ~2.7 Ga, which is associated with Ventersdorp magmatism (Schmitz and Bowring, 2003a,b). The absence of mafic granulites is consistent with the relatively low *P*-wave velocities in the lower crust of the Kaapvaal craton (Durrheim and Green, 1992; Nguuri *et al*., 2001; Niu and James, 2002), but it is not clear whether the lack of a mafic lower crust reflects the original crustal structure of this Archean craton (Nguuri *et al*., 2001) or reflects loss of a mafic complement some time after crust formation in the Archean (Niu and James, 2002).

Lower crustal xenoliths from the Hannuoba basalts, situated in the central zone of the North China Craton, show a diversity of compositions ranging from felsic to mafic metaigneous granulites and metapelites (Gao *et al*., 2000; Chen *et al*., 2001; Liu *et al*., 2001; Zhou *et al*., 2002); approximately half the xenoliths have evolved compositions (Liu *et al*., 2001). All granulite xenoliths equilibrated under high temperatures (700–1,000 °C), corresponding to depths of 25–40 km (Chen *et al*., 2001), but mafic granulites yield higher temperatures than metapelitic xenoliths, suggesting their derivation from deeper crustal levels (Liu *et al*., 2001). Liu *et al*. used regional seismic refraction data and the lithologies observed in the Hannuoba xenoliths to infer the lower-crust composition in this part of the North China craton. They describe a layered lower crust in which the upper portion (from 24 km to ~38 km, $V_p \sim 6.5$ km s^{-1}), consists largely of felsic granulites and metasediments, and is underlain by a "lowermost" crust (38–42 km, $V_p \sim 7.0$ km s^{-1}) composed of intermediate granulites, mafic granulites, pyroxenite, and peridotite. Thus, the bulk lower crust in this region is intermediate in composition, consistent with the relatively large proportion of evolved granulites at Hannuoba. Zircon geochronology shows that mafic granulites and some intermediate granulites were formed by basaltic underplating in the Cretaceous. This mafic magmatism intruded pre-existing Precambrian crust consisting of metapelites that had experienced high-grade metamorphism at 1.9 Ga (Liu *et al*. (2001) and references therein).

Fragmentary xenolithic evidence for the composition of the lower crust is available for three other Archean cratons. Two mafic garnet granulites from the Udachnaya kimberlite in the Siberian craton yield Archean lead–lead and Proterozoic samarium–neodymium mineral isochrons (Shatsky, Rudnick and Jagoutz, unpublished data). It is likely that that lead–lead isochrons are frozen isochrons yielding anomalously old ages due to ancient uranium loss; the best estimate of the true age of these mafic granulites is Proterozoic. Moser and Heaman (1997) report Archean uranium–lead ages for zircons derived from mafic lower-crustal xenoliths from the Superior Province, Canada. They suggest these samples represent the mafic lower crust presently imaged seismically beneath the Abitibi greenstone belt, but which is not exposed in the Kapuskasing uplift. These granulites experienced an episode of high-grade metamorphism at 2.4 Ga, which Moser and Heaman (1997) attribute to underplating of basaltic magmas associated with the opening of the Matachewan Ocean. Davis (1997) reports mafic to felsic granulite xenoliths from the Slave craton, Canada, that have Archean to Proterozoic uranium–lead zircon ages. The mafic granulites appear to derive from basaltic magmas that underplated the felsic-Archean crust during the intrusion of the 1.3 Ga McKenzie dike swarm.

The above case studies illustrate the utility of lower crustal xenolith studies in defining the age, lithology, and composition of the lower crust beneath Archean cratons. When viewed collectively, an interesting generality emerges: when mafic granulites occur within the lower crust of Archean cratons they are generally inferred to have formed from basaltic underplating related to post-Archean magmatic events (In addition to the studies mentioned above is the case of the thick, high-velocity lower crust beneath the Archean Wyoming Province and Medicine Hat Block, western North America, which is also inferred to have formed by Proterozoic underplating based on

uranium–lead zircon ages from lower crustal xenoliths (Gorman *et al*., 2002)). Only granulites from the Superior Province appear to represent Archean mafic lower crust (Moser and Heaman, 1997). This generality is based on still only a handful of studies of xenoliths from Archean cratons and more such studies are clearly needed. However, if this generality proves robust, it implies that the processes responsible for generation of crust in most Archean cratons did not leave behind a mafic lower crust, the latter of which is commonly observed in post-Archean regions (Rudnick (1992) and references therein). It may be that this mafic lower crust was never produced, or that it formed but was removed from the crust, perhaps via density foundering (R. W. Kay and S. M. Kay, 1991; Gao *et al*., 1998b; Jull and Kelemen, 2001). In either case, the apparent contrast in lower-crustal composition between Archean and post-Archean regions, originally pointed out by Durrheim and Mooney (1994), suggests different processes may have been operative in the formation of Archean crust (see Chapter 3.11). We return to the issue of what crust composition tells us about crustal generation processes in Section 3.01.5.

In summary, despite the uncertainties regarding the representativeness of any given lower-crustal xenolith suite (Rudnick, 1992), the above studies show that an accurate picture of the deep crust can be derived from such studies, especially when xenolith studies are combined with seismological observations of lower-crust velocities, to which we now turn.

3.01.3.5.2 Seismological evidence

The *P*-wave velocity of the lower crust varies from region to region, but average, temperature-corrected velocities for lower crust from a variety of different tectonic settings are high (6.9–7.2 km s^{-1}; Rudnick and Fountain, 1995; Christensen and Mooney, 1995). Such velocities are consistent with the dominance of mafic lithologies (mafic granulite and/or amphibolite) in these lower-crustal sections. High-grade metapelite, in which much of the quartz and feldspars have been removed by partial melting, is also characterized by high seismic velocities and thus may also be present (Rudnick and Fountain, 1995). Although seismically indistinct, some limit on the amount of metapelite in these high-velocity layers can be made on the basis of heat-flow and xenolith studies; these suggest that metapelite is probably a minor constituent of the lower crust (i.e., <10%; Rudnick and Fountain, 1995). In addition, average *P*-wave velocities for mafic granulite or amphibolite are higher than those observed in many lower-crustal sections (corrected to room-temperature velocities). Average room-temperature *P*-wave velocities for a variety of mafic lower crustal rock types are generally equal to or higher than 7 km s^{-1}: 7.0 ± 0.2 km s^{-1} for amphibolite, 7.0 to 7.2 ± 0.2 km s^{-1} for garnet-free mafic granulites, and 7.2 to 7.3 ± 0.2 km s^{-1} for garnet-bearing mafic granulites at 600 MPa (Rudnick and Fountain, 1995; Christensen and Mooney, 1995). Lower-crustal sections having temperature-corrected *P*-wave velocities of 6.9–7.0 km s^{-1} (e.g., Paleozoic orogens and Mesozoic/Cenozoic extensional and contractional terranes), are thus likely to have lower-velocity rock types present (up to 30% intermediate to felsic granulites), in addition to mafic granulites or amphibolites (Rudnick and Fountain, 1995).

Although the average lower-crustal seismic sections discussed above show high velocities, some sections are characterized by much lower velocities, indicating a significantly more evolved lower-crust composition. For example, the crust of a number of Archean cratons is relatively thin (~35 km) with low seismic velocities in the lower crust (6.5–6.7 km s^{-1}), suggesting an evolved composition (e.g., Yilgarn craton (Drummond, 1988), Kaapvaal craton (Durrheim and Green, 1992; Niu and James, 2002), and North China craton (Gao *et al*., 1998a,b)). As discussed above, it is not clear whether these thin and relatively evolved regions of Archean crust represent the original crustal architecture, formed by processes distinct from those responsible for thicker and more mafic crustal regions (e.g., Nguuri *et al*., 2001), or reflect loss of a mafic layer from the base of the original crust (Gao *et al*., 1998b; Niu and James, 2002). In addition, some Cenozoic–Mesozoic extensional and contractional regions, Paleozoic orogens, and active rifts show relatively slow lower-crustal velocities of 6.7–6.8 km s^{-1} and may contain >40% felsic and intermediate granulites (Rudnick and Fountain, 1995). Two extreme examples are the southern Sierra Nevada and Central Andean backarc. In both cases, the entire crustal columns are characterized by *P*-wave velocities of less than 6.4 km s^{-1} (Beck and Zandt, 2002; Wernicke *et al*., 1996). A relatively high-velocity ($Vp = 6.4–6.8$ km s^{-1}) layer of <5 km in thickness occurs only at the base of the Central Andean backarc at ~60 km depth.

In summary, the seismic velocity of the lower crust is variable from region to region, but is generally high, suggesting a dominance of mafic lithologies. However, most seismic sections require the presence of evolved compositions in addition to mafic lithologies in the lower crust (up to 30% for average velocity of 6.9 km s^{-1}) and a few regions (e.g., continental arcs and some Archean cratons) are characterized by slow lower crust, indicating a highly evolved average composition. This diversity of lithologies is

consistent with that seen in both crustal cross-sections and lower-crustal xenolith suites and also provides a mechanism (lithological layering) to explain the common occurrence of seismic reflections observed in many seismic reflection profiles (Mooney and Meissner, 1992).

3.01.3.5.3 Lower-crust composition

Table 7 lists previous estimates of the composition of the lower crust. These estimates include averages of exposed granulites (columns 1 and 2; Weaver and Tarney, 1984; Shaw *et al.*, 1994), averages of individual lower-crustal xenolith suites (columns 3–6, Condie and Selverstone, 1999; Liu *et al.*, 2001; Rudnick and Taylor, 1987; Villaseca *et al.*, 1999), the median composition of lower-crustal xenoliths (column 7; updated from Rudnick and Presper (1990), with data from papers cited in Table 6 (the complete geochemical database for lower crustal xenoliths is available on the GERM web site http://earthref.org/cgi-bin/erda.cgi?$n = 1,2,3,8$ and also on the Treatise web site), averages derived from linking seismic velocity data for the lower crust with the compositions of lower-crustal rock types (columns 8–10; Rudnick and Fountain, 1995; Wedepohl, 1995; Gao *et al.*, 1998a), and Taylor and McLennan's model lower crust (column 11). It is readily apparent from this table and Figures 12 and 13 that, compared to estimates of the upper-crust composition (Table 1), there is much greater variability in estimates of the lower-crust composition. For example, TiO_2, MgO, FeO_T, and Na_2O all vary by over a factor of 2, CaO varies by almost a factor of 7, and K_2O varies by over an order of magnitude between the different estimates (Figures 12 and 13). Trace elements show correspondingly large variations (Figure 13). In contrast, modern estimates of major elements in the upper crust generally fall within 20% of each other (Table 1 and Figure 2—gray shading) and

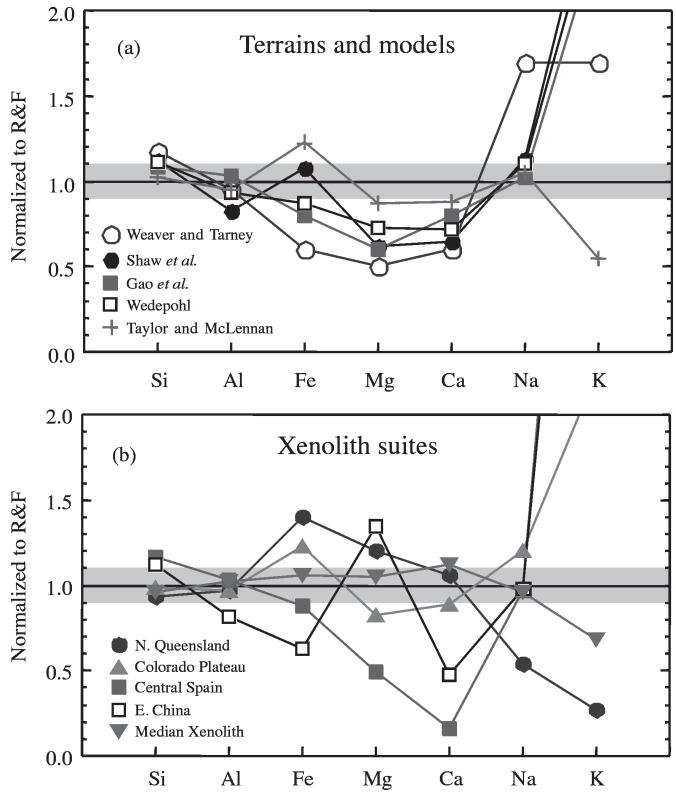

Figure 12 Comparison of different major-element estimates of the composition of the lower continental crust. All data normalized to the lower-crust composition of Rudnick and Fountain (1995), which is adopted here. Gray shaded field represents ±10% variation from the model of Rudnick and Fountain (1995). (a) Models based on granulite terrains (Scourian granulites: Weaver and Tarney, 1984; Kapuskasing Structure Zone: Shaw *et al.*, 1986), seismological models (Eastern China: Gao *et al.*, 1998a,b; western Europe: Wedepohl, 1995) and Taylor and McLennan (1985, 1995; modified by McLennan, 2001b) model lower crust. (b) Models based on weighted averages of lower crustal xenoliths. These include: Northern Queensland, Australia (Rudnick and Taylor, 1987); Colorado Plateau, USA (Condie and Selverstone, 1999); Central Spain (Villaseca *et al.*, 1999); eastern China (Liu *et al.*, 2001) and the median global lower crustal xenolith composition, updated from Rudnick and Presper (1990). Note that K data for eastern China and Central Spain are co-incident on this plot, making it hard to distinguish the separate lines.

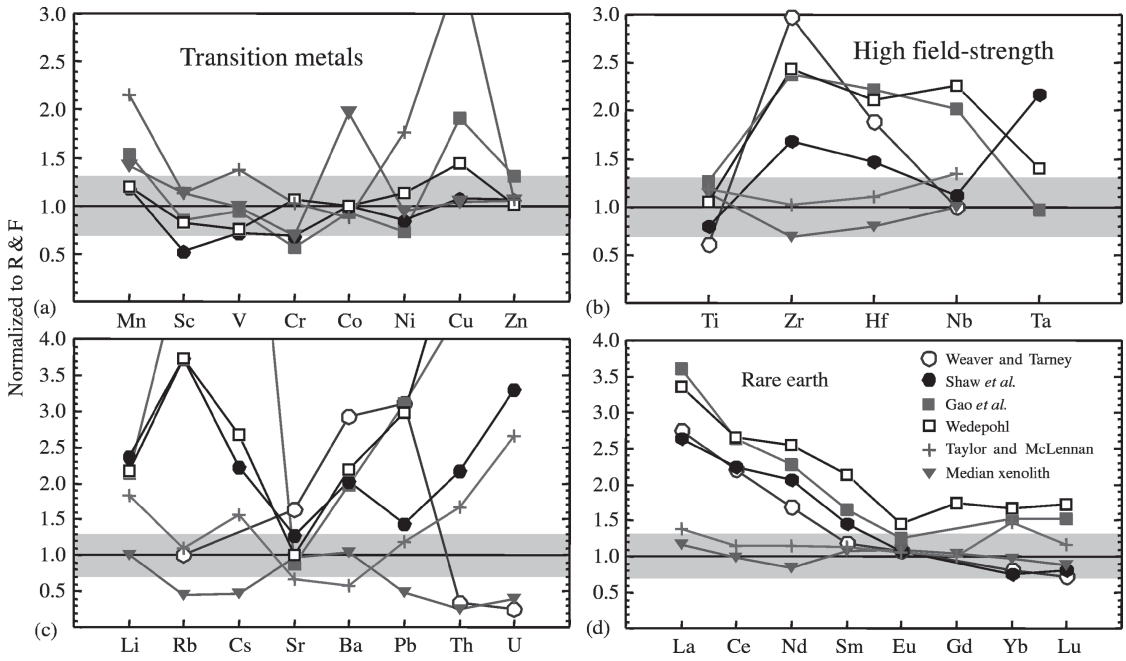

Figure 13 Comparison of different models of the trace-element composition of the lower continental crust. All values normalized to the lower-crust composition of Rudnick and Fountain (1995), which is adopted here as the "best estimate" of the global lower crust. Gray-shaded field represents ±30% variation from this value. Trace elements are divided into the following groups: (a) transition metals, (b) high-field strength elements, (c) alkali, alkaline earth, and actinides, and (d) REEs.

most trace elements fall with 50%. We now explore the possible reasons for these variations, with an eye towards determining a "best estimate" of the global lower-crust composition.

The two lower-crustal estimates derived from averages of surface granulites are generally more evolved than other estimates (Table 7, and Figures 12 and 13). Weaver and Tarney's (1984) lower-crustal estimate derives from the average of Archean Scourian granulites in the Lewisian complex, Scotland. It is one of the most evolved compositions given in the table and is characterized by a steeply fractionated REE pattern, which is characteristic of Archean granitoids of the tonalite–trondhjemite–granodiorite assemblage (see Chapter 3.11) and severe depletions in the large-ion lithophile elements, in addition to thorium and uranium (Rudnick *et al*., 1985). The estimate of Shaw *et al*. (1994) derives from a weighted average of the granulite-facies rocks of the Kapuskasing Structure zone, Canadian Shield. The average is intermediate in overall composition. As discussed in Section 3.01.3.4.1, the Kapuskasing cross-section provides samples down to depths of ~25 km, leaving the lower 20 km of lower crust unexposed. Seismic-velocity data show this unexposed deepest crust to be mafic in bulk composition, consistent with the limited data for lower-crustal xenoliths from the Superior province (Moser and Heaman, 1997). Thus, the lower-crustal estimates of Weaver and Tarney (1984) and Shaw *et al*. (1994) may be representative of evolved lower crust in Archean cratons lacking a high-velocity lower crust, but are unlikely to be representative of the global continental lower crust (Archean cratons constitute only ~7% of the total area of the continental crust (Goodwin, 1991)).

The lower-crustal estimates derived from particular xenolith suites (columns 3–6, Table 7) were selected to illustrate the great compositional heterogeneity in the deep crust. The average weighted composition of lower-crustal xenoliths from central Spain (Villaseca *et al*., 1999) is one of the most felsic compositions in Table 7 (with ~63 wt.% SiO_2, Figure 12(b)). It has higher K_2O content than nearly every estimate of the upper crust composition (Table 1), and has such a high heat production (0.8 $\mu W\ m^{-3}$), that a 40 km thickness of crust with average upper- and middle-crustal compositions given in Tables 3 and 5, respectively, would generate a surface heat flow of 41 $mW\ m^{-2}$. This is equivalent to 100% of surface heat flow through Archean crust, 85% of surface heat flow through Proterozoic crust, and 71% of the surface heat flow through Paleozoic crust (see Chapter 3.02). Assuming the heat flux through the Moho is ~17 $mW\ m^{-2}$ (see Chapter 3.02) this lower-crust composition could thus be representative of the lower crust in Phanerozoic regions with high surface heat flow, but clearly cannot be representative of the global

Table 7 Compositional estimates of the lower continental crust. Major elements in weight percent.

	1 *Weaver and Tamey (1984)*	*2* *Shaw et al. (1994)*	*3* *Rudnick and Taylor (1987)*	*4* *Condie and Selverstone (1999)*	*5* *Villaseca et al. (1999)*	*6* *Liu et al. (2001)*	*7* *Updated from Rudnick and Presper (1990)*	*8* *Rudnick and Fountain (1995)*	*9* *Wedepohl (1995)*	*10* *Gao et al. (1998a)*	*11* *Taylor and McLennan (1985, 1995)*
SiO_2	62.9	58.3	49.6	52.6	62.7	59.6	52.0	53.4	59.0	59.8	54.3
TiO_2	0.5	0.65	1.33	0.95	1.04	0.60	1.13	0.82	0.85	1.04	0.97[b]
Al_2O_3	16.0	17.4	16.4	16.4	17.4	13.9	17.0	16.9	15.8	14.0	16.1
FeO_T[a]	5.4	7.09	12.0	10.5	7.52	5.44	9.08	8.57	7.47	9.30	10.6
MnO	0.08	0.12	0.22	0.16	0.10	0.08	0.15	0.10	0.12	0.16	0.22
MgO	3.5	4.36	8.72	6.04	3.53	9.79	7.21	7.24	5.32	4.46	6.28
CaO	5.8	7.68	10.1	8.50	1.58	4.64	10.28	9.59	6.92	6.20	8.48
Na_2O	4.5	2.70	1.43	3.19	2.58	2.60	2.61	2.65	2.91	3.00	2.79
K_2O	1.0	1.47	0.17	1.37	3.41	3.30	0.54	0.61	1.61	1.75	0.64[b]
P_2O_5	0.19	0.24		0.21	0.16	0.13	0.13	0.10		0.21	
Mg#	53.4	52.3	56.5	50.5	45.6	76.2	58.6	60.1	55.9	46.1	51.4
Li		14				3.3	5	6	13	13	11
Be									1.7	1.1	1.0
B		3.2							5	7.6	8.3
N									34		
F									429	703	
S									408	231	
Cl									278	216	
Sc		16	33	28	17	20	29	31	25	26	35[b]
V		140	217		139	100	189	196	149	185	271[b]
Cr	88	168	276	133	178	490	145	215	228	123	219[b]
Co		38	31	20	22	31	41	38	38	36	33[b]
Ni	58	75	141	73	65	347	80	88	99	64	156[b]
Cu		28	29		40		32	26	37	50	90
Zn		83			83	89	85	78	79	102	83
Ga						15	17	13	17	19	18
Ge									1.4	1.24	1.6
As									1.3	1.6	0.8
Se									0.17	0.17	0.05
Br									0.28		
Rb	11	41	12	37	90	51	7	11	41	56	12[b]
Sr	569	447	196	518	286	712	354	348	352	308	230
Y	7	16	28		40	8	20	16	27	18	19
Zr	202	114	127	86	206	180	68	68	165	162	70
Nb	5	5.6	13	7.75	15	6.4	5.6	5.0	11	10	6.7[b]
Mo			0.8				0.8		0.6	0.54	0.8
Ru											
Pd										2.78	1
Ag									80	51	90

(continued)

Table 7 (continued).

	1 *Weaver and Tamey (1984)*	*2* *Shaw et al. (1994)*	*3* *Rudnick and Taylor (1987)*	*4* *Condie and Selverstone (1999)*	*5* *Villaseca et al. (1999)*	*6* *Liu et al. (2001)*	*7* *Updated from Rudnick and Presper (1990)*	*8* *Rudnick and Fountain (1995)*	*9* *Wedepohl (1995)*	*10* *Gao et al. (1998a)*	*11* *Taylor and McLennan (1985, 1995)*
Cd									0.101	0.097	0.098
In									0.052		0.050
Sn							1.3		2.1	1.34	1.5
Sb									0.30	0.09	0.2
I									0.14		
Cs		0.67	0.07			0.15	0.19	0.3	0.8	2.6	0.47[b]
Ba	757	523	212	564	994	1434	305	259	568	509	150
La	22	21	12	22	38	18	9.5	8	27	29	11
Ce	44	45	28	46	73	36	21	20	53	53	23
Pr			3.6				[2.1]		7.4		2.8
Nd	19	23	16	24	30	14	13.3	11	28	25	13
Sm	3.3	4.1	4.1	5.17	6.6	2.59	3.40	2.8	6.0	4.65	3.17
Eu	1.18	1.18	1.36	1.30	1.8	0.97	1.20	1.1	1.6	1.39	1.17
Gd			4.31	4.67	6.8		3.6	3.1	5.4		3.13
Tb	0.43	0.28	0.79	0.72		0.33	0.50	0.48	0.81	0.86	0.59
Dy			5.05		6.7		3.9	3.1	4.7		3.6
Ho			1.12				0.6	0.68	0.99		0.77
Er			3.25				2.0	1.9			2.2
Tm	0.19										0.32
Yb	1.2	1.13	3.19	2.09	4.0	0.79	1.70	1.5	2.5	2.29	2.2
Lu	0.18	0.2		0.37	0.65	0.12	0.30	0.25	0.43	0.38	0.29
Hf	3.6	2.8	3.3	1.9		4.6	1.9	1.9	4.0	4.2	2.1
Ta		1.3		0.5	2.1	0.3	0.5	0.6	0.8	0.6	0.7[b]
W			0.5				0.5		0.6	0.51	0.6[b]
Re											0.4
Os											0.05
Ir											0.13
Pt										2.87	
Au										1.58	3.4
Hg									0.021	0.0063	
Tl									0.26	0.38	0.23
Pb	13	6	3.3	9.8		12.9	4.1	4	12.5	13	5.0[b]
Bi									0.037	0.38	0.038
Th	0.42	2.6	0.54	1.64	5.74	0.49	0.50	1.2	6.6	5.23	2.0[b]
U	0.05	0.66	0.21	1.38	0.47	0.18	0.18	0.2	0.93	0.86	0.53[b]

[a] Total Fe as FeO. [b] Value from McLennan (2001b).

1. Weighted average of Scourian granulites, Scotland, from Weaver and Tarney (1984). 2. Weighted average of Kapuskasing Structural Zone granulites, from Shaw *et al.* (1994). 3. Average lower crustal xenoliths from the McBride Province, Queensland, Australia from Rudnick and Taylor (1987). 4. Average lower crustal xenoliths from the four corners region, Colorado Plateau, USA from Condie and Selverstone (1999). 5. Weighted mean composition calculated from lithologic proportions of lower crustal xenoliths from Central Spain from Villaseca *et al.*, (1999). 6. Weighted average of lower crustal xenoliths from Hannuoba according to seismic crustal model of North China Craton from Liu *et al.* (2001). 7. Median worldwide lower crustal xenoliths from Rudnick and Presper (1990), updated with data from more recent publications. Complete database available at http://earthref.org/cgi-bin/erda.cgi?$n = 1, 2, 3, 8$, and on Treatise website. 8. Average lower crust derived from global average seismic velocities and granulites from Rudnick and Fountain (1995). 9. Average lower crust in western Europe derived from seismic data and granulite xenolith compositions from Wedepohl (1995). 10. Average lower crust derived from seismic velocities and granulite data from the North China craton from Gao *et al.* (1998a). 11. Average lower crust from Taylor and McLennan (1985, 1995), updated by McLennan and Taylor (1996) and McLennan (2001b). Mg# = molar $100 \times Mg/(Mg + Fe_{tot})$.

average lower crust. Likewise, the "evolved" xenolith-derived lower crustal estimate of Liu *et al*. (2001) for the central zone of the North China craton, also has a high-K_2O content that exceeds that in most modern estimates of the upper continental crust (Table 1 and Figure 12(b)). Total crustal heat production calculated as described above using the Liu *et al*. composition for the lower crust yields a value of 0.95 $\mu W\ m^{-3}$, which corresponds to a surface heat flow of 34 $mW\ m^{-2}$. This composition is thus unlikely to be representative of the lower crust in Archean cratons, where average surface heat flow is $41 \pm 1\ mW\ m^{-2}$ (Nyblade and Pollack, 1993). However, surface heat flow through this part of the North China craton is unusually high ($50\ mW\ m^{-2}$; Hu *et al*., 2000), thus permitting a more radiogenic lower crust in this region. Other peculiarities of this bulk composition include an extreme Mg# of 76 (Mg# = 100 * molar Mg/(Mg + Fe)) and extreme nickel (347 ppm) and chromium (490 ppm) contents. These values are especially unusual given the rather felsic bulk composition of this estimate and reflect the very high Mg# mafic granulites present in this suite and the inclusion of up to 25% peridotite within the lower-crustal mixture modeled by Liu *et al*. (2001). This estimate also has the highest strontium and barium contents of all estimates (712 ppm and 1,434 ppm, respectively) and is the most HREE depleted (Table 7). The two remaining average lower-crustal xenolith suites (Rudnick and Taylor, 1987 and Condie and Selverstone, 1999) both have mafic compositions that more closely approximate the global average-xenolith composition (column 7 in Table 7).

It has been shown repeatedly from numerous xenolith studies that the majority of lower-crustal xenoliths are mafic in composition (Rudnick and Presper (1990), Rudnick (1992), and Downes (1993) and references therein). Thus, the "best estimate" of the lower crust made on the basis of xenolith studies is found in column 7 of Table 7, which gives the median composition of all analyzed lower-crustal xenoliths. Yet it remains unclear to what degree xenolith compositions reflect average lower crust. Uncertainties include the degree to which volcanic pipes sample a representative cross-section of the deep crust and whether certain xenoliths (e.g., felsic xenoliths and meta-carbonates) suffer preferential disaggregation or dissolution in the host magmas. In addition, large compositional variations are apparent from place to place (Figure 12(b)) and xenolith data are only available for limited regions of the continents.

For these reasons, the best estimates of lower-crustal composition rely on combining seismic velocities of the lower crust with compositions of "typical" lower-crustal lithologies to derive the bulk composition (Christensen and Mooney, 1995; Rudnick and Fountain, 1995; Wedepohl, 1995; Gao *et al*., 1998a). Wedepohl (1995) used seismic data from the European Geotraverse and Gao *et al*. (1998a) used data from the North China craton to estimate lower-continental crust composition. The resulting compositions derived from these studies (Table 7, and Figures 12 and 13) reflect the thin and more evolved crust in these regions relative to global averages, and produce too much heat to be representative of global lower crust (Rudnick *et al*., 1998; see Chapter 3.02).

The studies of Rudnick and Fountain (1995) and Christensen and Mooney (1995) are probably best representative of the global deep continental crust, as these authors used overlapping, but not identical, global seismic data sets and independent geochemical data sets to derive the bulk-crust composition. Christensen and Mooney (1995) do not provide the compositional data they used for their lower-crustal assemblages and they do not report a lower-crust composition; thus, one cannot derive an independent estimate of the bulk lower crust from their work. However, they do model the global lower crust (25–40 km depth) as containing ~7% tonalite gneiss and 93% mafic lithologies (including amphibolite, mafic granulite, and mafic-garnet granulite). Such a mafic-bulk composition is consistent with the results of Rudnick and Fountain (1995) (Table 7). Thus, we adopt the lower-crust composition of Rudnick and Fountain (1995) as the best available model of global lower-crust composition, with the proviso that our understanding will evolve as more extensive and detailed information becomes available about the seismic velocity structure of the lower crust. This composition has higher iron, magnesium, and calcium, and considerably lower potassium than most other estimates of the lower continental crust (Figure 12), reflecting the overall high *P*-wave velocities in the lower crust on a worldwide basis and the use of lower crustal xenoliths to derive the average mafic granulite composition. Reliance on xenolith data also accounts for the lower concentrations of highly incompatible trace elements in this composition (e.g., LREEs, rubidium, caesium, barium, thorium, and uranium) compared to most other estimates of the lower crust (Figure 13). For trace elements not considered by Rudnick and Fountain (1995), we adopt the averages of values given in Gao *et al*. (1998a), Wedepohl (1995), or studies focused specifically on the lower-crustal composition of particular trace elements (e.g., antimony, arsenic, molybdenum (Sims *et al*., 1990); boron (Leeman *et al*., 1992); tungsten (Newsom *et al*., 1996); rhenium; and osmium (Saal *et al*., 1998)). The resulting lower-crustal composition is given in Table 8.

Table 8 Recommended composition of the lower continental crust. Major elements in weight percent. Trace element concentration units the same as in Table 2.

Element	*Lower crust*	*Source*[a]	*Element*	*Lower crust*	*Source*[a]
SiO_2	53.4	1	Ag	65	2
TiO_2	0.82	1	Cd	0.1	2
Al_2O_3	16.9	1	In	0.05	4
FeOT	8.57	1	Sn	1.7	2
MnO	0.10	1	Sb	0.1	5
MgO	7.24	1	I	0.1	4
CaO	9.59	1	Cs	0.3	1
Na_2O	2.65	1	Ba	259	1
K_2O	0.61	1	La	8	1
P_2O_5	0.10	1	Ce	20	1
Li	13	2	Pr	2.4	7
Be	1.4	2	Nd	11	1
B	2	3	Sm	2.8	1
N	34	4	Eu	1.1	1
F	570	2	Gd	3.1	1
S	345	2	Tb	0.48	1
Cl	250	2	Dy	3.1	1
Sc	31	1	Ho	0.68	1
V	196	1	Er	1.9	1
Cr	215	1	Tm	0.24	7
Co	38	1	Yb	1.5	1
Ni	88	1	Lu	0.25	1
Cu	26	1	Hf	1.9	1
Zn	78	1	Ta	0.6	1
Ga	13	1	W	0.6	8
Ge	1.3	2	Re	0.18	9
As	0.2	5	Os	0.05	9
Se	0.2	2	Ir	0.05	10
Br	0.3	4	Pt	2.7	6
Rb	11	1	Au	1.6	11
Sr	348	1	Hg	0.014	2
Y	16	1	Tl	0.32	2
Zr	68	1	Pb	4	1
Nb	5	1	Bi	0.2	2
Mo	0.6	5	Th	1.2	1
Ru	0.75	6	U	0.2	1
Pd	2.8	4			

[a] Sources: 1. Rudnick and Fountain (1995). 2. Average of values given in Wedepohl (1995) and Gao *et al*. (1998a). 3. Leeman *et al*. (1992). 4. Wedepohl (1995). 5. Calculated assuming As/Ce = 0.01, Sb/Ce = 0.005 and Mo/Ce = 0.03 (Sims *et al*., 1990). 6. Assuming Ru/Ir ratio and Pt/Pd ratios equal to that of upper continental cust. 7. Value interpolated from REE pattern. 8. Average of all values in Table 7, plus correlation from Newsom *et al*. (1996), using W/Th = 0.5. 9. Saal *et al*. (1998). 10. Taylor and McLennan (1985). 11. Gao *et al*. (1998a)

It is interesting to note that the lower-crust composition of Rudnick and Fountain (1995) is quite similar to that of Taylor and McLennan (1985, 1995). However, this similarity is deceptive as Taylor and McLennan's "lower crust" actually represents the crust below the "upper crust" or between ~10 km depth and the Moho. Thus, Taylor and McLennan's lower crust is equivalent to the combined middle and lower crust given here, and is considerably less evolved than the crustal models adopted here (see Section 3.01.4 for a description of how Taylor and McLennan's crust composition was derived).

In summary, our knowledge of lower-crustal composition, like the middle crust, is limited by the ambiguity in deriving chemical compositions from seismic velocities, the lack of high-quality data for a number of trace elements and by the still fragmentary knowledge of the seismic structure of the continental crust. Although the various lower-crustal compositional models in Table 7 show large variations, the true uncertainty in the global model is likely to fall within the seismologically constrained estimates and thus the uncertainty is on the order of ≤30% for most major elements. Uncertainties in trace-element abundances are generally higher (Figure 13). Whereas concentrations of the transition metals between the different estimates generally fall within ~60%, uncertainties in the highly incompatible trace elements (e.g., caesium and thorium; Figure 13) and highly siderophile elements (PGE) can be as large as an order of magnitude. Despite these rather large uncertainties, there are some conclusions that can be drawn from this analysis. The lower crust has a mafic composition and is strongly depleted in potassium and other highly incompatible elements relative to higher levels of the crust. The lower crust is LREE enriched and probably has a positive europium anomaly (Figure 14). Like the upper and middle crust, it is also characterized by enrichment in lead relative to cerium and praseodymium and depletion in niobium relative to lanthanum. It is also likely to be enriched in strontium relative to neodymium (Figure 14).

3.01.4 BULK CRUST COMPOSITION

The earliest estimates of the continental crust composition were derived from analyses and observed proportions of upper crustal rock types (Clarke, 1889; Clarke and Washington, 1924; Ronov and Yaroshevsky, 1967). These estimates do not take into account the changes in both lithological proportions and metamorphic grade that are now recognized to occur with depth in the crust (see Section 3.01.3) and are thus more appropriately regarded as estimates of upper-crust composition. (It is interesting to note, however, the remarkably good correspondence of these earliest estimates with those of today (cf. Tables 1 and 9)) Taylor (1964) used a different approach to estimate bulk crust composition. Following Goldschmidt (1933), he assumed that the nearly constant REE pattern of sedimentary rocks reflected the REE pattern of the crust as a whole, and recreated that pattern by mixing "average" felsic- and mafic-igneous rocks in approximately equal proportions. His composition (Table 9) is also remarkably similar to more modern estimates

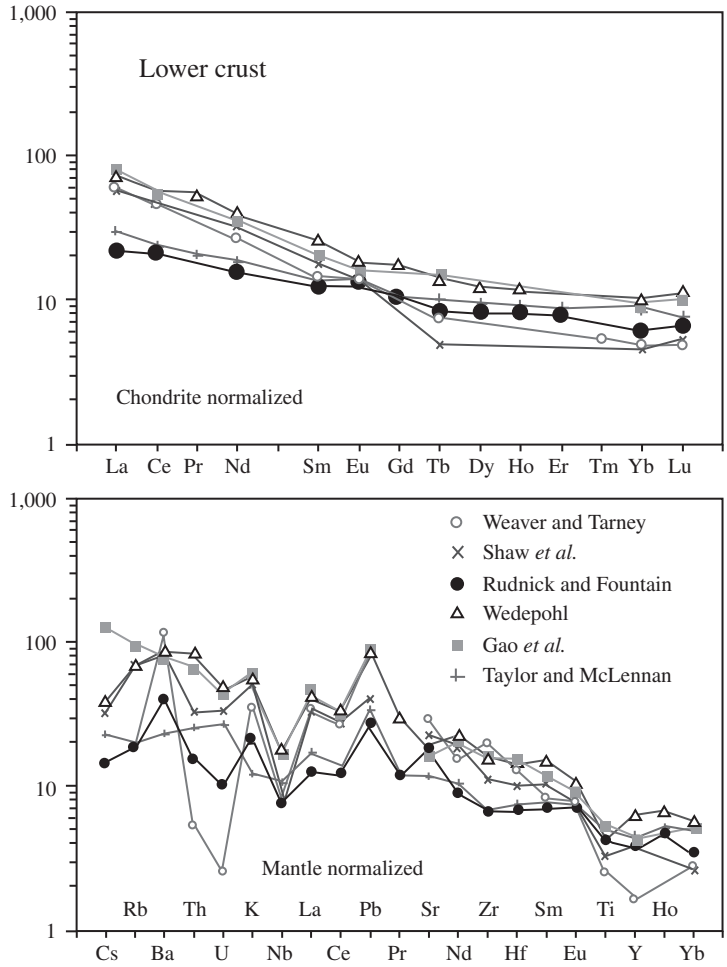

Figure 14 REE (upper) and multi-element plot (lower) of the compositions of the lower crust given in Table 7. Compositions derived from individual xenolith suites not shown. Chondrite values from Taylor and McLennan (1985) and primitive mantle values from McDonough and Sun (1995).

for a large number of elements, but like the earliest estimates, is more appropriately considered an upper crustal estimate since sediments derive strictly from upper crustal sources. Following the plate-tectonic revolution, Taylor (1967) modified his crust-composition model. Recognizing that the present site of continental growth is at convergent-plate margins, he developed the "island arc" or "andesite" model for crustal growth and hence crust composition. In this model (Taylor, 1967, 1977), the crust is assumed to have a composition equal to average convergent-margin andesite. Taylor and McLennan (1985) discussed the difficulties with this approach. Moreover, it is now recognized that basalts dominate present intra-oceanic arcs (see Chapter 3.18, and references therein).

Crust-composition estimates made since the 1970s derive from a variety of approaches. Smithson (1978) was the first to use seismic velocities to determine the lithological makeup of the deep crust. His crust composition is similar to other estimates, save for the very high alkali element contents (4 wt.% Na_2O and 2.7 wt.% K_2O), which presumably reflects the choice of granitic rocks used in his calculations. Holland and Lambert (1972), Weaver and Tarney (1984), and Shaw *et al*. (1986) recognized the importance of granulite-facies rocks in the deep crust and based their crustal models on the composition of rocks from high-grade terranes exposed at the Earth's surface and previous estimates of upper crustal composition.

Taylor and McLennan (1985, 1995), like Taylor's previous estimates (Taylor, 1967, 1977), derived their crust composition using an approach based on assumptions about its formation processes. They assumed that 75% of the crust grew during the Archean from bimodal volcanism and the remaining 25% originated from post-Archean accretion of island arcs having an average andesite composition (from Taylor, 1977). To constrain the proportions of mafic- to felsic-Archean volcanics, they used heat-flow data

Table 9 Compositional estimates of the bulk continental crust. Major elements in weight percent. Trace element concentration units the same as in Table 2.

	1 *Taylor (1964)*	*2* *Ronov and Yaroshevsky (1967)*	*3* *Holland and Lambert (1972)*	*4* *Smithson (1978)*	*5* *Weaver and Tarney (1984)*	*6* *Shaw* et al. *(1986)*	*7* *Christensen and Mooney (1995)*	*8* *Rudnick and Fountain (1995)*	*9* *Wedepohl (1995)*	*10* *Gao* et al. *(1998a)*	*11* *Taylor and McLennan (1985, 1995)*	*12* *This study*[a]
SiO_2	60.4	62.2	62.8	63.7	63.9	64.5	62.4	60.1	62.8	64.2	57.1	60.6
TiO_2	1.0	0.8	0.7	0.7	0.6	0.7	0.9	0.7	0.7	0.8	0.9	0.72
Al_2O_3	15.6	15.7	15.7	16.0	16.3	15.1	14.9	16.1	15.4	14.1	15.9	15.9
FeO_T[b]	7.3	6.3	5.5	5.3	5.0	5.7	6.9	6.7	5.7	6.8	9.1	6.71
MnO	0.12	0.10	0.10	0.10	0.08	0.09	0.10	0.11	0.10	0.12	0.18	0.10
MgO	3.9	3.1	3.2	2.8	2.8	3.2	3.1	4.5	3.8	3.5	5.3	4.66
CaO	5.8	5.7	6.0	4.7	4.8	4.8	5.8	6.5	5.6	4.9	7.4	6.41
Na_2O	3.2	3.1	3.4	4.0	4.2	3.4	3.6	3.3	3.3	3.1	3.1	3.07
K_2O	2.5	2.9	2.3	2.7	2.1	2.4	2.1	1.9	2.7	2.3	1.3	1.81
P_2O_5	0.24		0.20		0.19	0.14	0.20	0.20		0.18		0.13
Mg#	48.7	47.0	50.9	49.0	50.5	50.1	44.8	54.3	54.3	48.3	50.9	55.3
Li	20							11	18	17	13	17
Be	2.8								2.4	1.7	1.5	1.9
B	10					9.3			11	18	10	11
N	20								60			56
F	625								525	602		553
S	260								697	283		404
Cl	130								472	179		244
Sc	22					13		22	16	19	30	21.9
V	135					96		131	98	128	230	138
Cr	100				56	90		119	126	92	185	135
Co	25					26		25	24	24	29	26.6
Ni	75				35	54		51	56	46	105	59
Cu	55					26		24	25	38	75	27
Zn	70					71		73	65	81	80	72
Ga	15							16	15	18	18	16
Ge	1.5								1.4	1.25	1.6	1.3
As	1.8								1.7	3.1	1.0	2.5
Se	0.05								0.12	0.13	0.05	0.13
Br	2.5								1.0			0.88
Rb	90				61	76		58	78	69	37[c]	49
Sr	375				503	317		325	333	285	260	320
Y	33				14	26		20	24	17.5	20	19
Zr	165				210	203		123	203	175	100	132
Nb	20				13	20		8[d]	19	11	8[d]	8
Mo	1.5								1.1	0.65	1.0	0.8

Ru					0.1			0.57
Pd					0.4	1.74	1	1.5
Ag	70				70	52	80	56
Cd	0.20				0.10	0.08	0.10	0.08
In	0.1				0.05		0.05	0.05
Sn	2.0				2.3	1.5	2.5	1.7
Sb	0.2				0.3	0.2	0.2	0.2
I	0.5				0.8			0.7
Cs	3.0			2.6	3.4	2.8	1.5[c]	2
Ba	425	707	764	390	584	614	250	456
La	30	28		18	30	31.6	16	20
Ce	60	57		42	60	60.0	33	43
Pr	8.2				6.7		3.9	4.9
Nd	28	23		20	27	27.4	16	20
Sm	6	4.1		3.9	5.3	4.84	3.5	3.9
Eu	1.2	1.09		1.2	1.3	1.27	1.1	1.1
Gd	5.4				4.0		3.3	3.7
Tb	0.9	0.53		0.56	0.65	0.82	0.60	0.6
Dy	3				3.8		3.7	3.6
Ho	1.2				0.80		0.78	0.77
Er	2.8				2.1		2.2	2.1
Tm	0.48	0.24			0.30		0.32	0.28
Yb	3.0	1.5		2.0	2.0	2.2	2.2	*1.9*
Lu	0.50	0.23		0.33	0.35	0.35	0.30	0.30
Hf	3	4.7	5	3.7	4.9	4.71	3.0	3.7
Ta	2		4	0.7[d]	1.1	0.6	0.8[c]	0.7
W	1.5				1.0	0.7	1.0	1
Re					0.4		0.4	0.19
Os					0.05		0.05	0.041
Ir					0.05		0.10	0.037
Pt					0.4	1.81		0.5
Au	40				2.5	1.21	3.0	1.3
Hg	0.08				0.040	0.009		0.03
Tl	0.45				0.52	0.39	0.36	0.50
Pb	12.5	15	20	12.6	14.8	15	8.0	11
Bi	0.17				0.085	0.27	0.06	0.18
Th	9.6	5.7	9	5.6	8.5	7.1	4.2	5.6
U	2.7	1.3	1.8	1.4	1.7	1.2	1.1	1.3

Major elements recast to 100% anhydrous.
[a] See Table 10 for derviation of this estimate. [b] Total Fe as FeO. Mg# = molar $100 \times Mg/(Mg + Fe_{tot})$. [c] Updated by McLennan (2001b). [d] Updated by Barth *et al*. (2000).

from Archean cratons, which is relatively low and uniform at ~40 mW m^{-2} (see Chapter 3.02). Assuming that half the surface heat flow derives from the mantle yielded a mafic to felsic proportion of 2 : 1. This dominantly mafic Archean-crustal component is reflected in the major- and trace-element composition of their crust. Their crust has low SiO_2 and K_2O, high MgO and CaO, and very high FeO content. It also has the highest transition-metal concentrations and lowest incompatible element concentrations of all the models presented in Table 9.

Refinements of the Taylor and McLennan (1985) model are provided by McLennan and Taylor (1996) and McLennan (2001b). The latter is a modification of several trace-element abundances in the upper crust and as such, should not affect their compositional model for the bulk crust, which does not rely on their upper crustal composition. Nevertheless, McLennan (2001b) does provide modified bulk-crust estimates for niobium, rubidium, caesium, and tantalum (and these are dealt with in the footnotes of Table 9). McLennan and Taylor (1996) revisited the heat-flow constraints on the proportions of mafic and felsic rocks in the Archean crust and revised the proportion of Archean-aged crust to propose a more evolved bulk crust composition. This revised composition is derived from a mixture of 60% Archean crust (which is a 50 : 50 mixture of mafic and felsic end-member lithologies), and 40% average-andesite crust of Taylor (1977). McLennan and Taylor (1996) focused on potassium, thorium, and uranium, and did not provide amended values for other elements, although other incompatible elements will be higher (e.g., rubidium, barium, LREEs) and compatible elements lower in a crust composition so revised.

More recently, a number of studies have estimated the bulk-crust composition by deriving lithological proportions for the deep crust from seismic velocities (as discussed in Section 3.01.3) with upper crustal contributions based on data for surface rocks or previous estimates of the upper crust (Christensen and Mooney, 1995; Rudnick and Fountain, 1995; Wedepohl, 1995; Gao *et al*., 1998a) (Table 9). Like previous estimates of the crust, all of these show intermediate bulk compositions with very similar major-element contents. The greatest differences in major elements between these recent seismologically based estimates are for MgO, CaO, and K_2O, which show ~30% variation, with the Rudnick and Fountain (1995) estimate having the highest MgO and CaO, and lowest K_2O (Table 9, Figure 15). Most trace elements from these estimates fall within 30% total variation as well (Figure 16); the exceptions are trace elements for which very limited data exist (i.e., sulfur, chlorine, arsenic, tin, mercury, bismuth, and the PGEs).

Table 10 Recommended composition of the bulk continental crust.

Element	*Units*		*Element*	*Units*	
SiO_2	wt.%	60.6	Ag	ng g^{-1}	56
TiO_2	”	0.7	Cd	μg g^{-1}	0.08
Al_2O_3	”	15.9	In	”	0.052
FeOT	”	6.7	Sn	”	1.7
MnO	”	0.10	Sb	”	0.2
MgO	”	4.7	I[a]	”	0.7
CaO	”	6.4	Cs	”	2
Na_2O	”	3.1	Ba	”	456
K_2O	”	1.8	La	”	20
P_2O_5	”	0.1	Ce	”	43
Li	μg g^{-1}	16	Pr	”	4.9
Be	”	1.9	Nd	”	20
B	”	11	Sm	”	3.9
N[a]	”	56	Eu	”	1.1
F	”	553	Gd	”	3.7
S	”	404	Tb	”	0.6
Cl	”	244	Dy	”	3.6
Sc	”	21.9	Ho	”	0.77
V	”	138	Er	”	2.1
Cr	”	135	Tm	”	0.28
Co	”	26.6	Yb	”	1.9
Ni	”	59	Lu	”	0.30
Cu	”	27	Hf	”	3.7
Zn	”	72	Ta	”	0.7
Ga	”	16	W	”	1
Ge	”	1.3	Re[a]	ng g^{-1}	0.188
As	”	2.5	Os[a]	”	0.041
Se	”	0.13	Ir[a]	”	0.037
Br[a]	”	0.88	Pt	”	1.5
Rb	”	49	Au	”	1.3
Sr	”	320	Hg	μg g^{-1}	0.03
Y	”	19	Tl	”	0.50
Zr	”	132	Pb	”	11
Nb	”	8	Bi	”	0.18
Mo	”	0.8	Th	”	5.6
Ru[a]	ng g^{-1}	0.6	U	”	1.3
Pd	”	1.5		”	

The total-crust composition is calculated according to the upper, middle and lower-crust compositions obtained in this study and corresponding weighing factors of 0.317, 0.296 and 0.388. The weighing factors are based on the layer thickness of the global continental crust, recalculated from crustal structure and areal proportion of various tectonic units given by Rudnick and Fountain (1995).
[a] Middle crust is not considered due to lack of data.

Niobium and tantalum also show >30% total variation, but this is due to the very high niobium and tantalum contents of Wedepohl's estimate, which reflects his reliance on the old Canadian Shield data, for which niobium content is anomalously high (see discussion in Section 3.01.2.1). These elements were also compromised in the Rudnick and Fountain (1995) crust composition, which relied (indirectly) on the Canadian Shield data for the upper crust by adopting the Taylor and McLennan upper-crust composition (see discussions in Plank and Langmuir (1998) and Barth *et al*. (2000)). The values for niobium and tantalum in

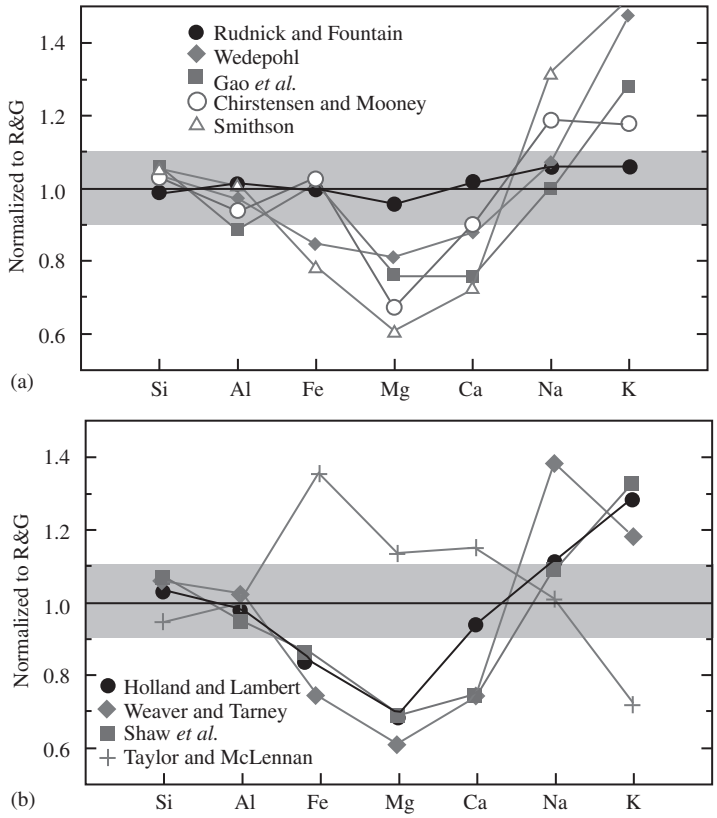

Figure 15 Comparison of different estimates of the major-element composition of the bulk continental crust. All data normalized to the new composition given here (Table 10, "R&G"); gray shading depicts 10% variation from this composition. (a) Models based on seismological data (Rudnick and Fountain, 1995; Wedepohl, 1995; Gao *et al*., 1998a; Christensen and Mooney, 1995 and Smithson, 1978). (b) Models based on both surface exposures (Holland and Lambert, 1972; Weaver and Tarney, 1984; Shaw *et al*., 1986) and Taylor and McLennan's (1985, 1995) model-generated crust composition.

the Rudnick and Fountain (1995) model given in Table 9 have been updated by Barth *et al*. (2000). These values are similar to those of Gao *et al*. (1998a) and thus the concentrations of these elements are known to within 30% in the bulk crust.

Of all the estimates in Table 9, that of Taylor and McLennan (1985, 1995) stands out as being the most mafic overall (Figures 15 and 16). This mafic composition stems from their model for Archean crust, which constitutes 75% of their crust and is composed of a 2 : 1 mixture of mafic- to felsic-igneous rocks. This relatively mafic crust composition was necessitated by their inferred low heat production in Archean crust and the inferred large proportion of the Archean-aged crust. However, such a high proportion of mafic rocks in the Archean crust is at odds with seismic data (summarized in Section 3.01.3), which show that the crust of most Archean cratons is dominated by low velocities, implying the presence of felsic (not mafic) compositions, even in the lower crust. In addition, some of the assumptions used by Taylor and McLennan (1985) regarding heat flow are not very robust, as recognized by McLennan and Taylor (1996) (see also discussion in Rudnick *et al*., 1998). First, the 20 mWm^{-2} of mantle heat flow they assumed for Archean cratons is probably too high (see Chapter 3.02), thus allowing for more heat production in the crust. Second, granulite-facies felsic rocks are often depleted in heat-producing elements (the Scourian granulites are an extreme example), thereby allowing a greater proportion of felsic rocks in the crust. Third, it is unlikely that 75% of the present continents were formed in the Archean (see Chapter 3.10) and, importantly, the observed low surface heat flow that is the rationale for Taylor and McLennan's (1985, 1995) dominantly mafic crust composition is restricted to Archean cratons, which constitute only ~7% of the present continental crust (Goodwin, 1991). Indeed, heat production of the Taylor and McLennan (1985, 1995) crustal model falls outside the range estimated for average continental crust by Jaupart and Mareschal (see Chapter 3.02)

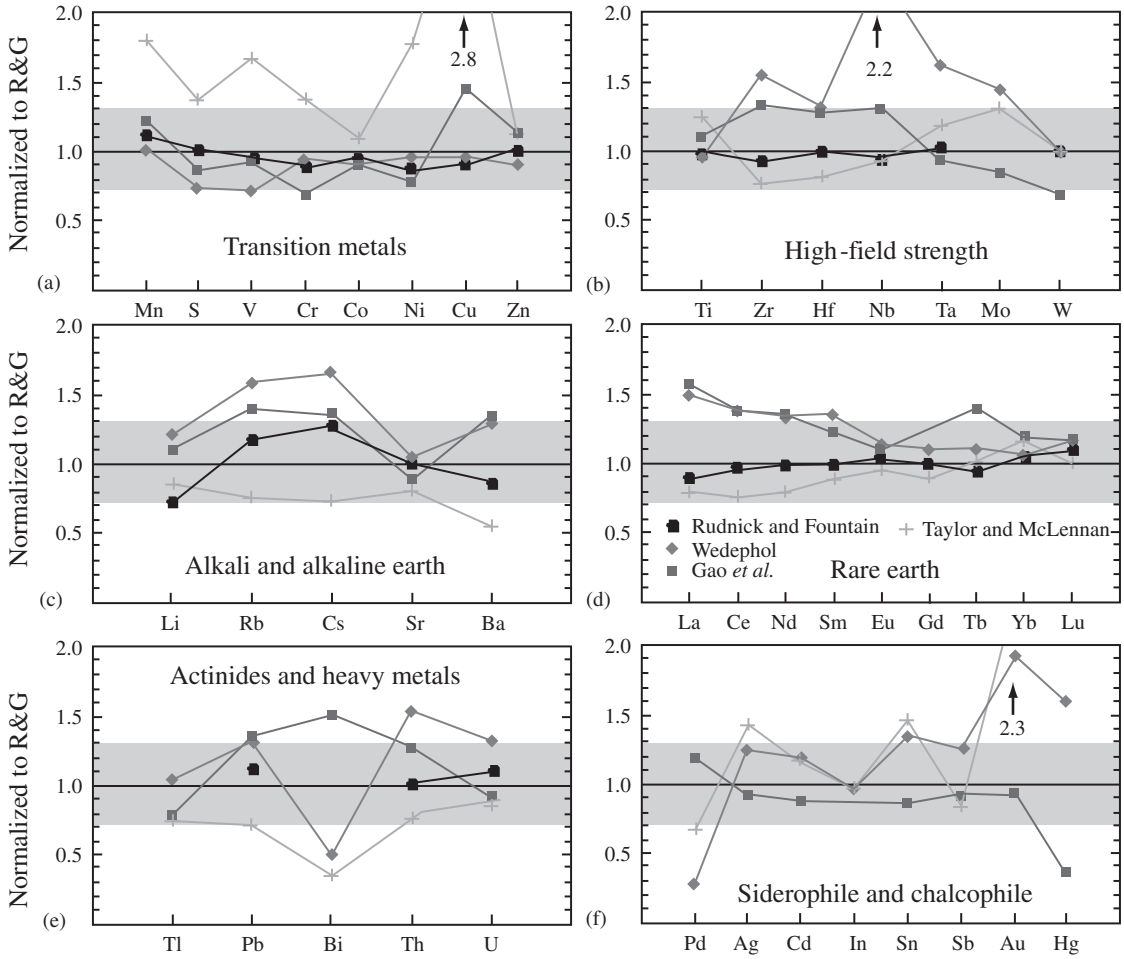

Figure 16 Comparison of the trace-element composition of bulk continental crust from seismological and model-based approaches. All data normalized to the new composition given here (Table 10, "R&G"). Gray shading depicts ±30% variation from Rudnick and Gao composition (this work). (a) Transition metals, (b) high-field strength elements, (c) alkali and alkaline earth metals, and (d) REEs, (e) actinides and heavy metals, and (f) siderophile and chalcophile elements.

(i.e., 0.58 $\mu W\ m^{-2}$ versus 0.79–0.99 $\mu W\ m^{-2}$). The modifications made to this model by McLennan and Taylor (1996) help to reconcile their model with the above observations, but the proportion of mafic rocks in Archean-aged crust still appears to be high (based on observed seismic velocities) and the total heat production (at 0.70 $\mu W\ m^{-2}$) may still be somewhat low.

3.01.4.1 A New Estimate of Crust Composition

In column 12 of Table 9 we present a new estimate of the bulk crust composition. This composition derives from our estimates of upper, middle, and lower crust given in Tables 3, 5, and 8, mixed in the proportions derived from the global compilation of Rudnick and Fountain (1995): 31.7% upper, 29.6% middle, and 38.8% lower crust. Our new crustal estimate thus relies heavily on the previously derived lower crust of Rudnick and Fountain (1995), the middle crust of Rudnick and Fountain and Gao *et al*. (1998a) and the new estimate of upper-crust composition provided here (Table 3). The latter is very similar to the upper crust of Taylor and McLennan (1985) (Figure 8), which was used by Rudnick and Fountain (1995) in calculating their bulk crust composition. The main differences lie in the concentrations of K_2O, rubidium, niobium, and tantalum, which are lower in the new estimate of the upper continental crust provided here. Accordingly, this new estimate has many similarities with that of Rudnick and Fountain (1995), but contains lower potassium, rubidium, niobium, and tantalum, and considers a wider range of trace elements than given in that model. The heat production of this new estimate is 0.89 $\mu W\ m^{-2}$, which falls in the

middle of the range estimated for average-crustal heat production by Jaupart and Mareschal (see Chapter 3.02).

Figures 15–17 show how this composition compares to other estimates of crust composition. Figure 15 shows that our new composition has generally higher MgO, CaO, and FeO, and lower Na_2O and K_2O than most other seismically based models. The differences between our model and that of Wedepohl (1995) and Gao *et al*. (1998a) likely reflect the regional character of these latter models (western Europe, eastern China), where the crust is thinner and more evolved than the global averages (Chirstensen and Mooney, 1995, and Rudnick and Fountain, 1995). The lower MgO and higher alkali elements in Christensen and Mooney's model compared to ours must stem from the differences in the chemical databases used to construct these two models, as the lithological proportions of the deep crust are very similar (Section 3.01.3). Rudnick and Fountain (1995) (and hence our current composition) used the compositions of lower-crustal xenoliths to constrain the mafic end-member of the deep crust. These xenoliths have high Mg# and low alkalis (Table 7), and thus may be chemically distinct from mafic rocks exposed on the Earth's surface (the chemical data used by Christensen and Mooney, 1995).

The variations between the different seismological-based crust compositions can be considered representative of the uncertainties that exist in our understanding of the bulk crust composition. Some elemental concentrations (e.g., silicon, aluminum, sodium) are known to within 20% uncertainty. The remaining major-element and many trace-element (transition metals, high-field strength elements, most REE) concentrations are known to within 30% uncertainty. Still some trace element concentrations are yet poorly constrained in the crust, including many of the highly siderophile elements (Figure 16).

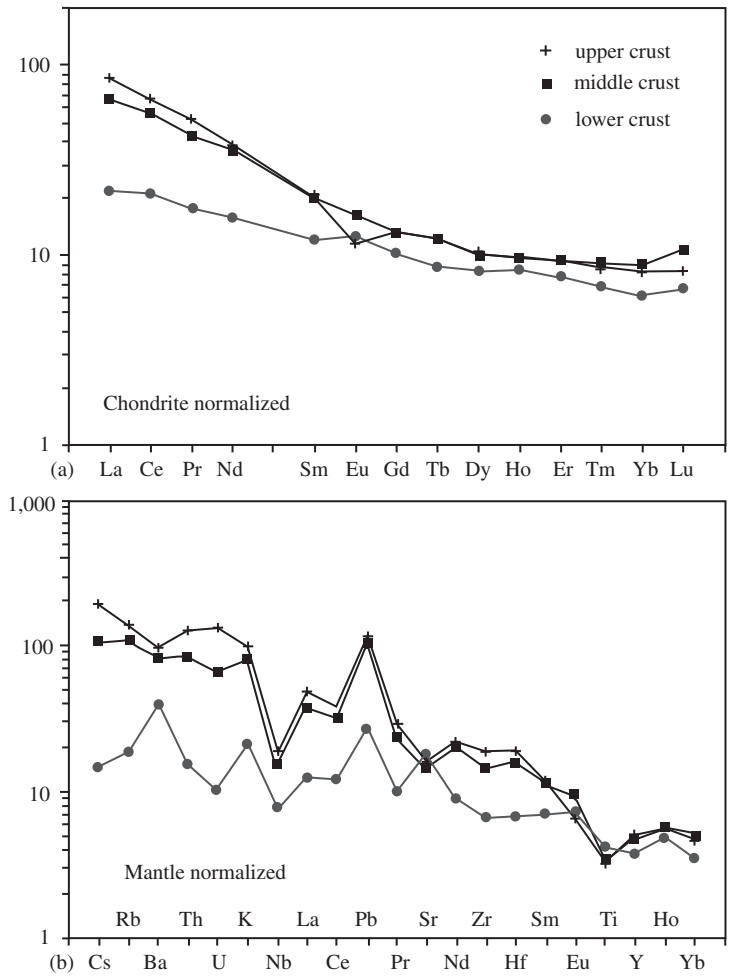

Figure 17 Comparison of (a) rare-earth and (b) additional trace-element compositions of the upper, middle, and lower crust recommended here. Chondrite values from Taylor and McLennan (1985), mantle-normalizing values from McDonough and Sun (1995).

3.01.4.2 Intracrustal Differentiation

Table 11 provides the composition of the upper, middle, lower, and bulk crust for comparison purposes and Figure 17 compares their respective REE and extended trace-element patterns. The upper crust has a large negative europium anomaly (Eu/Eu^*, Table 11) that is largely complemented by the positive europium anomaly of the lower crust; the middle crust has essentially no europium anomaly. Similar complementary anomalies exist for strontium. These features, in addition to the greater LREE enrichment of the upper crust relative to the lower crust, suggests that the upper crust is largely the product of intracrustal magmatic differentiation in the presence of plagioclase (see Taylor and McLennan, 1985; see Chapter 3.11). That is, the upper crust is dominated by granite that differentiated from the lower crust through partial melting, crystal fractionation and mixing processes. The middle crust has an overall trace-element pattern that is very similar to the upper crust, indicating that it too is dominated by the products of intracrustal differentiation. All segments of the crust are characterized by an overall enrichment of the most incompatible elements, as well as high La/Nb and low Ce/Pb ratios. These are characteristics of convergent margin magmas (see Chapter 3.18, and references therein) and thus have implications for the processes responsible for generation of the continental crust as discussed in the next section.

3.01.5 IMPLICATIONS OF THE CRUST COMPOSITION

Despite the uncertainties in estimating crust composition discussed in the previous section, there are a number of similarities that all crust-compositional models share and these may be important for understanding the origin of the crust. The crust is characterized by an overall *intermediate* igneous-rock composition, with relatively high Mg#. It is enriched in incompatible elements (Figure 18), and contains up to 50% of the silicate Earth's budget of these elements (Rudnick and Fountain, 1995). It is also well established that the crust is depleted in niobium relative to lanthanum, and has a subchondritic Nb/Ta ratio. These features are not consistent with formation of the crust by single-stage melting of peridotitic mantle, as discussed in Rudnick (1995), Kelemen (1995) and Rudnick *et al*. (2000) (see also Chapter 3.18).

If one assumes that the crust grows ultimately by igneous processes (i.e., magmatic transport of mass from the mantle into the crust), then the disparity between crust composition and the composition of primary mantle melts requires the operation of additional processes to produce the present crust composition. As reviewed in Rudnick (1995) and Kelemen (1995), these additional processes could include (but are not limited to):

(i) *Recycling of mafic/ultramafic lower crust and upper mantle via density foundering (often referred to as delamination within the geochemical literature)*. In this process, lithologically stratified continental crust is thickened during an orogenic event, causing the mafic lower crust to transform to eclogite, which has a higher density than the underlying mantle peridotite. Provided the right temperatures and viscosities exist (i.e., hot and goey), the base of the lithosphere will sink into the underlying asthenosphere. Numerical simulations of this process show that it is very likely to occur at the time of arc–continent collision (and in fact, may be impossible to avoid)(Jull and Kelemen, 2001).

(ii) *Production of crust from a mixture of silicic melts derived from subducted oceanic crust, and basaltic melts from peridotite*. This process is likely to have been more prevalent in a hotter, Archean Earth (although see Chapter 3.18 for an alternative view) and would have involved extensive silicic melt–peridotite reaction as the slab melts traverse the mantle wedge (Kelemen, 1995). The abundance of Archean-aged granitoids of the so-called "TTG" suite (trondhjemite, tonalite, granodiorite) are often cited as the surface manifestations of these processes (Drummond and Defant, 1990; Martin, 1994; see Chapter 3.11).

(iii) *Weathering of the crust, with preferential recycling of Mg ± Ca into the mantle via hydrothermally altered mid-ocean ridge basalt* (*Albarede, 1998*; *Anderson, 1982*). This hypothesis states that during continental weathering, soluble cations such as Ca^{2+}, Mg^{2+}, and Na^{+} are carried to the oceans while silicon and aluminum remain behind in the continental regolith. Whereas other elements (e.g., sodium) may be returned to the continents via arc magmatism, magnesium may be preferentially sequestered into altered seafloor basalts and returned to the mantle via subduction, producing a net change in the crust composition over time. However, one potential problem with this hypothesis is that examination of altered ocean-floor rocks suggests that magnesium may not be significantly sequestered there (see Chapter 3.15).

A fourth possibility, that ultramafic cumulates representing the chemical complement to the andesitic crust are present in the uppermost mantle, is not supported by studies of peridotite xenoliths, which show a predominance of restitic peridotite over cumulates (e.g., Wilshire *et al*., 1988). If such cumulates were originally there,

Table 11 Comparison of the upper, middle, lower and total continental crust compositions recommended here.

Element	*Upper crust*	*Middle crust*	*Lower crust*	*Total crust*
SiO_2	66.6	63.5	53.4	60.6
TiO_2	0.64	0.69	0.82	0.72
Al_2O_3	15.4	15.0	16.9	15.9
FeO_T	5.04	6.02	8.57	6.71
MnO	0.10	0.10	0.10	0.10
MgO	2.48	3.59	7.24	4.66
CaO	3.59	5.25	9.59	6.41
Na_2O	3.27	3.39	2.65	3.07
K_2O	2.80	2.30	0.61	1.81
P_2O_5	0.15	0.15	0.10	0.13
Total	100.05	100.00	100.00	100.12
Mg#	46.7	51.5	60.1	55.3
Li	24	12	13	16
Be	2.1	2.3	1.4	1.9
B	17	17	2	11
N	83		34	56
F	557	524	570	553
S	621	249	345	404
Cl	294	182	250	244
Sc	14.0	19	31	21.9
V	97	107	196	138
Cr	92	76	215	135
Co	17.3	22	38	26.6
Ni	47	33.5	88	59
Cu	28	26	26	27
Zn	67	69.5	78	72
Ga	17.5	17.5	13	16
Ge	1.4	1.1	1.3	1.3
As	4.8	3.1	0.2	2.5
Se	0.09	0.064	0.2	0.13
Br	1.6		0.3	0.88
Rb	82	65	11	49
Sr	320	282	348	320
Y	21	20	16	19
Zr	193	149	68	132
Nb	12	10	5	8
Mo	1.1	0.60	0.6	0.8
Ru	0.34		0.75	0.57
Pd	0.52	0.76	2.8	1.5
Ag	53	48	65	56
Cd	0.09	0.061	0.10	0.08
In	0.056		0.05	0.052
Sn	2.1	1.30	1.7	1.7
Sb	0.4	0.28	0.10	0.2
I	1.4		0.14	0.71
Cs	4.9	2.2	0.3	2
Ba	628	532	259	456
La	31	24	8	20
Ce	63	53	20	43
Pr	7.1	5.8	2.4	4.9
Nd	27	25	11	20
Sm	4.7	4.6	2.8	3.9
Eu	1.0	1.4	1.1	1.1
Gd	4.0	4.0	3.1	3.7
Tb	0.7	0.7	0.48	0.6
Dy	3.9	3.8	3.1	3.6
Ho	0.83	0.82	0.68	0.77
Er	2.3	2.3	1.9	2.1

(continued)

Table 11 (continued).

Element	*Upper crust*	*Middle crust*	*Lower crust*	*Total crust*
Tm	0.30	0.32	0.24	0.28
Yb	2.0	2.2	1.5	1.9
Lu	0.31	0.4	0.25	0.30
Hf	5.3	4.4	1.9	3.7
Ta	0.9	0.6	0.6	0.7
W	1.9	0.60	0.60	1
Re	0.198		0.18	0.188
Os	0.031		0.05	0.041
Ir	0.022		0.05	0.037
Pt	0.5	0.85	2.7	1.5
Au	1.5	0.66	1.6	1.3
Hg	0.05	0.0079	0.014	0.03
Tl	0.9	0.27	0.32	0.5
Pb	17	15.2	4	11
Bi	0.16	0.17	0.2	0.18
Th	10.5	6.5	1.2	5.6
U	2.7	1.3	0.2	1.3
Eu/Eu*	0.72	0.96	1.14	0.93
Heat production (μW m^{-3})	1.65	1.00	0.19	0.89
Nb/Ta	13.4	16.5	8.3	12.4
Zr/Hf	36.7	33.9	35.8	35.5
Th/U	3.8	4.9	6.0	4.3
K/U	9475	15607	27245	12367
La/Yb	15.4	10.7	5.3	10.6
Rb/Cs	20	30	37	24
K/Rb	283	296	462	304
La/Ta	36	42	13	29

they must have been subsequently removed via a process such as density foundering.

All of the above processes require return of mafic to ultramafic lithologies to the convecting mantle. These lithologies are the chemical complement of the present-day andesitic crust. Thus crustal recycling, in various forms, must have been important throughout Earth history.

Another implication of the distinctive trace element composition of the continental crust is that the primary setting of crust generation is most likely to be that of a convergent margin. The characteristic depletion of niobium relative to lanthanum seen in the crust (Figure 18) is a ubiquitous feature of convergent margin magmas (see review of Kelemen *et al.* (Chapter 3.18)) and is virtually absent in intraplate magmas. Simple mixing calculations indicate that the degree of niobium depletion seen in the crust suggests that at least 80% of the crust was generated in a convergent margin (Barth *et al.*, 2000; Plank and Langmuir, 1998).

3.01.6 EARTH'S CRUST IN A PLANETARY PERSPECTIVE

The other terrestrial planets show a variety of crustal types, but none that are similar to that of the Earth. Mercury has an ancient, heavily cratered crust with a high albedo (see review of Taylor and Scott (Chapter 1.18)). Its brightness plus the detection of sodium, and more recently the refractory element calcium, in the Mercurian atmosphere (Bida *et al.*, 2000) has led to the speculation that Mercury's crust may be anorthositic, like the lunar highlands (see Taylor, 1992 and references therein). The MESSENGER mission (http://messenger.jhuapl.edu/), currently planned to rendezvous with Mercury in 2007, should considerably illuminate the nature of the crust on Mercury.

In contrast to Mercury's ancient crust, high-resolution radar mapping of Venus' cloaked surface has revealed an active planet, both tectonically and volcanically (see review of Fegley (Chapter 1.19) and references therein). Crater densities are relatively constant, suggesting a relatively young surface ($\sim$300–500 Ma, Phillips *et al.*, 1992; Schaber *et al.*, 1992; Strom *et al.*, 1994). It has been suggested that this statistically random crater distribution may reflect episodes of mantle overturn followed by periods of quiescence (Schaber *et al.*, 1992; Strom *et al.*, 1994). Most Venusian volcanoes appear to erupt basaltic magmas, but a few are pancake-shaped, which may signify the eruption of a highly viscous lava such as rhyolite (e.g., Ivanov and Head, 1999). The unimodal topography of Venus is

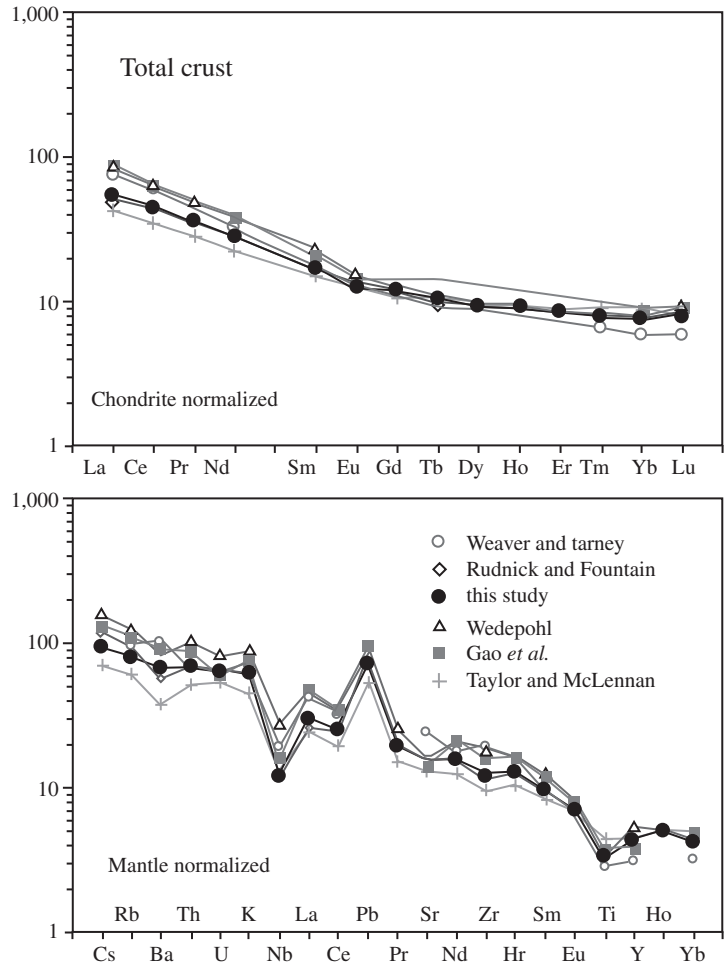

Figure 18 REE (upper) and multi-element plot (lower) of the compositions of the continental crust given in Table 9. Chondrite values from Taylor and McLennan (1985), mantle-normalizing values from McDonough and Sun (1995).

distinct from that of the Earth and there appear to be no equivalents to Earth's oceanic and continental dichotomy. It is possible that the high elevations on Venus were produced tectonically by compression of basaltic rocks made rigid by the virtual absence of water (Mackwell *et al*., 1998).

Of the terrestrial planets, only Mars has the bimodal topographic distribution seen on the Earth (Smith *et al*., 1999). In addition, evolved igneous rocks, similar to the andesites found in the continents on Earth, have also been observed on the Martian surface, although their significance and relative abundance is a matter of contention (see review by McSween (Chapter 1.22)). However, the bimodal topography of Mars appears to be an ancient feature (Frey *et al*., 2002), unlike the Earth's, which is a product of active plate tectonics. It remains to be seen whether the rocks that compose the high-standing southern highlands of Mars bear any resemblance to those of Earth's continental crust (McLennan, 2001a; Wanke *et al*., 2001).

3.01.7 SUMMARY

The crust is the Earth's major repository of incompatible elements and thus factors prominently into geochemical mass-balance calculations for the whole Earth. For this reason, and to understand the processes by which it formed, determining the composition of the continental crust has been a popular pursuit of geochemists from the time the first rocks were analyzed.

It has been known for over a century that the continental crust has an average composition approximating to andesite (when cast as an igneous rock type) (Clarke, 1889, Clarke and Washington, 1924). The myriad studies on continental crust composition carried out in the intervening years have refined our picture of the crust's composition, particularly for trace elements.

Based on seismic investigations the crust can be divided into three regions: upper, middle, and lower continental crust. The upper crust is

the most accessible region of the solid earth and its composition is estimated from both weighted averages of surface samples and studies of shales and loess. The latter is a particularly powerful means of estimating the average upper crustal concentrations of insoluble to moderately soluble trace elements. Most estimates of the major-element composition of the upper continental crust fall within 20% standard deviation of the mean and thus the composition of this important reservoir appears to be reasonably well known. The concentrations of some trace elements also appear to be known to within 20% (most of the transition metals, rubidium, strontium, yttrium, zirconium, niobium, barium, REE, hafnium, tantalum, lead, thorium, and uranium), whereas others are less-precisely known. In particular, very few estimates have been made of the upper crust's halogen, sulfur, germanium, arsenic, selenium, indium, and platinum-group element concentration.

Lacking the access and widescale natural sampling by sediments afforded the upper crust, the composition of the deep crust must be inferred from more indirect means. Both heat flow and seismic velocities have been employed towards this end. Heat flow provides bounds on the potassium, thorium, and uranium content of the crust, and seismic-wave speeds can be interpreted, with some caveats, in terms of rock types, whose compositions are derived from averages of appropriate deep-crustal lithologies. The middle crust is perhaps the least well characterized of the three crustal regions. This is due to the lack of systematic geochemical studies of amphibolite-facies crustal lithologies. In contrast, the lower crust has been the target of a number of geochemical investigations, yet there is wide variation in different estimates of lower-crust composition. This reflects, in part, the highly heterogeneous character of this part of the Earth. However, some generalities can be made. Heat production must decrease and seismic velocities are observed to increase with depth in the crust. Thus the lower crust is, on an average, mafic in composition and depleted in heat-producing elements. Curiously, the lower crust of many Archean cratons, where heat flow is lowest, has relatively slow *P*-wave velocities. Such low velocities imply the dominance of evolved rock types and thus these rocks must be highly depleted in potassium, thorium, and uranium compared to their upper crustal counterparts.

The andesitic continental crust composition is difficult to explain if the crust is generated by single-stage melting of peridotitic mantle, and additional processes must therefore be involved in its generation. All of these processes entail return of mafic or ultramafic crustal material (which is complementary to the present continental crust) to the convecting mantle. Thus crustal recycling, in various forms, must have been important throughout Earth history and is undoubtedly related to the plate-tectonic cycle on our planet. Crustal recycling, along with the presence of abundant water to facilitate melting (Campbell and Taylor, 1985), may be the major factor responsible for our planet's unique crustal dichotomy.

ACKNOWLEDGMENTS

We thank Sandy Romeo and Yongshen Liu for their able assistance in the preparation of this manuscript and updating of the lower-crustal xenolith database. Reviews by Kent Condie and Scott McLennan and comments from Herbert Palme and Rich Walker improved the presentation. This work was supported by NSF grant EAR 99031591 to R.L.R., a National Nature Science Foundation of China grant (40133020) and a Chinese Ministry of Science and Technology grant (G1999043202) to S.G.

REFERENCES

Albarede F. (1998) The growth of continental crust. In *Continents and their Mantle Roots*, Tectonophysics (eds. A. Vauchez and R. O. Meissner). Elsevier, Amsterdam, vol. 296 (1–2), pp. 1–14.

Alirezaei S. and Cameron E. M. (2002) Mass balance during gabbro-amphibolite transition, Bamble sector, Norway: implications for petrogenesis and tectonic setting of the gabbros. *Lithos* **60**(1–2), 21–45.

Anderson A. T. (1982) Parental basalts in subduction zones: implications for continental evolution. *J. Geophys. Res.* **87**, 7047–7060.

Aoki K.-I. (1971) Petrology of mafic inclusion from Itinomegata, Japan. *Contrib. Mineral. Petrol.* **30**, 314–331.

Arculus R. J. and Smith D. (1979) Eclogite, pyroxenite, and amphibolite inclusions in the Sullivan Buttes latite, Chino Valley, Yavapai County, Arizona. In *The Mantle Sample: Inclusions in Kimberlites and Other Volcanics* (eds. F. R. Boyd and H. O. A. Meyer). American Geophysical Union, Washington, DC, pp. 309–317.

Arculus R. J., Ferguson J., Chappell B. W., Smith D., McCulloch M. T., Jackson I., Hensel H. D., Taylor S. R., Knutson J., and Gust D. A. (1988) Trace element and isotopic characteristics of eclogites and other xenoliths derived from the lower continental crust of southeastern Australia and southwestern Colorado Plateau USA. In *Eclogites and Eclogite-Facies Rocks* (ed. D. C. Smith). Elsevier, Amsterdam, pp. 335–386.

Baldridge W. S. (1979) Mafic and ultramafic inclusion suites from the Rio Grande Rift (New Mexico) and their bearing on the composition and thermal state of the lithosphere. *J. Volcanol. Geotherm. Res.* **6**, 319–351.

Barth M., McDonough W. F., and Rudnick R. L. (2000) Tracking the budget of Nb and Ta in the continental crust. *Chem. Geol.* **165**, 197–213.

Barth M., Rudnick R. L., Carlson R. W., Horn I., and McDonough W. F. (2002) Re–Os and U–Pb geochronological constraints on the eclogite-tonalite connection in the Archean Man Shield, West Africa. *Precamb. Res.* **118**(3–4), 267–283.

Beck S. L. and Zandt G. (2002) The nature of orogenic crust in the central Andes. *J. Geophys. Res. Solid Earth* **107**(B10) (article no. 2230).

Behn M. D. and Kelemen P. B. (2003) The relationship between seismic P-wave velocity and the composition of anhydrous igneous and meta-igneous rocks. *Geochem. Geophys. Geosys.* (**4**)1041, doi: 10.1029/2002GC000393.

Berckhemer H. (1969) Direct evidence for the composition of the lower crust and Moho. *Tectonophysics* **8**, 97–105.

Berg J. H., Moscati R. J., and Herz D. L. (1989) A petrologic geotherm from a continental rift in Antarctica. *Earth Planet. Sci. Lett.* **93**, 98–108.

Bida T. A., Killen R. M., and Morgan T. H. (2000) Discovery of calcium in Mercury's atmosphere. *Nature* **404**, 159–161.

Bohlen S. R. and Mezger K. (1989) Origin of granulite terranes and the formation of the lowermost continental crust. *Science* **244**, 326–329.

Borodin L. S. (1998) Estimated chemical composition and petrochemical evolution of the upper continental crust. *Geochem. Int.* **37**(8), 723–734.

Bowring S. A. and Williams I. S. (1999) Priscoan (4.00–4.03 Ga) orthogneisses from northwestern Canada. *Contrib. Mineral. Petrol.* **134**(1), 3–16.

Bradley S. D. and McCallum M. E. (1984) Granulite facies and related xenoliths from Colorado-Wyoming kimberlite. In *Kimberlites: II. The Mantle and Crust–Mantle Relationships* (ed. J. Kornprobst). Elsevier, Amsterdam, vol. 11B, pp. 205–218.

Broadhurst J. R. (1986) Mineral reactions in xenoliths from the Colorado Plateau: implications for lower crustal conditions and fluid composition. In *The Nature of the Lower Continental Crust*, Geol. Soc. Spec. Publ. (eds. J. B. Dawson, D. A. Carswell, J. Hall, and K. H. Wedepohl). London, vol. 24, pp. 331–349.

Brittan J. and Warner M. (1996) Seismic velocity, heterogeneity, and the composition of the lower crust. *Tectonophysics* **264**, 249–259.

Brittan J. and Warner M. (1997) Wide-angle seismic velocities in heterogeneous crust. *Geophys. J. Int.* **129**, 269–280.

Burke M. M. and Fountain D. M. (1990) Seismic properties of rocks from an exposure of extended continental crust—new laboratory measurements from the Ivrea zone. *Tectonophysics* **182**, 119–146.

Cameron K. L. and Ward R. L. (1998) Xenoliths of Grenvillian granulite basement constrain models for the origin of voluminous Tertiary rhyolites, Davis Mountains, west Texas. *Geology* **26**(12), 1087–1090.

Cameron K. L., Robinson J. V., Niemeyer S., Nimz G. J., Kuentz D. C., Harmon R. S., Bohlen S. R., and Collerson K. D. (1992) Contrasting styles of pre-Cenozoic and mid-Tertiary crustal evolution in northern Mexico: evidence from deep crustal xenoliths from La Olivina. *J. Geophys. Res.* **97**, 17353–17376.

Campbell I. H. and Taylor S. R. (1985) No water, no granites—no oceans, no continents. *Geophys. Res. Lett.* **10**, 1061–1064.

Chen S., O'Reilly S. Y., Zhou X., Griffin W. L., Zhang G., Sun M., Feng J., and Zhang M. (2001) Thermal and petrological structure of the lithosphere beneath Hannuoba, Sino-Korean craton, China: evidence from xenoliths. *Lithos* **56**, 267–301.

Chen W. and Arculus R. J. (1995) Geochemical and isotopic characteristics of lower crustal xenoliths, San Francisco volcanic field, Arizona, USA. *Lithos* **36**(3–4), 203–225.

Chen Y. D., O'Reilly S. Y., Kinny P. D., and Griffin W. L. (1994) Dating lower crust and upper-mantle events—an ion microprobe study of xenoliths from kimberlitic pipes, South-Australia. *Lithos* **32**(1–2), 77–94.

Chen Y. D., O'Reilly S. Y., Griffin W. L., and Krogh T. E. (1998) Combined U–Pb dating and Sm–Nd studies on lower crustal and mantle xenoliths from the delegate basaltic pipes, southeastern Australia. *Contrib. Mineral. Petrol.* **130**(2), 154–161.

Christensen N. I. (1982) Seismic velocities. In *Handbook of Physical Properties of Rocks* (ed. R. S. Carmichael). CRC Press, Boca Raton, FL, vol. II, pp. 1–228.

Christensen N. I. and Mooney W. D. (1995) Seismic velocity structure and composition of the continental crust: a global view. *J. Geophys. Res.* **100**(B7), 9761–9788.

Clarke F. W. (1889) The relative abundance of the chemical elements. *Phil. Soc. Washington Bull.* **XI**, 131–142.

Clarke F. W. and Washington H. S. (1924) The composition of the Earth's crust. *USGS Professional Paper* **127**, 117pp.

Clitheroe G., Gudmundsson O., and Kennett B. L. N. (2000) The crustal thickness of Australia. *J. Geophys. Res. Solid Earth* **105**(B6), 13697–13713.

Cogley J. G. (1984) Continental margins and the extent and number of the continents. *Rev. Geophys. Space Phys.* **22**, 101–122.

Cohen R. S., O'Nions R. K., and Dawson J. B. (1984) Isotope geochemistry of xenoliths from East Africa: implications for development of mantle reservoirs and their interaction. *Earth Planet. Sci. Lett.* **68**, 209–220.

Collerson K. D., Hearn B. C., MacDonald R. A., Upton B. F., and Park J. G. (1988) Granulite xenoliths from the Bearpaw mountains, Montana: constraints on the character and evolution of lower continental crust. *Terra Cognita* **8**, 270.

Condie K. C. (1993) Chemical composition and evolution of the upper continental crust: contrasting results form surface samples and shales. *Chem. Geol.* **104**, 1–37.

Condie K. C. (1997) *Plate Tectonics and Crustal Evolution*. Butterworth-Heinemann, Oxford, UK.

Condie K. C. and Selverstone J. (1999) The crust of the Colorado plateau: new views of an old arc. *J. Geol.* **107**(4), 387–397.

Condie K. C., Latysh N., Van Schmus W. R., Kozuch M., and Selverstone J. (1999) Geochemistry, Nd and Sr isotopes, and U/Pb zircon ages of Navajo Volcanic Field, Four Corners area, southwestern United States. *Chem. Geol.* **156**(1–4), 95–133.

Davis G. L. (1977) The ages and uranium contents of zircons from kimberlites and associated rocks. *Carnegie Inst. Wash. Yearbook* **76**, 631–635.

Davis G. L. and Grew E. S. (1977) Age of zircon from a crustal xenolith, Kilbourne Hole, New Mexico. *Carnegie Inst. Wash. Yearbook* **77**, 897–898.

Davis W. J. (1997) U–Pb zircon and rutile ages from granulite xenoliths in the Slave province: evidence for mafic magmatism in the lower crust coincident with Proterozoic dike swarms. *Geology* **25**(4), 343–346.

Dawson J. B. (1977) Sub-cratonic crust and upper-mantle models based on xenolith suites in kimberlite and nephelinitic diatremes. *J. Geol. Soc.* **134**, 173–184.

Dawson J. B. and Smith J. V. (1987) Reduced sapphirine granulite xenoliths from the Lace Kimberlite, South Africa: implications for the deep structure of the Kaapvaal Craton. *Contrib. Mineral. Petrol.* **95**, 376–383.

Dawson J. B., Harley S. L., Rudnick R. L., and Ireland T. R. (1997) Equilibration and reaction in Archaean quartz-sapphirine granulite xenoliths from the Lace Kimberlite pipe, South Africa. *J. Metamorph. Geol.* **15**(2), 253–266.

Dessai A. G. and Vaselli O. (1999) Petrology and geochemistry of xenoliths in lamprophyres from the Deccan Traps: implications for the nature of the deep crust boundary in western India. *Min. Mag.* **63**(5), 703–722.

Dessai A. G., Knight K., and Vaselli O. (1999) Thermal structure of the lithosphere beneath the Deccan Trap along the western Indian continental margin: evidence from xenolith data. *J. Geol. Soc. India* **54**(6), 585–598.

Dobosi G., Kempton P. D., Downes H., Embey-Isztin A., Thirlwall M., and Greenwood P. (2003) Lower crustal granulite xenoliths from the Pannonian Basin, Hungary: Part 2. Sr–Nd–Pb–Hf and O isotope evidence for formation of continental lower crust by tectonic emplacement of oceanic crust. *Contrib. Mineral. Petrol.* **144**, 671–683.

Dodge F. C. W., Lockwood J. P., and Calk L. C. (1988) Fragments of the mantle and crust from beneath the Sierra Nevada batholith: xenoliths in a volcanic pipe near Big Creek, California. *Geol. Soc. Am. Bull.* **100**, 938–947.

Dodge F. W., Calk L. C., and Kistler R. W. (1986) Lower crustal xenoliths, Chinese Peak lava flow, central Sierra Nevada. *J. Petrol.* **27**, 1277–1304.

Domenick M. A., Kistler R. W., Dodge F. W., and Tatsumoto M. (1983) Nd and Sr isotopic study of crustal and mantle inclusions from the Sierra Nevada and implications for batholith petrogenesis. *Geol. Soc. Am. Bull.* **94**, 713–719.

Dostal J. and Capedri S. (1979) Rare earth elements in high-grade metamorphic rocks from the western Alps. *Lithos* **12**, 41–49.

Dostal J., Dupuy C., and Leyreloup A. (1980) Geochemistry and petrology of meta-igneous granulitic xenoliths in Neogene volcanic rocks of the Massif Central, France—implications for the lower crust. *Earth Planet. Sci. Lett.* **50**, 31–40.

Downes H. (1993) The nature of the lower continental crust of Europe petrological and geochemical evidence from xenoliths. *Phys. Earth Planet. Inter.* **79**(1–2), 195–218.

Downes H., and Leyreloup A. F. (1986) Granulitic xenoliths from the French massif central—petrology, Sr and Nd isotope systematics and model age estimates. In *The Nature of the Lower Continental Crust* (eds. B. Dawson, D. A. Carswell, J. Hall, and K. H. Wedepohl). Geological Society of London, London, pp. 319–330.

Downes H., Dupuy C., and Leyreloup A. F. (1990) Crustal evolution of the Hercynian belt of western Europe: evidence from lower-crustal granulitic xenoliths (French Massif-Central). *Chem. Geol.* **83**(3–4), 209–231.

Downes H., Kempton P. D., Briot D., Harmon R. S., and Leyreloup A. F. (1991) Pb and O isotope systematics in granulite facies xenoliths, French Massif-Central—implications for crustal processes. *Earth Planet. Sci. Lett.* **102** (3–4), 342–357.

Downes H., Peltonen P., Manttari I., and Sharkov E. V. (2002) Proterozoic zircon ages from lower crustal granulite xenoliths, Kola Peninsula, Russia: evidence for crustal growth and reworking. *J. Geol. Soc.* **159**, 485–488.

Drummond B. J. (1988) A review of crust upper mantle structure in the Precambrian areas of Australia and implications for Precambrian crustal evolution. *Precamb. Res.* **40**(1), 101–116.

Drummond M. S. and Defant M. J. (1990) A model for trondhjemite-tonalite-dacite genesis and crustal growth via slab melting: archean to modern comparisons. *J. Geophys. Res.* **95**(B13), 21503–21521.

Ducea M. (2001) The California arc: thick granitic batholiths, eclogitic residues, lithospheric-scale thrusting, and magmatic flare-ups. *GSA Today* **11**(11), 4–10.

Ducea M. N. and Saleeby J. B. (1996) Buoyancy sources for a large, unrooted mountain range, the Sierra Nevada, California: evidence from xenolith thermobarometry. *J. Geophys. Res. Solid Earth* **101**(B4), 8229–8244.

Ducea M. N. and Saleeby J. B. (1998) The age and origin of a thick mafic-ultramafic keel from beneath the Sierra Nevada batholith. *Contrib. Mineral. Petrol.* **133**(1–2), 169–185.

Durrheim R. J. and Green R. W. E. (1992) A seismic refraction investigation of the Archaean Kaapvaal craton, South Africa, using mine tremors as the energy source. *Geophys. J. Int.* **108**, 812–832.

Durrheim R. J. and Mooney W. D. (1994) The evolution of the Precambrian lithosphere: seismological and geochemical constraints. *J. Geophys. Res.* **99**, 15359–15374.

Eade K. E. and Fahrig W. F. (1971) Chemical Evolutionary Trends of Continental Plates—preliminary Study of the Canadian Shield. *Geol. Sur. Can. Bull.* **179**, 51pp.

Eade K. E. and Fahrig W. F. (1973) Regional, Lithological, and Temporal Variation in the Abundances of some Trace Elements in the Canadian Shield. Geol. Sur. Canada Paper 72–46, Ottawa, Ontario.

Eberz G. W., Clarke D. B., Chatterjee A. K., and Giles P. S. (1991) Chemical and isotopic composition of the lower crust beneath the Meguma Lithotectonic Zone, Nova Scotia: evidence from granulite facies xenoliths. *Contrib. Mineral. Petrol.* **109**, 69–88.

Edwards A. C., Lovering J. F., and Ferguson J. (1979) High pressure basic inclusions from the Kayrunnera kimberlitic breccia pipe in New South Wales, Australia. *Contrib. Mineral. Petrol.* **69**, 185–192.

Ehrenberg S. N. and Griffin W. L. (1979) Garnet granulite and associated xenoliths in minette and serpentinite diatremes of the Colorado Plateau. *Geology* **7**, 483–487.

Embey-Isztin A., Scharbert H. G., Deitrich H., and Poultidis H. (1990) Mafic granulite and clinopyroxenite xenoliths from the Transdanubian volcanic region (Hungary): implication for the deep structure of the Pannonian Basin. *Min. Mag.* **54**, 463–483.

Embey-Isztin A., Downes H., Kempton P. D., Dobosi G., and Thirlwall M. (2003) Lower crustal granulite xenoliths from the Pannonian Basin, Hungary: Part 1. Mineral chemistry, thermobarometry and petrology. *Contrib. Mineral. Petrol.* **144**, 652–670.

Ertan I. E. and Leeman W. P. (1999) Fluid inclusions in mantle and lower crustal xenoliths from the Simcoe volcanic field, Washington. *Chem. Geol.* **154**(1–4), 83–95.

Esperança S. and Garfunkel Z. (1986) Ultramafic xenoliths from the Mt. Carmel area (Karem Maharal Volcano), Israel. *Lithos* **19**, 43–49.

Esperança S., Carlson R. W., and Shirey S. B. (1988) Lower crustal evolution under central Arizona: Sr, Nd, and Pb isotopic and geochemical evidence from the mafic xenoliths of Camp Creek. *Earth Planet. Sci. Lett.* **90**, 26–40.

Esser B. K. and Turekian K. K. (1993) The osmium isotopic composition of the continental crust. *Geochim. Cosmochim. Acta* **57**, 3093–3104.

Fahrig W. F., and Eade K. E. (1968) The chemical evolution of the Canadian Shield. *Geochim. Cosmochim. Acta* **5**, 1247–1252.

Fountain D. M. (1976) The Ivrea-Verbano and Strona-Ceneri zones, northern Italy: a cross-section of the continental crust—new evidence from seismic velocities of rock samples. *Tectonophysics* **33**, 145–165.

Fountain D. M. and Salisbury M. H. (1981) Exposed cross-sections through the continental crust: implications for crustal structure, petrology, and evolution. *Earth Planet. Sci. Lett.* **56**, 263–277.

Fountain D. M., and Salisbury M. H. (1995) Seismic properties of rock samples from the Pikwitonei granulite belt—God's lake domain crustal cross section, Manitoba. *Can. J. Earth Sci.* **33**(5), 757–768.

Fountain D. M., Percival J., and Salisbury M. H. (1990a) Exposed cross sections of the continental crust-synopsis. In *Exposed Cross-sections of the Continental Crust* (eds. M. H. Salisbury and D. M. Fountain). Kluwer, Amsterdam, pp. 653–662.

Fountain D. M., Salisbury M. H., and Percival J. (1990b) Seismic structure of the continental crust based on rock velocity measurements from the Kapuskasing uplift. *J. Geophys. Res.* **95**, 1167–1186.

Fountain D. M., Salisbury M. H., and Furlong K. P. (1987) Heat production and thermal conductivity of rocks from the Pikwitonei-Sachigo continental cross section, central Manitoba: implications for the thermal structure of Archean crust. *Can. J. Earth Sci.* **24**, 1583–1594.

Francis D. M. (1976) Corona-bearing pyroxene granulite xenoliths and the lower crust beneath Nunivak Island, Alaska. *Can. Mineral.* **14**, 291–298.

Frey H. V., Roark J. H., Shockey K. M., Frey E. L., and Sakimoto S. E. H. (2002) Ancient lowlands on Mars. *Geophys. Res. Lett.* **29**(10), 22-1–22-4.

Gallet S., Jahn B.-M., van Vliet Lanoë B., Dia A., and Rossello E. (1998) Loess geochemistry and its implications for particle origin and composition of the upper continental crust. *Earth Planet. Sci. Lett.* **156**, 157–172.

Gao S., Luo T.-C., Zhang B.-R., Zhang H.-F., Han Y.-W., Hu Y.-K., and Zhao Z.-D. (1998a) Chemical composition of the continental crust as revealed by studies in east China. *Geochim. Cosmochim. Acta* **62**, 1959–1975.

Gao S., Zhang B.-R., Jin Z.-M., Kern H., Luo T.-C., and Zhao Z.-D. (1998b) How mafic is the lower continental crust? *Earth Planet. Sci. Lett.* **106**, 101–117.

Gao S., Kern H., Liu Y. S., Jin S. Y., Popp T., Jin Z. M., Feng J. L., Sun M., and Zhao Z. B. (2000) Measured and calculated seismic velocities and densities for granulites from xenolith occurrences and adjacent exposed lower crustal sections: a comparative study from the North China craton. *J. Geophys. Res. Solid Earth* **105**(B8), 18965–18976.

Goldschmidt V. M. (1933) Grundlagen der quantitativen Geochemie. *Fortschr. Mienral. Kirst. Petrogr.* **17**, 112.

Goldschmidt V. M. (1958) *Geochemistry*. Oxford University Press, Oxford.

Goodwin A. M. (1991) *Precambrian Geology*. Academic Press, London.

Gorman A. R., Clowes R. M., Ellis R. M., Henstock T. J., Spence G. D., Keller G. R., Levander A., Snelson C. M., Burianyk M. J. A., Kanasewich E. R., Asudeh I., Hajnal Z., and Miller K. C. (2002) Deep probe: imaging the roots of western North America. *Can. J. Earth Sci.* **39**(3), 375–398.

Grapes R. H. (1986) Melting and thermal reconstitution of pelitic xenoliths, Wehr volcano, East Eifel, West Germany. *J. Petrol.* **27**, 343–396.

Gregoire M., Mattielli N., Nicollet C., Cottin J. Y., Leyrit H., Weis D., Shimizu N., and Giret A. (1994) Oceanic mafic granulite xenoliths from the Kerguelen archipelago. *Nature* **367**, 360–363.

Gregoire M., Cottin J. Y., Giret A., Mattielli N., and Weis D. (1998) The meta-igneous granulite xenoliths from Kerguelen archipelago: evidence of a continent nucleation in an oceanic setting. *Contrib. Mineral. Petrol.* **133**(3), 259–283.

Griffin W. L. and O'Reilly S. Y. (1986) The lower crust in eastern Australia: xenolith evidence. In *The Nature of the Lower Continental Crust*, Geol. Soc. London Spec. Publ. (eds. B. Dawson, D. A. Carswell, J. Hall, and K. H. Wedepohl). London, vol. 25, pp. 363–374.

Griffin W. L. and O'Reilly S. Y. (1987) Is the continental Moho the crust–mantle boundary? *Geology* **15**, 241–244.

Griffin W. L., Carswell D. A., and Nixon P. H. (1979) Lower-crustal granulites and eclogites from Lesotho, southern Africa. In *The Mantle Sample: Inclusions in Kimberlites* (eds. F. R. Boyd and H. O. A. Meyer). American Geophysical Union, Washington, DC, pp. 59–86.

Griffin W. L., Sutherland F. L., and Hollis J. D. (1987) Geothermal profile and crust–mantle transition beneath east-central Queensland: volcanology, xenolith petrology and seismic data. *J. Volcanol. Geotherm. Res.* **31**, 177–203.

Griffin W. L., Jaques A. L., Sie S. H., Ryan C. G., Cousens D. R., and Suter G. F. (1988) Conditions of diamond growth: a proton microprobe study of inclusions in West Australian diamonds. *Contrib. Mineral. Petrol.* **99**, 143–158.

Hacker B. R., Gnos E., Ratschbacher L., Grove M., McWilliams M., Sobolev S. V., Wan J., and Wu Z. H. (2000) Hot and dry deep crustal xenoliths from Tibet. *Science* **287**(5462), 2463–2466.

Halliday A. N., Aftalion M., Upton B. G. J., Aspen P., and Jocelyn J. (1984) U–Pb isotopic ages from a granulite-facies xenolith from Partan Craig in the Midland Valley of Scotland. *Trans. Roy. Soc. Edinburgh: Earth Sci.* **75**, 71–74.

Hanchar J. M., Miller C. F., Wooden J. L., Bennett V. C., and Staude J.-M. G. (1994) Evidence from xenoliths for a dynamic lower crust, eastern Mojave desert, California. *J. Petrol.* **35**, 1377–1415.

Harley S. L. (1989) The origin of granulites: a metamorphic perspective. *Geol. Mag.* **126**, 215–247.

Hart R. J., Nicolaysen L. O., and Gale N. H. (1981) Radioelement concentrations in the deep profile through Precambrian basement of the Vredefort structure. *J. Geophys. Res.* **86**, 10639–10652.

Hart R. J., Andreoli M. A. G., Tredoux M., and Dewit M. J. (1990) Geochemistry across an exposed section of Archean crust at Vredefort, South Africa with implications for midcrustal discontinuities. *Chem. Geol.* **82**(1–2), 21–50.

Haskin M. A. and Haskin L. A. (1966) Rare earths in European shales: a redetermination. *Science* **154**, 507–509.

Haskin L. A., Wildeman T. R., Frey F. A., Collins K. A., Keedy C. R., and Haskin M. A. (1966) Rare earths in sediments. *J. Geophys. Res. B: Solid Earth* **71**(24), 6091–6105.

Hattori Y., Suzuki K., Honda M., and Shimizu H. (2003) Re–Os isotope systematics of the Taklimakan Desert sands, moraines and river sediments around the Taklimakan Desert, and of Tibetan soils. *Geochim. Cosmochim. Acta* **67**, 1195–1206.

Hayob J. L., Essene E. J., Ruiz J., Ortega-Gutiérrez F., and Aranda-Gómez J. J. (1989) Young high-temperature granulites form the base of the crust in central Mexico. *Nature* **342**, 265–268.

Heier K. S. (1973) Geochemistry of granulite facies rocks and problems of their origin. *Phil. Trans. Roy. Soc. London* **A273**, 429–442.

Heinrichs H., Schulz-Dobrick B., and Wedepohl K. H. (1980) Terrestrial geochemistry of Cd, Bi, Tl, Pb, Zn, and Rb. *Geochim. Cosmochim. Acta* **44**, 1519–1533.

Hickey-Vargas R., Abdollahi M. J., Parada M. A., Lopezescobar L., and Frey F. A. (1995) Crustal xenoliths from Calbuco volcano, Andean southern volcanic zone—implications for crustal composition and magma–crust interaction. *Contrib. Mineral. Petrol.* **119**(4), 331–344.

Holbrook W. S. and Kelemen P. B. (1993) Large igneous province on the US Atlantic margin and implications for magmatism during continental breakup. *Nature* **364**, 433–436.

Holbrook W. S., Mooney W. D., and Christensen N. I. (1992) The seismic velocity structure of the deep continental crust. In *Continental Lower Crust* (eds. D. M. Fountain, R. Arculus, and R. W. Kay). Elsevier, Amsterdam, pp. 1–44.

Holland J. G. and Lambert R. S. J. (1972) Major element chemical composition of shields and the continental crust. *Geochim. Cosmochim. Acta* **36**, 673–683.

Hölttä P., Huhma H., Manttari I., Peltonen P., and Juhanoja J. (2000) Petrology and geochemistry of mafic granulite xenoliths from the Lahtojoki kimberlite pipe, eastern Finland. *Lithos* **51**(1–2), 109–133.

Hu S., He L., and Wang J. (2000) Heat flow in the continental area of China: a new data set. *Earth Planet. Sci. Lett.* **179**, 407–419.

Huang Y. M., van Calsteren P., and Hawkesworth C. J. (1995) The evolution of the lithosphere in southern Africa—a perspective on the basic granulite xenoliths from kimberlites in South-Africa. *Geochim. Cosmochim. Acta* **59**(23), 4905–4920.

Hunter R. H., Upton B. G. J., and Aspen P. (1984) Meta-igneous granulite and ultramafic xenoliths from basalts of the Midland Valley of Scotland: petrology and mineralogy of the lower crust and upper mantle. *Trans. Roy. Soc. Edinburgh* **75**, 75–84.

Ivanov M. A. and Head J. W. (1999) Stratigraphic and geographic distribution of steep-sided domes on Venus: preliminary results from regional geological mapping and implications for their origin. *J. Geophys. Res. Planet.* **104**(E8), 18907–18924.

Jahn B. M., Gallet S., and Han J. M. (2001) Geochemistry of the Xining, Xifeng, and Jixian sections, Loess Plateau of China: eolian dust provenance and paleosol evolution during the last 140 ka. *Chem. Geol.* **178**(1–4), 71–94.

James D. E., Padovani E. R., and Hart S. R. (1980) Preliminary results on the oxygen isotopic composition of the lower crust, Kilbourne Hole Maar, New Mexico. *Geophys. Res. Lett.* **7**, 321–324.

Jones A. P., Smith J. V., Dawson J. B., and Hansen E. C. (1983) Metamorphism, partial melting, and K-metasomatism of garnet-scapolite-kyanite granulite xenoliths from Lashaine, Tanzania. *J. Geol.* **91**, 143–166.

Jull M. and Kelemen P. B. (2001) On the conditions for lower crustal convective instability. *J. Geophys. Res. B: Solid Earth* **106**(4), 6423–6446.

Kalamarides R. I., Berg J. H., and Hank R. A. (1987) Lateral isotopic discontinuity in the lower crust: an example from Antarctica. *Science* **237**, 1192–1195.

Kay R. W. and Kay S. M. (1981) The nature of the lower continental crust: inferences from geophysics, surface geology, and crustal xenoliths. *Rev. Geophys. Space Phys.* **19**, 271–297.

Kay R. W. and Kay S. M. (1991) Creation and destruction of lower continental crust. *Geol. Rundsch.* **80**, 259–278.

Kay S. M. and Kay R. W. (1983) Thermal history of the deep crust inferred from granulite xenoliths, Queensland, Australia. *Am. J. Sci.* **283**, 486–513.

Kelemen P. B. (1995) Genesis of high Mg# andesites and the continental crust. *Contrib. Mineral. Petrol.* **120**, 1–19.

Kempton P. D. and Harmon R. S. (1992) Oxygen-isotope evidence for large-scale hybridization of the lower crust during magmatic underplating. *Geochim. Cosmochim. Acta* **55**, 971–986.

Kempton P. D., Harmon R. S., Hawkesworth C. J., and Moorbath S. (1990) Petrology and geochemistry of lower crustal granulites from the Geronimo volcanic field, south-eastern Arizona. *Geochim. Cosmochim. Acta* **54**, 3401–3426.

Kempton P. D., Downes H., Sharkov E. V., Vetrin V. R., Ionov D. A., Carswell D. A., and Beard A. (1995) Petrology and geochemistry of xenoliths from the northern Baltic shield: evidence for partial melting and metasomatism in the lower crust beneath an Archaean terrane. *Lithos* **36** (3–4), 157–184.

Kempton P. D., Downes H., and Embey-Isztin A. (1997) Mafic granulite xenoliths in Neogene alkali basalts from the western Pannonian Basin: insights into the lower crust of a collapsed orogen. *J. Petrol.* **38**(7), 941–970.

Kempton P. D., Downes H., Neymark L. A., Wartho J. A., Zartman R. E., and Sharkov E. V. (2001) Garnet granulite xenoliths from the northern Baltic shield the underplated lower crust of a palaeoproterozoic large igneous province. *J. Petrol.* **42**(4), 731–763.

Kern H., Gao S., and Liu Q.-S. (1996) Seismic properties and densities of middle and lower crustal rocks exposed along the North China geoscience transect. *Earth Planet. Sci. Lett.* **139**, 439–455.

Ketcham R. A. (1996) Distribution of heat-producing elements in the upper and middle crust of southern and west central Arizona: evidence from core complexes. *J. Geophys. Res.* (B) **101**, 13611–13632.

Kopylova M. G., O'Reilly S. Y., and Genshaft Y. S. (1995) Thermal state of the lithosphere beneath Central Mongolia: evidence from deep-seated xenoliths from the Shavaryn-Saram volcanic centre in the Tariat depression, Hangai, Mongolia. *Lithos* **36**, 243–255.

Kuno H. (1967) Mafic and ultramafic nodules from Itinomegata, Japan. In *Ultramafic and Related Rocks* (ed. P. J. Wiley). Wiley, New York, pp. 337–342.

Kyle P. R., Wright A., and Kirsch I. (1987) Ultramafic xenoliths in the late Cenozoic McMurdo volcanic group, western Ross Sea embayment, Antarctica. In *Mantle Xenoliths* (ed. P. H. Nixon). Wiley, New York, pp. 287–294.

Le Bas M. J. and Streckeisen A. L. (1991) The IUGS systematics of igneous rocks. *J. Geol. Soc. London* **148**, 825–833.

Lee C.-Y., Chung S. L., Chen C.-H., and Hsieh Y. L. (1993) Mafic granulite xenoliths from Penghu Islands: evidence for basic lower crust in SE China continental margin. *J. Geol. Soc. China* **36**(4), 351–379.

Leech M. L. (2001) Arrested orogenic development: eclogitization, delamination, and tectonic collapse. *Earth Planet. Sci. Lett.* **185**(1–2), 149–159.

Leeman W. P., Menzies M. A., Matty D. J., and Embree G. F. (1985) Strontium, neodymium, and lead isotopic compositions of deep crustal xenoliths from the Snake River Plain: evidence for Archean basement. *Earth Planet. Sci. Lett.* **75**, 354–368.

Leeman W. P., Sisson V. B., and Reid M. R. (1992) Boron geochemistry of the lower crust-evidence from granulite terranes and deep crustal xenoliths. *Geochim. Cosmochim. Acta* **56**(2), 775–788.

LePichon X., Henry P., and Goffe B. (1997) Uplift of Tibet: from eclogites to granulites-implications for the Andean Plateau and the Variscan belt. *Tectonophysics* **273**(1–2), 57–76.

Leyreloup A., Dupuy C., and Andriambololona R. (1977) Catazonal xenoliths in French Neogene volcanic rocks: constitution of the lower crust: 2. Chemical composition and consequences of the evolution of the French Massif Central Precambrian crust. *Contrib. Mineral. Petrol.* **62**, 283–300.

Leyreloup A., Bodinier J. L., Dupuy C., and Dostal J. (1982) Petrology and geochemistry of granulite xenoliths from Central Hoggar (Algeria)—implications for the lower crust. *Contrib. Mineral. Petrol.* **79**, 68–75.

Liu Y. S., Gao S., Jin S. Y., Hu S. H., Sun M., Zhao Z. B., and Feng J. L. (2001) Geochemistry of lower crustal xenoliths from Neogene Hannuoba basalt, North China craton: implications for petrogenesis and lower crustal composition. *Geochim. Cosmochim. Acta* **65**(15), 2589–2604.

Lombardo B. and Rolfo F. (2000) Two contrasting eclogite types in the Himalayas: implications for the Himalayan orogeny. *J. Geodynam.* **30**(1–2), 37–60.

Loock G., Seck H. A., and Stosch H.-G. (1990) Granulite facies lower crustal xenoliths from the Eifel, West Germany: petrological and geochemical aspects. *Contrib. Mineral. Petrol.* **105**, 25–41.

Lovering J. F. and White A. J. R. (1964) The significance of primary scapolite in granulitic inclusions from deep-seated pipes. *J. Petrol.* **5**, 195–218.

Lovering J. F. and White A. J. R. (1969) Granulitic and eclogitic inclusions from basic pipes at Delegate, Australia. *Contrib. Mineral. Petrol.* **21**, 9–52.

Lucassen F., Lewerenz S., Franz G., Viramonte J., and Mezger K. (1999) Metamorphism, isotopic ages and composition of lower crustal granulite xenoliths from the Cretaceous Salta Rift, Argentina. *Contrib. Mineral. Petrol.* **134**(4), 325–341.

Luosto U. and Korhonen H. (1986) Crustal structure of the baltic shield based on off-fennolora refraction data. *Tectonophysics* **128**, 183–208.

Luosto U., Flüh E. R., Lund C.-E., and Group W. (1989) The crustal structure along the POLAR profile from seismic refraction investigations. *Tectonophysics* **162**, 51–85.

Luosto U., Tiira T., Korhonen H., Azbel I., Burmin V., Buyanov A., Kosminskaya I., Ionkis V., and Sharov N. (1990) Crust and upper mantle structure along the DSS Baltic profile in SE Finland. *Geophys. J. Int.* **101**, 89–110.

Mackwell S. J., Zimmerman M. E., and Kohlstedt D. L. (1998) High-temperature deformation of dry diabase with application to tectonics on Venus. *J. Geophys. Res. B: Solid Earth* **103**, 975–984.

Markwick A. J. W. and Downes H. (2000) Lower crustal granulite xenoliths from the Arkhangelsk kimberlite pipes: petrological, geochemical and geophysical results. *Lithos* **51**(1–2), 135–151.

Markwick A. J. W., Downes H., and Veretennikov N. (2001) The lower crust of SE Belarus: petrological, geophysical, and geochemical constraints from xenoliths. *Tectonophysics* **339**(1–2), 215–237.

Martin H. (1994) The Archean grey gneisses and the genesis of continental crust. In *Archean Crustal Evolution* (ed. K. C. Condie). Elsevier, Amsterdam, pp. 205–259.

Mattie P. D., Condie K. C., Selverstone J., and Kyle P. R. (1997) Origin of the continental crust in the Colorado Plateau: geochemical evidence from mafic xenoliths from the Navajo volcanic field, southwestern USA. *Geochim. Cosmochim. Acta* **61**(10), 2007–2021.

Mayer A., Mezger K., and Sinigoi S. (2000) New Sm–Nd ages for the Ivrea-Verbano Zone, Sesia and Sessera valleys (Northern-Italy). *J. Geodynamics* **30**(1–2), 147–166.

McBirney A. R. and Aoki K.-I. (1973) Factors governing the stability of plagioclase at high pressures as shown by spinel-gabbro xenoliths from the Kerguelen archipelago. *Am. Mineral.* **58**, 271–276.

McCulloch M. T., Arculus R. J., Chappell B. W., and Ferguson J. (1982) Isotopic and geochemical studies of nodules in kimberlite have implications for the lower continental crust. *Nature* **300**, 166–169.

McDonough W. F. and Sun S.-S. (1995) Composition of the Earth. *Chem. Geol.* **120**, 223–253.

McDonough W. F., Rudnick R. L., and McCulloch M. T. (1991) The chemical and isotopic composition of the lower eastern Australian lithosphere: a review. In *The Nature of the Eastern Australian Lithosphere*, Geol. Soc. Austral. Spec. Publ. (ed. B. Drummond). Sydney, vol. 17, pp. 163–188.

McDonough W. F., Sun S.-S., Ringwood A. E., Jagoutz E., and Hofmann A. W. (1992) Potassium, rubidium, and cesium in the Earth and Moon and the evolution of the mantle of the Earth. *Geochim. Cosmochim. Acta* **56**, 1001–1012.

McLennan S. M. (2001a) Crustal heat production and the thermal evolution of Mars. *Geophys. Res. Lett.* **28**(21), 4019–4022.

McLennan S. M. (2001b) Relationships between the trace element composition of sedimentary rocks and upper continental crust. *Geochem. Geophys. Geosys.* **2** (article no. 2000GC000109).

McLennan S. M. and Taylor S. R. (1996) Heat flow and the chemical composition of continental crust. *J. Geol.* **104** 396–377.

McLennan S. M., Nance W. B., and Taylor S. R. (1980) Rare earth element-thorium correlations in sedimentary rocks, and the composition of the continental crust. *Geochim. Cosmochim. Acta* **44**, 1833–1839.

Mehnert K. R. (1975) The Ivrea zone: a model of the deep crust. *Neus Jahrb. Mineral. Abh.* **125**, 156–199.

Meltzer A. and Christensen N. (2001) Nanga Parbat crustal anisotrophy: implication for interpretation of crustal velocity structure and shear-wave splitting. *Geophys. Res. Lett.* **28**(10), 2129–2132.

Mengel K. (1990) Crustal xenoliths from Tertiary volcanics of the northern Hessian depression: petrological and chemical evolution. *Contrib. Mineral. Petrol.* **104**, 8–26.

Mengel K. and Wedepohl K. H. (1983) Crustal xenoliths in Tertiary volcanics from the northern Hessian depression. In *Plateau Uplift* (eds. K. Fuchs, *et al.*). Springer, Berlin, pp. 332–335.

Mengel K., Sachs P. M., Stosch H. G., Worner G., and Loock G. (1991) Crustal xenoliths from Cenozoic volcanic fields of West Germany implications for structure and composition of the continental crust. *Tectonophysics* **195**(2–4), 271.

Meyer H. O. A. and Brookins D. G. (1976) Sapphirine, sillimanite, and garnet in granulite xenoliths from Stockdale kimberlite, Kansas. *Am. Mineral.* **61**, 1194–1202.

Miller J. D. and Christensen N. I. (1994) Seismic signature and geochemistry of an island arc: a multidisciplinary study of the Kohistan accreted terrane, northern Pakistan. *J. Geophys. Res.* (B) **99**, 11623–11642.

Mittlefehldt D. W. (1984) Genesis of clinopyroxene-amphibole xenoliths from Birket Ram: trace element and petrologic constraints. *Contrib. Mineral. Petrol.* **88**, 280–287.

Mittlefehldt D. W. (1986) Petrology of high pressure clinopyroxenite series xenoliths, Mount Carmel, Israel. *Contrib. Mineral. Petrol.* **94**, 245–252.

Moecher D. P., Valley J. W., and Essene E. J. (1994) Extraction and carbon isotope analysis of CO_2 from scapolite in deep crustal granulites and xenoliths. *Geochim. Cosmochim. Acta* **58**(2), 959–967.

Mooney W. D. and Meissner R. (1992) Multi-genetic origin of crustal reflectivity: a review of seismic reflection profiling of the continental lower crust and Moho. In *Continental Lower Crust* (eds. D. M. Fountain, R. Arculus, and R. W. Kay). Elsevier, pp. 45–80.

Moser D. E. and Heaman L. M. (1997) Proterozoic zircon growth in Archean lower crust xenoliths, southern Superior craton: a consequence of Matachewan ocean opening. *Contrib. Mineral. Petrol.* **128**, 164–175.

Moser D. E., Flowers R. M., and Hart R. J. (2001) Birth of the Kaapvaal tectosphere 3.08 billion years ago. *Science* **291**(5503), 465–468.

Nasir S. (1992) The lithosphere beneath the northwestern part of the Arabian plate (Jordan)—evidence from xenoliths and geophysics. *Tectonophysics* **201**(3–4), 357–370.

Nasir S. (1995) Mafic lower crustal xenoliths from the northwestern part of the Arabian plate. *Euro. J. Mineral.* **7**(1), 217–230.

Nasir S. and Safarjalani A. (2000) Lithospheric petrology beneath the northern part of the Arabian plate in Syria: evidence from xenoliths in alkali basalts. *J. African Earth Sci.* **30**(1), 149–168.

Nesbitt H. W. and Young G. M. (1984) Prediction of some weathering trends of plutonic and volcanic rocks based on thermodynamic and kinetic considerations. *Geochim. Cosmochim. Acta* **48**, 1523–1534.

Newsom H. E., Sims K. W. W., Noll P. D., Jr., Jaeger W. L., Maehr S. A., and Beserra T. B. (1996) The depletion of tungsten in the bulk silicate Earth: constraints on core formation. *Geochim. Cosmochim. Acta* **60**, 1155–1169.

Nguuri T. K., Gore J., James D. E., Webb S. J., Wright C., Zengeni T. G., Gwavava O., and Snoke J. A. (2001) Crustal structure beneath southern Africa and its implications for the formation and evolution of the Kaapvaal and Zimbabwe cratons. *Geophys. Res. Lett.* **28**(13), 2501–2504.

Nimz G. J., Cameron K. L., Cameron M., and Morris S. L. (1986) Petrology of the lower crust and upper mantle beneath southeastern Chihuahua, Mexico. *Geofísica Int.* **25**, 85–116.

Niu F. L. and James D. E. (2002) Fine structure of the lowermost crust beneath the Kaapvaal craton and its implications for crustal formation and evolution. *Earth Planet. Sci. Lett.* **200**(1–2), 121–130.

Nyblade A. A. and Pollack H. N. (1993) A global analysis of heat flow from Precambrian terrains: implications for the thermal structure of Archean and Proterozoic lithosphere. *J. Geophys. Res.* **98**, 12207–12218.

Okrusch M., Schröder B., and Schnütgen A. (1979) Granulite-facies metabasite ejecta in the Laacher Sea area, Eifel, West Germany. *Lithos* **12**, 251–270.

O'Reilly S. Y., Griffin W. L., and Stabel A. (1988) Evolution of Phanerozoic eastern Australian lithosphere: isotopic evidence for magmatic and tectonic underplating. In *Oceanic and Continental Lithosphere: Similarities and Differences*, J. Petrol. Spec. Vol. (eds. M. A. Menzies and K. G. Cox). Oxford University Press, Oxford, pp. 89–108.

Owen J. V., Greenough J. D., Hy C., and Ruffman A. (1988) Xenoliths in a mafic dyke at Popes Harbour, Nova Scotia: implications for the basement to the Meguma Group. *Can. J. Earth Sci.* **25**, 1464–1471.

Padovani E. R. and Carter J. L. (1977) Aspects of the deep crustal evolution beneath south central New Mexico. In *The Earth's Crust* (ed. J. G. Heacock). American Geophysical Union, Washington, DC, pp. 19–55.

Padovani E. R. and Hart S. R. (1981) Geochemical constraints on the evolution of the lower crust beneath the Rio Grande rift. In *Conference on the Processes of Planetary Rifting*. Lunar and Planetary Science Institute, pp. 149–152.

Padovani E. R., Hall J., and Simmons G. (1982) Constraints on crustal hydration below the Colorado Plateau from V_p measurements on crustal xenoliths. *Tectonophysics* **84**, 313–328.

Pearcy L. G., DeBari S. M., and Sleep N. H. (1990) Mass balance calculations for two sections of island arc crust and implications for the formation of continents. *Earth Planet. Sci. Lett.* **96**, 427–442.

Pearson N. J., O'Reilly S. Y., and Griffin W. L. (1995) The crust–mantle boundary beneath cratons and craton margins: a transect across the south-west margin of the Kaapvaal craton. *Lithos* **36**(3–4), 257–287.

Percival J. A. and Card K. D. (1983) Archean crust as revealed in the Kapuskasing uplift, Superior province, Canada. *Geology* **11**, 323–326.

Percival J. A., Fountain D. M., and Salisbury M. H. (1992) Exposed cross sections as windows on the lower crust. In *Continental Lower Crust* (eds. D. M. Fountain, R. Arculus, and R. W. Kay). Elsevier, Amsterdam, pp. 317–362.

Peucker-Ehrenbrink B. and Jahn B.-M. (2001) Rhenium-osmium isotope systematics and platinum group element concentations: loess and the upper continental crust. *Geochem. Geophys. Geosys.* **2**, 2001GC000172.

Phillips R. J., Raubertas R. F., Arvidson R. E., Sarkar I. C., Herrick R. R., Izenberg N., and Grimm R. E. (1992) Impact craters and Venus resurfacing history. *J. Geophys. Res. Planet.* **97**(E10), 15923–15948.

Pinet C. and Jaupart C. (1987) The vertical distribution of radiogenic heat production in the Precambrian crust of Norway and Sweden: geothermal implications. *Geophys. Res. Lett.* **14**, 260–263.

Plank T. and Langmuir C. H. (1998) The chemical composition of subducting sediment and its consequences for the crust and mantle. *Chem. Geol.* **145**, 325–394.

Poldervaart A. (1955) The chemistry of the Earth's crust. *Geol. Soc. Am. Spec. Pap.* **62**, 119–144.

Quick J. E., Sinigoi S., and Mayer A. (1995) Emplacement of mantle peridotite in the lower continental crust, Ivrea-Verbano zone, northwest Italy. *Geology* **23**(8), 739–742.

Reid M. R., Hart S. R., Padovani E. R., and Wandless G. A. (1989) Contribution of metapelitic sediments to the composition, heat production, and seismic velocity of the lower crust of southern New Mexico. *Earth Planet. Sci. Lett.* **95**, 367–381.

Roberts S. and Ruiz J. (1989) Geochemical zonation and evolution of the lower crust in Mexico. *J. Geophys. Res.* **94**, 7961–7974.

Rogers N. W. (1977) Granulite xenoliths from Lesotho kimberlites and the lower continental crust. *Nature* **270**, 681–684.

Rogers N. W. and Hawkesworth C. J. (1982) Proterozoic age and cumulate origin for granulite xenoliths, Lesotho. *Nature* **299**, 409–413.

Ronov A. B. and Yaroshevsky A. A. (1967) Chemical structure of the Earth's crust. *Geokhimiya* **11**, 1285–1309.

Ronov A. B. and Yaroshevsky A. A. (1976) A new model for the chemical structure of the Earth's crust. *Geokhimiya* **12**, 1761–1795.

Ross D. C. (1985) Mafic gneissic complex (batholithic root?) in the southernmost Sierra Nevada, California. *Geology* **13**, 288–291.

Rudnick R. L. (1990a) Continental crust: growing from below. *Nature* **347**, 711–712.

Rudnick R. L. (1990b) Nd and Sr isotopic compositions of lower crustal xenoliths from North Queensland, Australia: implications for Nd model ages and crustal growth processes. *Chem. Geol.* **83**, 195–208.

Rudnick R. L. (1992) Xenoliths—samples of the lower continental crust. In *Continental Lower Crust* (eds. D. M. Fountain, R. Arculus, and R. W. Kay). Elsevier, Amsterdam, pp. 269–316.

Rudnick R. L. (1995) Making continental crust. *Nature* **378**, 571–578.

Rudnick R. L. and Cameron K. L. (1991) Age diversity of the deep crust in northern Mexico. *Geology* **19**, 1197–1200.

Rudnick R. L. and Goldstein S. L. (1990) The Pb isotopic compositions of lower crustal xenoliths and the evolution of lower crustal Pb. *Earth Planet. Sci. Lett.* **98**, 192–207.

Rudnick R. L. and Fountain D. M. (1995) Nature and composition of the continental crust: a lower crustal perspective. *Rev. Geophys.* **33**(3), 267–309.

Rudnick R. L. and Presper T. (1990) Geochemistry of intermediate to high-pressure granulites. In *Granulites and Crustal Evolution* (eds. D. Vielzeuf and P. Vidal). Kluwer, Amsterdam, pp. 523–550.

Rudnick R. L. and Taylor S. R. (1987) The composition and petrogenesis of the lower crust: a xenolith study. *J. Geophys. Res.* **92**(B13), 13981–14005.

Rudnick R. L. and Taylor S. R. (1991) Petrology and geochemistry of lower crustal xenoliths from northern Queensland and inferences on lower crustal composition. In *The Eastern Australian Lithosphere*, Geol. Soc. Austral. Spec. Publ. (ed. B. Drummond), 189–208.

Rudnick R. L. and Williams I. S. (1987) Dating the lower crust by ion microprobe. *Earth Planet. Sci. Lett.* **85**, 145–161.

Rudnick R. L., McLennan S. M., and Taylor S. R. (1985) Large ion lithophile elements in rocks from high-pressure granulite facies terrains. *Geochim. Cosmochim. Acta* **49**, 1645–1655.

Rudnick R. L., McDonough W. F., McCulloch M. T., and Taylor S. R. (1986) Lower crustal xenoliths from Queensland, Australia: evidence for deep crustal assimilation and fractionation of continental basalts. *Geochim. Cosmochim. Acta* **50**, 1099–1115.

Rudnick R. L., McDonough W. F., and O'Connell R. J. (1998) Thermal structure, thickness and composition of continental lithosphere. *Chem. Geol.* **145**, 399–415.

Rudnick R. L., Ireland T. R., Gehrels G., Irving A. J., Chesley J. T., and Hanchar J. M. (1999) Dating mantle metasomatism: U–Pb geochronology of zircons in cratonic mantle xenoliths from Montana and Tanzania. In *Proceedings of the VIIth International Kimberlite Conference* (eds. J. J. Gurney, J. L. Gurney, M. D. Pascoe, and S. R. Richardson). Red Roof Design, Cape Town, pp. 728–735.

Rudnick R. L., Barth M., Horn I., and McDonough W. F. (2000) Rutile-bearing refractory eclogites: missing link between continents and depleted mantle. *Science* **287**, 278–281.

Ruiz J., Patchett P. J., and Arculus R. J. (1988a) Nd–Sr isotope composition of lower crustal xenoliths—evidence for the origin of mid-Tertiary felsic volcanics in Mexico. *Contrib. Mineral. Petrol.* **99**, 36–43.

Ruiz J., Patchett P. J., and Ortega-Gutierrez F. (1988b) Proterozoic and Phanerozoic basement terranes of Mexico from Nd isotopic studies. *Geol. Soc. Am. Bull.* **100**, 274–281.

Rutter M. J. (1987) The nature of the lithosphere beneath the Sardinian continental block: mantle and deep crustal inclusions in mafic alkaline lavas. *Lithos* **20**, 225–234.

Saal A. E., Rudnick R. L., Ravizza G. E., and Hart S. R. (1998) Re–Os isotope evidence for the composition, formation and age of the lower continental crust. *Nature* **393**, 58–61.

Sachs P. M. and Hansteen T. H. (2000) Pleistocene underplating and metasomatism of the lower continental crust: a xenolith study. *J. Petrol.* **41**(3), 331–356.

Saleeby J. B. (1990) Progress in tectonic and petrogenetic studies in an exposed cross-section of young (c. 100 Ma) continental crust southern Sierra Nevada, California. In *Exposed Cross-sections of the Continental Crust* (eds. M. H. Salisbury, and D. M. Fountain). Kluwer Academic, Norwell, MA, pp. 137–159.

Schaaf P., Heinrich W., and Besch T. (1994) Composition and Sm–Nd isotopic data of the lower crust beneath San-Luis-Potosi, Central Mexico—evidence from a granulite-facies xenolith suite. *Chem. Geol.* **118**(1–4), 63–84.

Schaber G. G., Strom R. G., Moore H. J., Soderblom L. A., Kirk R. L., Chadwick D. J., Dawson D. D., Gaddis L. R., Boyce J. M., and Russell J. (1992) Geology and distribution of impact craters on Venus-what are they telling us. *J. Geophys. Res. Planet.* **97**(E8), 13257–13301.

Scherer E. K., Cameron K. L., Johnson C. M., Beard B. L., Barovich K. M., and Collerson K. D. (1997) Lu–Hf geochronology applied to dating Cenozoic events affecting lower crustal xenoliths from Kilbourne Hole, New Mexico. *Chem. Geol.* **142**, 63–78.

Schmitz M. D. and Bowring S. A. (2000) The significance of U–Pb zircon dates in lower crustal xenoliths from the southwestern margin of the Kaapvaal craton, southern Africa. *Chem. Geol.* **172**, 59–76.

Schmitz M. D. and Bowring S. A. (2003a) Constraints on the thermal evolution of continental lithosphere from U–Pb accessory mineral thermochronometry of lower crustal xenoliths, southern Africa. *Contrib. Mineral. Petrol.* **144**, 592–618.

Schmitz M. D. and Bowring S. A. (2003b) Ultrahigh-temperature metamorphism in the lower crust during Neoarchean Ventersdorp rifting and magmatism, Kaapvaal craton, southern Africa. *Geol. Soc. Am. Bull.* **115**, 533–548.

Schulze D. J. and Helmstaedt H. (1979) Garnet pyroxenite and eclogite xenoliths from the Sullivan Buttes latite, Chino valley, Arizona. In *The Mantle Sample: Inclusions in Kimberlites and Other Volcanics* (eds. F. R. Boyd and H. O. A. Meyer). American Geophysics Union, Washington, DC, pp. 318–329.

Sclater J. G., Jaupart C. J., and Galson D. (1980) The heat flow through oceanic and continental crust and the heat loss of the earth. *Rev. Geophys. Space Phys.* **18**, 269–311.

Selverstone J. and Stern C. R. (1983) Petrochemistry and recrystallization history of granulite xenoliths from the Pali-Aike volcanic field, Chile. *Am. Mineral.* **68**, 1102–1111.

Sewell R. J., Hobden B. J., and Weaver S. D. (1993) Mafic and ultramafic mantle and deep-crustal xenoliths from Banks Peninsula, South-Island, New-Zealand. *NZ J. Geol. Geophys.* **36**(2), 223–231.

Shatsky V., Rudnick R. L., and Jagoutz E. (1990) Mafic granulites from Udachnaya pipe, Yakutia: samples of Archean lower crust? *Deep Seated Magmatism and Evolution of Lithosphere of the Siberian Platform*, 23–24.

Shatsky V. S., Sobolev N. V., and Pavlyuchenko V. S. (1983) Fassaïte-garnet-anorthite xenolith from the Udachnaya kimberlite pipe, Yakutia. *Dokl. Akad. Nauk. SSSR* **272**(1), 188–192.

Shaw D. M., Reilly G. A., Muysson J. R., Pattenden G. E., and Campbell F. E. (1967) An estimate of the chemical composition of the Canadian Precambrian shield. *Can. J. Earth Sci.* **4**, 829–853.

Shaw D. M., Dostal J., and Keays R. R. (1976) Additional estimates of continental surface Precambrian shield composition in Canada. *Geochim. Cosmochim. Acta* **40**, 73–83.

Shaw D. M., Cramer J. J., Higgins M. D., and Truscott M. G. (1986) Composition of the Canadian Precambrian shield and the continental crust of the Earth. In *The Nature of the Lower Continental Crust* (eds. J. B. Dawson, D. A. Carswell, J. Hall, and K. H. Wedepohl). Geol. Soc. London, London, vol. 24, pp. 257–282.

Shaw D. M., Dickin A. P., Li H., McNutt R. H., Schwarcz H. P., and Truscott M. G. (1994) Crustal geochemistry in the Wawa-Foleyet region, Ontario. *Can. J. Earth Sci.* **31**(7), 1104–1121.

Sims K. W. W., Newsom H. E., and Gladney E. S. (1990) Chemical fractionation during formation of the Earth's core and continental crust: clues from As, Sb, W, and M., and In *Origin of the Earth* (eds. H. E. Newsom, J. H. Jones, and J. H. Newson). Oxford University Press, Oxford, pp. 291–317.

Smith D. E., Zuber M. T., Solomon S. C., Phillips R. J., Head J. W., Garvin J. B., Banerdt W. B., Muhleman D. O., Pettengill G. H., Neumann G. A., Lemoine F. G., Abshire J. B., Aharonson O., Brown C. D., Hauck S. A., Ivanov A. B., McGovern P. J., Zwally H. J., and Duxbury T. C. (1999) The global topography of Mars and implications for surface evolution. *Science* **284**(5419), 1495–1503.

Smith R. D., Cameron K. L., McDowell F. W., Niemeyer S., and Sampson D. E. (1996) Generation of voluminous silicic magmas and formation of mid-Cenozoic crust beneath north-central Mexico: evidence from ignimbrites, associated lavas, deep crustal granulites, and mantle pyroxenites. *Contrib. Mineral. Petrol.* **123**, 375–389.

Smithson S. B. (1978) Modeling continental crust-structural and chemical constraints. *Geophys. Res. Lett.* **5**(9), 749–752.

Stolz A. J. (1987) Fluid activity in the lower crust and upper mantle: mineralogical evidence bearing on the origin of amphibole and scapolite in ultramafic and mafic granulite xenoliths. *Min. Mag.* **51**, 719–732.

Stolz A. J. and Davies G. R. (1989) Metasomatized lower crustal and upper mantle xenoliths from north Queensland: chemical and isotopic evidence bearing on the composition and source of the fluid phase. *Geochim. Cosmochim. Acta* **53**, 649–660.

Stosch H.-G. and Lugmair G. W. (1984) Evolution of the lower continental crust: granulite facies xenoliths from the Eifel, West Germany. *Nature* **311**, 368–370.

Stosch H.-G., Ionov D. A., Puchtel I. S., Galer S. J. G., and Sharpouri A. (1995) Lower crustal xenoliths from Mongolia and their bearing on the nature of the deep crust beneath cental Asia. *Lithos* **36**, 227–242.

Strom R. G., Schaber G. G., and Dawson D. D. (1994) The global resurfacing of Venus. *J. Geophys. Res. Planet.* **99**(E5), 10899–10926.

Sun W., Bennett V. C., Eggins S. M., Kamenetsky V. S., and Arculus R. J. (2003) Evidence for enhanced mantle to crust rhenium transfer from undegassed arc magmas. *Nature* **422**, 294–297.

Sutherland F. L. and Hollis J. D. (1982) Mantle–lower crust petrology from inclusions in basaltic rocks in eastern Australia—an outline. *J. Volcanol. Geotherm. Res.* **14**, 1–29.

Tanaka T. and Aoki K.-I. (1981) Petrogenetic implications of REE and Ba data on mafic and ultramafic inclusions from Itinome-gata, Japan. *J. Geol.* **89**, 369–390.

Taylor S. R. (1964) Abundance of chemical elements in the continental crust—a new table. *Geochim. Cosmochim. Acta* **28**, 1273–1285.

Taylor S. R. (1967) The origin and growth of continents. *Tectonophysics* **4**, 17–34.

Taylor S. R. (1977) Island arc models and the composition of the continental crust. In *Island Arcs, Deep Sea Trenches and Back-Arc Basins* (ed. M. Talwani). American Geophysical Union, Washington, DC, pp. 325–336.

Taylor S. R. (1992) *Solar System Evolution*. Cambridge University Press, Cambridge.

Taylor S. R. and McLennan S. M. (1981) The composition and evolution of the continental crust: rare Earth element evidence from sedimentary rocks. *Phil. Trans. Roy. Soc. London* **A301**, 381–399.

Taylor S. R. and McLennan S. M. (1985) *The Continental Crust: Its Composition and Evolution*. Blackwell, Oxford.

Taylor S. R., and McLennan S. M. (1995) The geochemical evolution of the continental crust. *Rev. Geophys.* **33**, 241–265.

Taylor S. R., McLennan S. M., and McCulloch M. T. (1983) Geochemistry of loess, continental crustal composition and crustal model ages. *Geochim. Cosmochim. Acta* **47**, 1897–1905.

Teng F., McDonough W. F., Rudnick R. L., Dalpé C., Tomascak P. B., Chappell B. W., and Gao S. (2003) Lithium isotopic composition and concentration of the upper continental crust. *Geochim. Cosmochim. Acta* (submitted).

Thomas C. W. and Nixon P. H. (1987) Lower crustal granulite xenoliths in carbonatite volcanoes of the western rift of East Africa. *Min. Mag.* **51**, 621–633.

Toft P. B., Hills D. V., and Haggerty S. E. (1989) Crustal evolution and the granulite to eclogite transition in xenoliths from kimberlites in the West African craton. *Tectonophysics* **161**, 213–231.

Tredoux M., Hart R. J., Carlson R. W., and Shirey S. B. (1999) Ultramafic rocks at the center of the Vredefort structure:

further evidence for the crust on edge model. *Geology* **27**(10), 923–926.

Trzcienski W. E. and Marchildon N. (1989) Kyanite-garnet-bearing Cambrian rocks and Grenville granulites from the Ayers Cliff, Quebec, Canada, Lamprophyre Dike Suite—deep crustal fragments from the northern appalachians. *Geology* **17**(7), 637–640.

Upton B. G. J., Aspen P., and Chapman N. A. (1983) The upper mantle and deep crust beneath the British Isles: evidence from inclusion suites in volcanic rocks. *J. Geol. Soc. London* **140**, 105–122.

Upton B. G. J., Aspen P., Rex D. C., Melcher F., and Kinny P. (1998) Lower crustal and possible shallow mantle samples from beneath the Hebrides: evidence from a xenolithic dyke at Gribun, western Mull. *J. Geol. Soc.* **155**, 813–828.

Upton B. G. J., Aspen P., and Hinton R. W. (2001) Pyroxenite and granulite xenoliths from beneath the Scottish northern Highlands terrane: evidence for lower-crust/upper-mantle relationships. *Contrib. Mineral. Petrol.* **142**(2), 178–197.

Urrutia-Fucugauchi J. and Uribe-Cifuentes R. M. (1999) Lower-crustal xenoliths from the Valle de Santiago maar field, Michoacan-Guanajuato volcanic field, central Mexico. *Int. Geol. Rev.* **41**(12), 1067–1081.

van Breeman O. and Hawkesworth C. J. (1980) Sm–Nd isotopic study of garnets and their metamorphic host rocks. *Trans. Roy. Soc. Edinburgh* **71**, 97–102.

van Calsteren P. W. C., Harris N. B. W., Hawkesworth C. J., Menzies M. A., and Rogers N. W. (1986) Xenoliths from southern Africa: a perspective on the lower crust. In *The Nature of the Lower Continental Crust*, Geol. Soc. London Spec. Publ. (eds. J. B. Dawson, D. A. Carswell, J. Hall, and K. H. Wedepohl). London, vol. 25, pp. 351–362.

Vidal P. and Postaire B. (1985) Étude par la méthode Pb–Pb de roches de haut grade métamorphique impliquées dans la chaîne Hercynienne. *Chem. Geol.* **49**, 429–449.

Vielzeuf D. (1983) The spinel and quartz associations in high grade xenoliths from Tallante (S. E. Spain) and their potential use in geothermometry and barometry. *Contrib. Mineral. Petrol.* **82**, 301–311.

Villaseca C., Downes H., Pin C., and Barbero L. (1999) Nature and composition of the lower continental crust in central Spain and the granulite-granite linkage: inferences from granulitic xenoliths. *J. Petrol.* **40**(10), 1465–1496.

Voshage H., Hofmann A. W., Mazzucchelli M., Rivalenti G., Sinigoi S., Raczek I., and Demarchi G. (1990) Isotopic evidence from the Ivrea zone for hybrid lower crust formed by magmatic underplating. *Nature* **347**, 731–736.

Wanke H., Bruckner J., Dreibus G., Rieder R., and Ryabchikov I. (2001) Chemical composition of rocks and soils at the pathfinder site. *Space Sci. Rev.* **96**(1–4), 317–330.

Warren R. G., Kudo A. M., and Keil K. (1979) Geochemistry of lithic and single-crystal inclusions in basalts and a characterization of the upper mantle-lower crust in the Engle Basin, Rio Grande Rift, New Mexico. In *Rio Grande Rift: Tectonics and Magmatism* (ed. R. E. Riecker). American Geophysical Union, Washington, DC, pp. 393–415.

Wass S. Y. and Hollis J. D. (1983) Crustal growth in south-eastern Australia—evidence from lower crustal eclogitic and granulitic xenoliths. *J. Metamorph. Geol.* **1**, 25–45.

Weaver B. L. and Tarney J. (1980) Continental crust composition and nature of the lower crust: constraints from mantle Nd–Sr isotope correlation. *Nature* **286**, 342–346.

Weaver B. L. and Tarney J. (1981) Lewisian gneiss geochemistry and Archaean crustal development models. *Earth Planet. Sci. Lett.* **55**, 171–180.

Weaver B. L. and Tarney J. (1984) Empirical approach to estimating the composition of the continental crust. *Nature* **310**, 575–577.

Weber M. B. I., Tarney J., Kempton P. D., and Kent R. W. (2002) Crustal make-up of the northern Andes: evidence based on deep crustal xenolith suites, Mercaderes, SW Colombia. *Tectonophysics* **345**(1–4), 49–82.

Wedepohl H. (1995) The composition of the continental crust. *Geochim. Cosmochim. Acta* **59**, 1217–1239.

Wedepohl K. H. (1969–1978) *Handbook of Geochemistry*. Springer, Berlin.

Wendlandt E., DePaolo D. J., and Baldridge W. S. (1993) Nd and Sr isotope chronostratigraphy of Colorado Plateau lithosphere: implications for magmatic and tectonic underplating of the continental crust. *Earth Planet. Sci. Lett.* **116**, 23–43.

Wendlandt E., DePaolo D. J., and Baldridge W. S. (1996) Thermal history of Colorado Plateau lithosphere from Sm–Nd mineral geochronology of xenoliths. *Geol. Soc. Am. Bull.* **108**(7), 757–767.

Wernicke B., Clayton R., Ducea M., Jones C. H., Park S., Ruppert S., Saleeby J., Snow J. K., Squires L., Fliedner M., Jiracek G., Keller R., Klemperer S., Luetgert J., Malin P., Miller K., Mooney W., Oliver H., and Phinney R. (1996) Origin of high mountains in the continents: the southern Sierra Nevada. *Science* **271**, 190–193.

Wilde S. A., Valley J. W., Peck W. H., and Graham C. M. (2001) Evidence from detrital zircons for the existence of continental crust and oceans on the Earth 4.4 Gyr ago. *Nature* **409**(6817), 175–178.

Wilkinson J. F. G. (1975) An Al-spinel ultramafic-mafic inclusion suite and high pressure megacrysts in an analcimite and their bearing on basaltic magma fractionation at elevated pressures. *Contrib. Mineral. Petrol.* **53**, 71–104.

Wilkinson J. F. G. and Taylor S. R. (1980) Trace element fractionation trends of thoeiitic magma at moderate pressure: evidence from an Al-spinel ultramafic-mafic inclusion suite. *Contrib. Mineral. Petrol.* **75**, 225–233.

Wilshire H. W., Meyer C. E., Nakata J. K., Calk L. C., Shervais J. W., Nielson J. E., and Schwarzman E. C. (1988) *Mafic and Ultramafic Xenoliths from Volcanic Rocks of the Western United States*. Prof. Paper, USGS, Washington, DC, West Sussex, UK.

Windley B. F. (1995) *The Evolving Continents*. Wiley.

Wörner G., Schmincke H.-U., and Schreyer W. (1982) Crustal xenoliths from the Quaternary Wehr volcano (East Eifel). *Neus. Jahrb. Mineral. Abh.* **144**(1), 29–55.

Yardley B. W. D. (1986) Is there water in the deep continental crust? *Nature* **323**, 111.

Yu. J. H., O'Reilly S. Y., Griffin W. L., Xu X. S., Zhang M., and Zhou X. M. (2003) The thermal state and composition of the lithospheric mantle beneath the Leizhou Peninsula South China. *J. Volcanol. Geotherm. Res.* **122**(3–4), 165–189.

Zashu S., Kaneoka I., and Aoki K.-I. (1980) Sr isotope study of mafic and ultramafic inclusions from Itinome-gata, Japan. *Geochem. J.* **14**, 123–128.

Zheng J. P., Sun M., Lu F. X., and Pearson N. (2003) Mesozoic lower crustal xenoliths and their significance in lithospheric evolution beneath the Sino-Korean craton. *Tectonophysics* **361**(1–2), 37–60.

Zhou X. H., Sun M., Zhang G. H., and Chen S. H. (2002) Continental crust and lithospheric mantle interaction beneath North China: isotopic evidence from granulite xenoliths in Hannuoba, Sino-Korean craton. *Lithos* **62**(3–4), 111–124.

© 2003, Elsevier Ltd. All rights reserved
No part of this publication may be reproduced, stored in a retrieval system or transmitted in any form or by any means, electronic, mechanical, photocopying, recording or otherwise, without prior written permission of the Publisher.

Treatise On Geochemistry
ISBN (set): 0-08-043751-6
Volume 3; (ISBN: 0-08-044338-9); pp. 1–64